الجمهورية الجزائرية الديمقراطية الشعبية

People's Democratic Republic of Algeria

وزارة التعليم العالي والبحث العلمي

Ministry of Higher Education and Scientific Research

جامعة زيان عاشور بالجلفة

Ziane Achour University of Djelfa

كلية العلوم والتكنولوجيا

Faculty of Science and Technology

Department: Electrical Engineering

Order N°: …. / 2025

Defense authorization N°…………/2025

DOCTORAL THESIS

3rd Cycle Doctoral (D-LMD)

Presented by

BOUGHEZALA HAMAD HAITHEM

With a view to obtaining the doctoral diploma in 3rd Cycle Doctoral (D-LMD)

Branch: Electrical Engineering

Specialty: Electrical Control

Topic

Contribution to the Control of Five Phase Permanent Magnet Synchronous Motor

Supported, on 11 / 01/2025, before the jury composed of:

Last and first name	Grade	Institution of affiliation	Designation
Mr. Abdelkader Rouibah	Professor	Ziane Achour University of Djelfa	President
Mr. Kouider Laroussi	Professor	Ziane Achour University of Djelfa	Supervisor
Mr. Kouzou Abdellah	Professor	Ziane Achour University of Djelfa	Co-Supervisor
Mr. Elbar Mohamed	MCA	Ziane Achour University of Djelfa	Examiner
Mr. Cherrak Naas	MCA	Ziane Achour University of Djelfa	Examiner
Mr. Samir Benammar	MCA	M. Bougara University of Boumerdes	Examiner

Djelfa University, FST, 2025

الجمهورية الجزائرية الديمقراطية الشعبية

République Algérienne Démocratique et Populaire

وزارة التعليم العالي والبحث العلمي

Ministère de l'Enseignement Supérieur et de la Recherche Scientifique

جامعة زيان عاشور بالجلفة

Université Ziane Achour de Djelfa

كلية العلوم والتكنولوجيا

Faculté des Sciences et de la Technologie

Département : Electrotechnique

N° d'Ordre : …. / 2025

Autorisation de Soutenance N°…………/2025

THESE DE DOCTORAT

Doctorat 3ème Cycle (D-LMD)

Présentée par

BOUGHEZALA HAMAD HAITHEM

En vue de l'obtention du diplôme de Docteur en 3ème Cycle D-LMD

Filière : Génie Electrique

Spécialité : Commande Electrique

Thème

Contribution au Contrôle du Moteur Synchrone à Aimant Permanent à Cinq Phases

Soutenue publiquement, le 11/01/2025, devant le jury composé de :

Nom et Prénom	Le Grade	Institute affiliation	Désignation
Mr. Abdelkader Rouibah	Professeur	Université de Ziane Achour, Djelfa	President
Mr. Kouider Laroussi	Professeur	Université de Ziane Achour, Djelfa	Rapporteur
Mr. Kouzou Abdellah	Professeur	Université de Ziane Achour, Djelfa	A- Rapporteur
Mr. Elbar Mohamed	MCA	Université de Ziane Achour, Djelfa	Examinateur
Mr. Cherrak Naas	MCA	Université de Ziane Achour, Djelfa	Examinateur
Mr. Samir Benammar	MCA	Université de M. Bougara, Boumerdes	Examinateur

Université De Djelfa, FST, 2025

Dedications

I dedicate this modest work:

-To the most precious persons to my heart, my mother and my father, your unwavering faith in me has been my guiding light. Your endless sacrifices, unwavering love, and constant prayers have been instrumental in my journey. I am eternally grateful for your presence and strength.

-To my entire family, especially to the generous wife, who is my back in life,

and to all my dearest children: Abdennour, Abdelbassir, Amara, and Bochra.

-To my dear brothers and my dear sisters.

-To my entire friends

-To my entire co-workers

Thank you.

Acknowledgements

I would like to begin by thanking Almighty God, the all-powerful and merciful, who has granted me the strength and patience to accomplish this work.

*I want to start by expressing my deepest appreciation to Professor **Kouider Laroussi**, my thesis advisor, for his unwavering support and guidance during the course of this research project. His commitment to excellence and vast expertise have played a crucial role in the successful culmination of this study.*

*I would also like to extend my sincere thanks to the co-supervisor, Professor. **Kouzou Abdellah**, for his significant contribution to this research. His presence, expertise, and attention to detail have played a crucial role in the successful outcome of this thesis.*

*I would like to express my gratitude to Dr. **Saad Khadar**, a doctor at the University of Djelfa, for accepting the role of the chairperson for the defence of this thesis.*

My sincere thanks go to the members of the jury who accepted to be the examiners of this thesis and dedicated their time and thorough attention to assessing this work. I am immensely grateful for their interest in my research.

***Dr. Cherrak Naas** from the University of Djelfa.*

***Dr. Elbar Mohamed** from the University of Djelfa.*

***Dr. Benammar Samir** from the University of Boumerdes*

*A big thank you goes to Dr. **Youssfi M. Amine.an** esteemed scholar at the University of Djelfa, fora respected doctor **Toumi Djaafar** and **Dr. Khalil oussama** from University of El-Oued their valuable guidance, advice, and the provision of data and documents relevant to the scope of this research project.*

Finally, I would like to express my gratitude to all the individuals who have contributed directly or indirectly to the completion of this work.

Boughezala Hamad Haithem

Abstract

In order to contribute the control of a Five-Phase Permanent Magnet Synchronous Motor, this thesis focuses on a well-designed backstepping control system, improved using a genetic algorithm and a strong sliding mode observer (SMO) to achieve high-performance sensorless control of a 5-phase Permanent Magnet Synchronous Motor (5Φ-PMSM). Initially, A strong nonlinear strategy based on backstepping control is used to track the desired speed and direct-axis current reference values. Using the Lyapunov theorem, the stability of the entire control system is verified to ensure that the tracking errors converge. Some backstepping control gains are picked at random, though, which could affect the quality of the controller. A novel numerical method based on the genetic algorithm (GA) is suggested for determining the control gains and finding the best gains while staying within the 5Φ-PMSM drive's physical limits. Moreover, to cut down on the number of sensors needed, a slide model observer is created to gather data on the electromotive force of the 5Φ-PMSM drive. An adaptive back EMF observer is then used to measure the motor's speed and rotor position. As a final step, the suggested approach was modelled to work in real time on the FPGA using the OPAL-RT 4500 simulator. These real-time simulation results show how well the suggested approach performs in different test scenarios.

Key words: backstepping control, Five-phase permanent magnet synchronous motor, genetic algorithm, OPAL-RT 4500 simulator, slide model observer.

Résumé

Afin de contribuer au contrôle du moteur synchrone à cinq phases avec des aimants permanents, cette thèse se concentre d'un système de contrôle bien conçu, amélioré à l'aide d'un algorithme génétique et d'un puissant observateur à mode glissant (OMG),pour réaliser un contrôle sans capteur de haute performance d'une machine synchrone à cinq phases (5Φ-PMSM), une stratégie non linéaire robuste, basée sur le contrôle backstepping est initialement utilisée pour suivre les valeurs de référence souhaitées de vitesse et de courant dans l'axe direct. Cette approche s'appuie sur le théorème de Lyapunov, la stabilité de l'ensemble du système de contrôle est vérifiée afin de s'assurer que les erreurs de suivi convergent. Certains gains du contrôle backstepping sont choisis de manière aléatoire, ce qui pourrait cependant affecter la qualité du contrôleur. Une nouvelle méthode numérique, basée sur l'algorithme génétique (GA), est proposée pour déterminer les gains de contrôle optimaux tout en respectant les limites physiques de l'appareil 5Φ-PMSM. En outre, pour réduire le nombre de capteurs nécessaires, un observateur à modèle glissant a été conçu pour estimer des données sur la force électromotrice de l'appareil 5Φ-PMSM. Un observateur adaptatif de le F.E.M est ensuite utilisé pour estimer la vitesse du moteur et la position du rotor. Enfin, l'approche proposée a été modélisée pour fonctionner en temps réel sur un FPGA à l'aide du simulateur OPAL-RT 4500. Les résultats de simulation en temps réel démontrent l'efficacité de l'approche proposée dans différents scénarios de test.

Les mots clés : Backstepping Contrôle, Moteur synchrone à cinq phases, Algorithme génétique, Simulateur OPAL-RT 4500, Observateur de mode glissant.

ملخص

من أجل المساهمة في التحكم في المحرك المغنطيسي الدائم المتزامن خماسي الأطوار، تتحدث هذه الأطروحة عن نظام تحكم جيد التصميم بالتخطّي الخلفي، جرى تحسينه باستخدام خوارزمية جينية ومراقب قوي بالنموذج الانزلاقي (SMO) لجعل التحكم عالي الأداء بدون حساس في محرك مغناطيسي دائم مكون من خمسة اطوار. في البداية، تم استخدام إستراتيجية قوية غير خطية تستند إلى التحكم بالتخطّي الخلفي لتعقب القيم المرجعية المطلوبة للسرعة والمحور المباشر. باستخدام نظرية ليابونوف، تم التحقق من استقرار نظام التحكم بأكمله للتأكد من أن أخطاء التتبع متقاربة. مع ذلك، بعض معاملات التحكم على التخطّي الخلفي يتم اختيارها عشوائياً، والتي يمكن أن تؤثر على جودة التحكم. لذا تم استخدام أسلوب رقمي جديد يستند إلى الخوارزمية الجينية من أجل تحديد معاملات التحكم وإيجاد أفضل المكاسب مع البقاء ضمن الحدود الفيزيائية للمحرك المغنطيسي الدائم المتزامن ذو خمسة اطوار. وعلاوة على ذلك، وبغية خفض عدد أجهزة الاستشعار اللازمة، تم تصميم نموذج مراقب منزلق لجمع البيانات عن القوة الدافعة الكهربية للمحرك المغنطيسي الدائم المتزامن ذو خمسة اطوار. ويُستخدم كذلك المراقب لقياس سرعة المحرك وموقع الدوار. وكخطوة نهائية، اصيغ النهج المقترح ليعمل في الوقت الحقيقي على استخدام جهاز المحاكاة OPAL-RT4500. وتبين نتائج المحاكاة الآنية هذه مدى نجاح النهج المقترح في مختلف سيناريوهات الاختبار.

الكلمات المفتاحية: التحكم بالخطّوة الخلفية، المحرك المغناطيسي الدائم المتزامن خماسي الاطوار، الخوارزمية الجينية، جهاز المحاكاةPOPAL-RT 4500 .مراقب بالنموذج الانزلاقي (SMO)

Table of Contents

Chapter IV. Optimized Sensorless Control of Five-Phases Permanent Magnet Synchronous Motor using Genetic Algorithm

Abreviations list

- PMSMs: permanent magnet synchronous Motors
- ,5Φ-PMSM: five Phase Permanent Magnet Synchronous Motor
- MRAS: model reference adaptive system.
- EKF: Extended Kalman filter
- SMO: Sliding Mode Observer
- AI: Artificial Intelligence
- EMF: Electromotive force
- MMF: Magnetomotive force
- HF: High Frequency
- DSP: Digital signal processor
- DC machine: Direct Current machine
- AC machine: Alternative Current machine
- VSI: Voltage Source Inverter
- CSI: Current Source Inverter
- PWM: Pulse-Width Modulation
- IGBT: Insulated gate bipolar transistors
- MOSFET: metal-oxide-semiconductor field-effect transistor
- DCMI: Diode Clamped Inverter.
- FCMI: Flying Capacitor Inverter
- PI: proportional integral control
- PID: proportional integral Derivative control.
- V/F control: voltage proportional with the frequency control
- DTC: direct torque control
- FOC: field-oriented control
- RFOC: rotor-flux oriented control
- SMC: sliding mode control
- MPC: model predictive control
- I q : q-axis current
- Id : d-current
- X(t) : state variable or state vector
- S(x): Sliding control Surface
- ρ: is a positive constant
- r: degree relative of sliding surface
- e(t): state error relative
- A: is the state matrix of the observer
- B: is a control input matrix
- C: is output matrix
- Vs: is input vector of Luenmberger observer
- G: gain matrix of Luenmberger observer
- $\dot{X}$: the derivative of state variable
- $\hat{X}$ `: the estimated value of the state variable
- Y: the output system
- L d: direct inductance
- L q: Quadratic inductance
- L l: leakage inductance
- PWM: Pulse width modulation
- (α-β) (α1, β1, α2, β2): stationary frame or the stator reference frame
- (d-q) (d1, q1, d2, q2): rotational frame or rotor reference frame
- (U V): Synchronous reference frame
- (a, b, c, d, e): natural frame for 5P-PMSM representation
- GA: Genetic Algorithms
- [Vs]: stator voltages
- [Is]: stator currents
- [Φs]: stator Flux
- $\left[\varphi_m\right]$: Matrix Vector of the flux created by the permanent magnets
- [Rs]: stator resistances

- $\left[L_{s0}\right]$: is the proper inductances matrix of stator windings,
- $\left[L_{s1}\right]$: The mutual inductances matrix of stat
- Lm: is the main stator inductance
- Ls: is linkage inductance.
- P: is pair of pol number.
- Θ: rotor angular position
- Ω: mechanical speed
- w: is the electrical speed
- Tem: electro-magnetic torque
- TL: eternal load torque
- J: is inertia moment of the motor and load combined.
- F:is the friction coefficient
- Ω: :is the mechanical energy delivered by rotor
- $\left[I_s\right]^T$ is the transposed matrix of stator current
- θ_{co} is the angle between the a-axis of referential frame and the d1-axis (coordinate angle)
- wco: is the speed coordinate
- ws: is the synchronous speed.
- K: is a constant factor depend of the power transformation from original frame to new reference frame
- [T]: Park matrix transformation
- [Iα1, Iβ1, Iα2, Iβ2]: Stator currents in stationary frame
- [Vα1, Vβ1, Vα2, Vβ2]: Stator voltages in stationary frame
- [φα1, φβ1, φα2, βd2]: Stator voltages in stationary frame
- [Iq1, Id1, Iq2, Id2]: Stator currents in rotational frame
- [Vq1, Vd1, Vq2, Vd2]: Stator voltages in rotational frame
- [φq1, φd1, φq2, φd2]: Stator voltages in rotational frame
- Ld1, Lq1: are the direct and quadratic inductances of principal frame
- Ld3, Lq3: are the direct and quadratic inductances of secondar frame
- [A]: is the system (or state) matrix
- [B]: is the input matrix
- [C]: represent the output matrix,
- [E]: represent the disturbance input matrix
- D: is the disturbance input of system
- Vdc: is the DC-link source
- (T1, T2……. T10) are ten symmetrical controllable semiconductors
- (D1, D2……. D10) are a ten symmetrical protective diode.
- VNO: is the voltage between the neutral of the machine and the neutral of the source VAN: is phase voltage of machine
- SVM: Space Vector Modulation
- PWM: Pulse Width Modulation
- Ts: is the sampling time (period) (Vmk, tmk, Vlk, tlk): are the middle vectors, switching time of middle vector, large vectors and switching time respectively of sector number k.
- (Vm(k+1), tl(k+1)): the middle vectors and switching time respectively of sector number k+1.
- f (x, u): system function
- V_1(x): first Lyapunov function
- (x): derivative of first Lyapunov function
- f (x1, x2): system of the second order
- Z1: the tracking error
- 1: Derivative of the tracking error

- : is the derivative of desired output.
- x_1^* is the desired reference output
- $V_2(x)$: second Lyapunov function
- (x): derivative of second Lyapunov function
- k_1, k_2: positives constants of Lyapunov functions
- X_{c2}: virtual command of control
- u: the global control
- $\ddot{x}^*$: second derivative of variable.
- K_1^2: square of gain.
- T_{em}: Electromagnet torque
- T_L: Load charge torque.
- *J:* motor inertia
- *B:* viscous friction
- Φm: Permanent Electromagnet
- w^*: reference speed
- $Id1ref$, $Vd1ref$: reference current and voltage in rotational frame
- C1, C2, C3, C4: are the backstepping control gains
- Z1, Z 2, Z 3, Z 4: are the backstepping control error
- Ls : Principal frame inductance
- L_{Ls}: secondary frame inductance
- OPAL-RT OP4500: Real-time estimator
- n: random numbers
- $P_{seli:}$ Probability of individual selection
- $P_{fi:}$ Probability of individual fitness
- Pcross: Probability of crossover
- Pmu: Probability of mutation
- Ps: Probability of selection
- P1, P2: are selection probability of two competitors (parents).
- (F_1, F_2, F_3): Possibility of children
- DNA: Deoxyribonucleic Nuclear Acid
- Γ:The fitness functions
- $\Delta\omega$: the relative errors of speed
- Δi : errors of current
- $\Delta T_{r\omega}$: the time response errors of speed and current
- ΔT_{ri} : the time response errors of current
- $D(\omega)$: the overshoots of speed
- $D(i)$: the overshoots of current
- L: is an SMO observer gain
- sgn (s): signum function
- H(s): is the discontinuity term as signum function
- $\hat{x}, \hat{y}$: are the estimated state variable
- L, K: are SMO observer gain
- PLL: Phase-Locked Loop
- Sat(s): is saturation function
- K_1, K_2 :are the observer gains
- χ : is positive constant of sat function
- Sα, Sβ: are the sliding surface in stationary frame.
- e_α, e_β: the back EMF of the stationary frame components.
- m, m_1 are constants that are obtained by applying the given stability conditions.
- Λ: constant of correction
- $K_{P\omega}$ and $K_{I\omega}$:are the PI speed gains
- RT-LAB: real time software lab

LIST OF FIGURES

Chapter I: State of the Art Sensorless Control of Multiphase Machines

Chapter II: Modeling of Five Phase Permanent Magnet Synchronous Motor

Chapter III: Backstepping Control of Five Phases Permanent Magnet Synchronous Motor

Chapter IV: Optimized Sensorless Control of Five-Phases Permanent Magnet Synchronous Motor using Genetic Algorithm

LIST OF TABLES

General Introduction

General Introduction

Multiphase permanent magnet synchronous motors (PMSMs) have an increasing interest during recent years compared to other motors (multiphase induction motor) [1][2],due to their considerable features such as high efficiency, low inertia, better dynamic response, reliable operation, excellent robustness, high power factor, small size, simple structure, as well as less maintenance requirement [3][4]. Thus multiphase PMSMs are suitable candidate in practical applications which require high performance such as automobiles, home appliances, renewable energy, ship propulsions, robotics actuations, aerospace applications, and so forth [1],[5]-[6].

Nevertheless, the non-linearity and multivariable of the dynamic model of the 5Φ-PMSM makes a control difficult due to the intense coupling between the mechanical speed and the electrical quantities of the machine, unmatched perturbations due to parameters variations, make this motor obviously hard to control [3][5]. Generally, these machines can be controlled by the traditional fixed gain PI, PID controllers[7], which have been used in most practical applications because of their applicability and simplicity[8]. In this approach, the PI controller performs admirably and offers certain respectable results. However, it is difficult to acquire adequate performance requirements when the motor parameter uncertainties like changes in load, temperature fluctuations, or vibrations, exacerbate the uncertainties and mismatches. These disturbances can further complicate the ability to maintain consistent performance.[3][9].To solve these problems, various design nonlinear techniques have been presented in the literature to PMSM control systems such as input-output linearization control[10], sliding mode control[11], direct torque control[12], backstepping control[13]. But the problem or difficulties facing these control schemes primarily revolve around maintaining stability, oscillations, chattering and disturbances. Among the above control techniques, the backstepping control is an effective strategy due to the robustness and it presents superior dynamic performance [14],Moreover, that offers greater flexibility and stability for a wide range of nonlinear control problems.

Problem Description

Since this technique depends on the control gains as the backstepping control, to achieve the high performance such as a faster dynamic of the stator current and the mechanical speed. The prevailing method for determining these gains involves empirical tuning, requiring a series of experiments to identify gain values that yield the desired performance. However, this approach often proves challenging and not consistently effective in producing optimal results. Consequently, the incorporation of stochastic search techniques such as genetic algorithms becomes essential to ascertain suitable gains. Prior research has indeed substantiated the effectiveness of such strategies in yielding optimal outcomes for optimal gain selection[15][16].

In other side, most control techniques typically require the knowledge for accurate position and speed information to obtain high-performance of variable speed motor drives [2]. It can be found by speed sensors. such as resolvers, hall sensor, and encoders. However, the use of real sensors makes the system more expensive and complicated, decreases system dependability, and limits the application in harsh environments. For these reasons, the PMSM sensorless control approach is seen to be an appropriate and successful solution, where position and speed signals is obtained by electromagnetic information instead of mechanical sensors. In this domain, various sensorless control methods have been designed in the literature to eliminate the speed sensor for three-phase PMSM such as model reference adaptive system (MRAS)[17], Kalman filter (EKF)[18], sliding mode observer (SMO)[2], and neural network based approaches[19]. Nonetheless, few operations that focus on speed sensorless control of multiphase machines PMSM such as MRAS estimator [3], EKF technique [20], and SMO algorithm [9]. In [20], the author designed a robust sensorless control based on an extended Kalman filter for 5P-PMSM drive. Despite motor parameter variations, the designed observer provides satisfactory performance for step reference speed. However, the design of this observer needs complex algorithm and high computational effort, which are not conducive to the real time application. In [3], a 5Φ-PMSM speed estimation was developed using MRAS estimator for sensorless speed control. Despite the fact that the MRAS estimator has high dynamic performance and high accuracy estimation, but the performance of MRAS estimator is sensitive to the variation of the stator resistance which constraints its performance at low-speed regions. Another nonlinear observer method based on SMO was designed in [9] to estimate the back EMF, rotor position and motor speed. The SMO methods have better dynamic behaviour, simple, robust and requires less computational time. Nonetheless, its major drawback of SMO method is the chattering issue produced by the discontinuity of the signum function [2] , [4]. One method to alleviate the chattering effect is to replace the signum function by a saturation or sigmoid function [9], showing a good performance.

Motivation for research

In numerous industrial applications, the use of backstepping control combined with SMO provides fast and accurate speed tracking, for ensuring high performance in dynamic environments. The optimization by a genetic algorithm generates the optimum tuning of the backstepping control gains, using sliding mode observers (SMO)to achieve efficient and robust control of motor speeds without the need for physical sensors, which reduces the cost of the system and enhances the reliability of the system.furthermore, sliding mode observers' robustness makes it possible for the system to successfully reject noise and disruptions, which is essential for preserving steady functioning in industrial settings.

Objectives of thesis

The main objectives of the control scheme suggested in this work is its ability to reduce the aforementioned drawbacks. They are summarized as:

- This thesis presents an optimized backstepping control using genetic algorithm for sensorless speed regulation to be applied for 5Φ-PMSM drive.
- The guarantee of an accurate determination of backstepping control gains, assuring the required performances. In fact, the suggested algorithm is based on a simple technique compared to the earlier works published in [15]-[16].
- Then, a simple slide model observer based on the saturation function is developed for sensorless speed regulation to ensure precise speed estimation over a wide speed range. The observer design can reduce chattering problem and maintain robust under the load torque disturbances and the parameter uncertainties in real-time, particularly the stator resistance, the stator inductance and the friction coefficient where the main aim is to eliminate the speed tracking errors in comparison with the previous observers[4],[9], [11],[20].
- The asymptotic stability of the overall system is analysed via Lyapunov theorem.
- The proposed sensorless control is different from the previous strategies (e.g. those presented in [16]-[20]), where the majority of these approaches suffer from the challenges of tuning time and computational complexity. Thus, the overall system concept provides a very competitive solution for high-performance control of multi-phase PMSM drive.

Organization of thesis

There are four chapters in this thesis in addition to appendices. An overview of the research issue is provided in chapter one. It discusses the purpose and motivation behind the study., presents the problem description, and highlights the key findings. Additionally, the goal of the current thesis is explained in this chapter, t provides a summary of the causes behind multiphase machines and introduces the basic principles of sensorless control for multiphase machines, highlighting their advantages. It also covers the types of controls and observers used to manage them, along with emerging trends and advancements in multiphase sensorless control.

Chapter II clarifies about the five-phase permanent magnet synchronous motors and their mathematical model, including electrical and mechanical equations that determine the behavior of the machine in the three different frames, in natural frame, rotating frame and in a stationary frame.

In addition, the association of inverter with 5Φ-PMSM have been detailed in this chapter and simulated of this association in MATLAB Simulink software.

In Chapter III, nonlinear backstepping control theory applied to 5Φ-PMSM is introduced. The entire control system is explained, and a block diagram shows how the backstepping control plan works without a speed sensor. Furthermore, the proposed control will be tested in various operating mode, reversible speed, load torque changed, and fault open phase through simulations using the MATLAB Simulink software.

Chapter VI is divided into two parts. The first presents a review of the Genetic Algorithm approach and the method of optimizing the backstepping control. The optimum gains obtained are shown in this chapter. The second part includes the sensorless optimized backstepping control using a sliding mode observer (SMO) to estimate the speed and rotor position, which are used for the experimentation in this research work. he performance of the control system is evaluated under various operating conditions across a wide range of speed operations, in Load torque change, robustness test and industrial test trajectories. The simulated results for each test are checked in the real time estimation in order to validate the performance of proposed control.

In Chapter V, the primary conclusions are presented, and the work discussed in the thesis is summarized. Additionally, it raises several points that aren't thoroughly examined in this thesis but might serve as a springboard for additional research on the topic. The last chapter contains the list of references consulted for this thesis.

.

Chapter I.

State of the Art

Sensorless Control of Multiphase Machines

I.1. Introduction

The traditional three-phase motors lack operational reliability, as the failure of a single stator phase can render the motor inoperable. The high evolution of electric machines increases rapidly in recent years lead to exploration and adoption of multiphase machines, due to their enhanced efficiency, power density, and fault tolerance property, these multiphase machines offer distinct advantages over their conventional counterparts, particularly in demanding applications such as electric vehicles, aerospace, and renewable energy systems. One critical aspect of effectively harnessing the potential of these machines lies in their precise control, achieved through sensorless control strategies instead of mechanical sensors due to their reliability advantages[21][22].

The fundamental premise of sensorless control involves estimating the machine`s parameters, by leveraging measured electrical quantities and advanced mathematical algorithms, such as rotor position, speed, and other internal states.As multiphase machines present unique characteristics due to their phase configuration, sensorless control approaches need to be adapted and optimized for these machines' specific characteristics[23].

This chapter provides an overview of one modern method and its advantages for controlling multiphase machines, such as sensorless control, which have become of interest to researchers in recent years. The primary focus of the review revolves around the contemporary advancements in multiphase drives. Additionally, it highlights the benefits of sensorless control for multiphase machines. Also, it touched on the details of its main structure, such as inverters, control methods, and types of observers, due to their importance in the effectiveness of sensorless control. In addition, it presents the challenges, merging trends, and advancements of sensorless techniques of multiphase machines.

I.2. Sensorless Control historical overview

The inception of sensorless control strategies dates back to the early 1980s; however, it wasn't until the late 1990s and early 2000s that sensorless control found extensive utilization in industrial applications [24]. During the early phases of sensorless control development, model-based methods were at the forefront. These approaches utilized mathematical representations of the machinery to estimate rotor speed and position from phase current and voltage data. Although model-based sensorless control techniques are known for their high accuracy, their complexity can make implementation challenging, and they are vulnerable to noise and external disturbances.

In recent years, interest in non-model-based sensorless control strategies has significantly increased. These methods eliminate the need for a mathematical model of the machine, making them easier to implement. Additionally, they offer greater robustness to noise and disturbances compared to model-based approaches[25].

A pivotal advancement in the sensorless control for multiphase machines emerged in the early 2000s with the introduction of adaptive sensorless control strategies. These innovative strategies possess the unique capability to dynamically adapt their parameters in real time, effectively compensating for variations in the machine and its surroundings. This inherent adaptability imparts remarkable resilience to noise and disturbances, setting them apart as a robust solution. Another significant innovation was the development of hybrid sensorless control strategies in the late 2000s. Hybrid sensorless control strategies combine two or more different sensorless control techniques to achieve the best possible performance. That can be useful for industrial applications where high accuracy and reliability are required[26].

Lately, there has been a surge in harnessing machine learning and artificial intelligence (AI) to enhance sensorless control strategies. Machine learning, for instance, enables the training of neural networks to precisely estimate the machine rotor's speed and position using data from phase currents and voltages. AI is crucial in advancing sensorless control methods that are both highly effective and capable of evolving by learning from experience, enabling continuous improvement in their performance

I.3. Sensorless control and closed loop operation

A closed-loop control system employs a feedback mechanism where the output of the system is measured and subsequently fed back to the input. This iterative process allows for continuous adjustments, ensuring effective control over the system's behavior. The feedback loop corrects any errors in the system and maintains the desired output. Sensorless control, on the other hand, utilizes mathematical models of the machine's behavior [27]. These models describe the system's dynamics and are used to estimate variables and parameters. In closed-loop operation, feedback from the estimated values is used to adjust the control action. Figure (I.1) illustrates the scheme of a closed-loop feedback system.

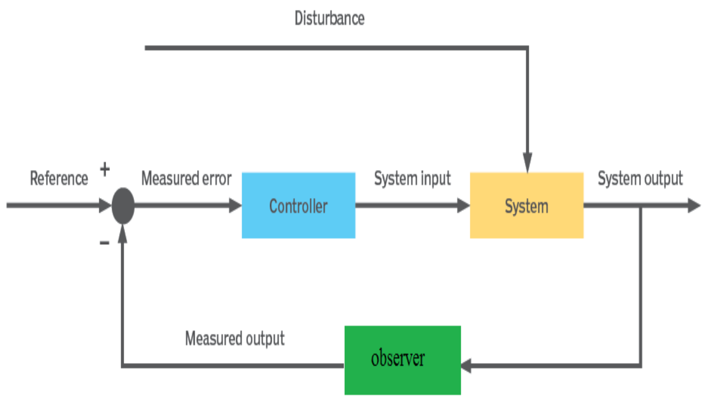

Figure. (I.1): Principle of system closed-loop feedback control

The sensorless control is typically implemented as a closed-loop system. In this architecture, measurements from sensors or estimated states from sensorless techniques are feedback to adjust system inputs. The main principle is to compare the desired states or references with actual states and employ corrective actions to minimize deviations. This iterative process imbues control systems with precision, robustness, and the ability to counteract disturbances, uncertainties, and changing operating conditions[28].

Feedback estimation is important in controlling of systems for a number of reasons.

- ✓ First, it allows for the control of the system without the need for mechanical sensors. This can improve the reliability and robustness of the system, as well as reduce the cost and complexity.
- ✓ The feedback estimation can improve the performance of the system. For example, it can be used to compensate for disturbances or errors in the system model. This can lead to improved accuracy and precision, as well as reduced noise and vibration.
- ✓ The feedback estimation can be used to monitor the health of the system by tracking the estimated parameters of the system, it is possible to detect and diagnose faults early on. This can help to prevent catastrophic failures and extend the life of the system.

I.4. Sensorless control technique classification

Generally, the sensorless control of electric machine can be classified into two families based on the speed range of operation as follow:

- ✓ The first family includes methods that operate in the medium speed range (10% to 100% of the base speed) and high speed range (100% to 200% of the base speed) [29].
- ✓ The second family includes methods that operate in the zero and low speed range (0% to10%ofthebasespeed)[30].

Furthermore, the machine model-based methods are preferred for sensorless control in the medium and high-speed range compared to non-model-based methods. Whereas machine model-based methods are preferred for sensorless control in the medium and high-speed range compared to non-model-based methods. However, among the non-model-based methods, some are based on artificial intelligence. Similarly, among the machine model-based methods, there are both non-adaptive and adaptive approaches.[31]. It is important to note that all these methods are unable to operate in the zero to low speed range[32].

The next Figure (I.2) illustrates the classification of sensorless control methods.

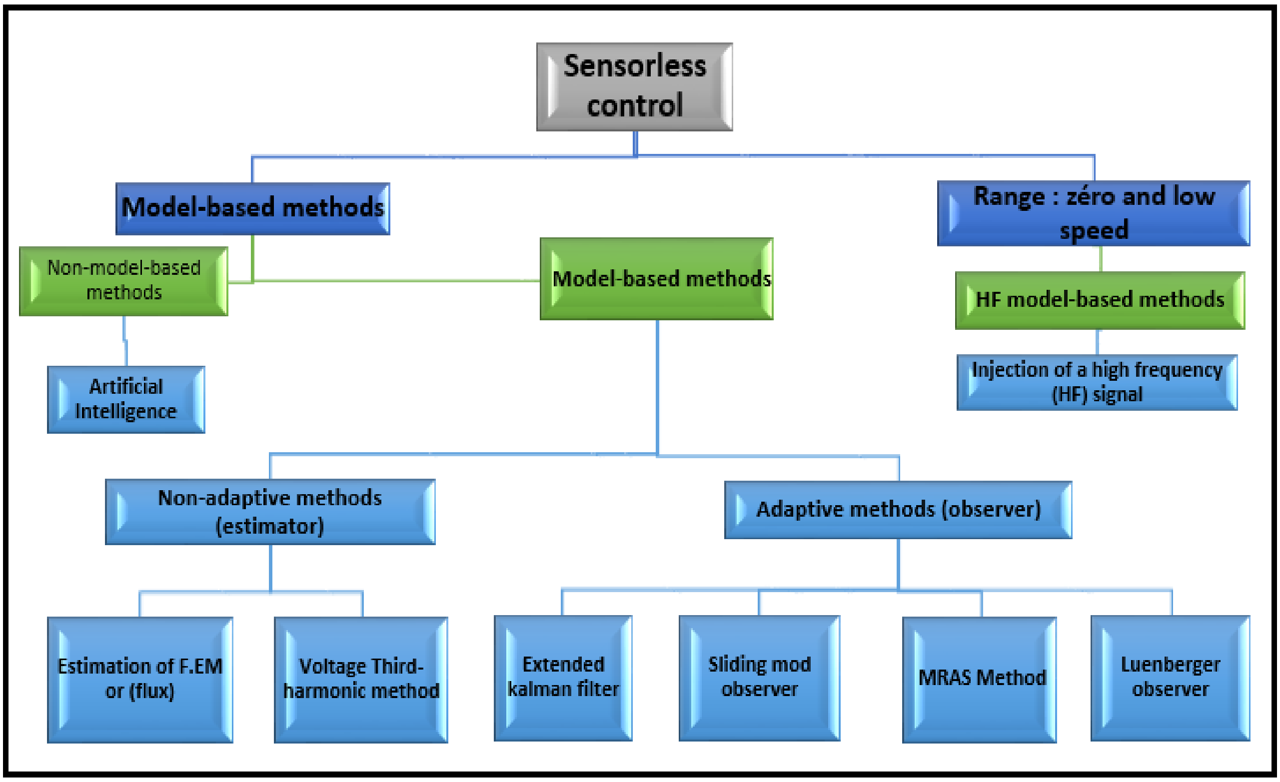

Figure (I.2): Summary of sensorless control methods for electrical machines

There are two main types of sensorless control techniques:

I.4.1. Non-model-based sensorless control techniques

Non-model-based methods based on (artificial intelligence) are utilized for sensorless control in the medium and high-speed range. These methods operate on the principles of fuzzy logic, neural networks, machine learning, and other similar techniques. The primary advantage of these methods is that they do not rely on an analytical model of the machine [33][34]. However, their implementation can be challenging, and they require significant learning time

I.4.2. Model-based sensorless control techniques

This technique used to provide sensorless control in the medium and high-speed range, it utilizes a mathematical model of the motor, and these methods estimate the rotor's position and speed from measured electrical signals, such as electromotive force (EMF) or magnetic flux. This is achieved by measuring the machine's voltages and currents. The primary advantage of these methods is their ease of implementation and low computation time. However, their sensitivity to noise from measurement probes can affect their precision and robustness. Among these machine model-based methods, a distinction is made between non-adaptive and adaptive methods [35]:

I.4.2.1. Non-adaptive methods

Their principle involves directly estimating the machine's quantities that contain rotor information, such as EMF or flux, from its state model. This is done without the use of a corrective term to compensate for the error between the quantities estimated by the model and the quantities measured on the machine [33][36]. Consequently, these methods are highly sensitive to the parametric uncertainties of the machine. As a result, non-adaptive methods are classified as 'Estimators'."

I.4.2.2. Adaptive methods

This method differs from non-adaptive methods in that they use a corrective term. Their operating principle involves correcting the error between the quantities estimated from the state model and the quantities measured on the machine using this corrective term. This correction guarantees the convergence of the estimated quantities towards the measured quantities.[33][37],as well as, these methods are robust to parametric uncertainties of the machine. Adaptive methods are classified as “Observers” due to their ability to estimate the state of a system based on measurements.

I.4.2.3. High Frequency (HF) model-based methods

These methods are utilized to provide sensorless control in the zero to low-speed range[38] . The operating principle of these methods is based on a model of the HF machine. This is achieved by injecting an HF signal into the machine to exploit the anisotropy of the magnetic circuit, which results either from the geometric saliency of the rotor or from the magnetic saliency, for the estimation of the position of the rotor[39]. Since this saliency is independent of the rotor speed, these methods are efficient when the machine is stopped and at low speeds. However, their disadvantage lies in the torque ripples resulting from the injection of the HF signal into the machine.

I.5. Sensorless control of multiphase machines

The principle of sensorless control for multiphase machines is similar to that of conventional three-phase machines. However, one of the main challenges of sensorless control for multiphase machines is the complexity of the machine model. Multiphase machines have more phases and more complex interactions between the phases than traditional three-phase machines. This makes it more difficult to develop accurate machine models for sensorless control there are some additional considerations that need to be taken into account due to the increased number of phases where the interactions between the phases are more complex. To address this, sensorless control algorithms for multiphase machines often use more sophisticated machine models, such as space vector models or multi-dimensional space vector models[21].

Another challenge is that the sensorless control algorithm needs to estimate the rotor position and speed of the multiphase machine using the measured currents and voltages. This becomes particularly difficult at low speeds. To overcome this, sensorless control algorithms for multiphase machines often employ multiple observers or combine various estimation methods

I.5.1. Structure of sensorless control of multiphase machines

The implementation of sensorless control for multi-phase machines necessitates meticulous consideration of several factors and a specific set of requirements. The requirements can vary depending on the type of machine and the application[38], understanding of the electrical properties and characteristics of multi-phase machines is essential to implement effective sensorless control. Also, the choice of sensorless control algorithm must be ensure a very high level of performance, precision and ease of implementation, taking these requirements into account, and examining the strengths and weaknesses of the algorithm methods, the adaptive “Observers” methods are the most suitable of sensorless control of multiphase machines.

Additionally, to execute the control algorithm and produce the control signals for the machine while running the sensorless software, a microcontroller or digital signal processor (DSP) serves as the hardware that processes the data.[40], In addition, many sensorless control systems also use additional hardware and software components, including a Real-time operating system which can be used to ensure that the sensorless control algorithm and controller are able to respond to changes in the system in a timely manner, and the communication interface is used to communicate between the microcontroller and the inverter.

Generally, there are several common components used in most sensorless control systems, as illustrated in the following schematic Figure (I.3), such as:

1. Current and voltage measurement: The first step is to measure the currents and voltages of the multiphase machine. This is done using current and voltage sensors.
2. Machine model: The next step is to use the measured currents and voltages to estimate the machine states, such as the rotor position, speed, and flux. This is done using a machine model.
3. Observer: The observer is used to estimate the machine states based on the measured currents and voltages and the machine model. The observer is designed to be robust to noise and disturbances.
4. Controller: The controller uses the estimated machine states to generate control signals for the inverter. The controller is designed to achieve the desired performance of the multiphase machine, such as speed control or torque control.
5. Inverter: The inverter converts the control signals from the controller into gate signals for the power transistors. Inverters are commonly used to vary the speed of machines by adjusting the frequency and voltage of the power supplied that drives the multiphase machine.

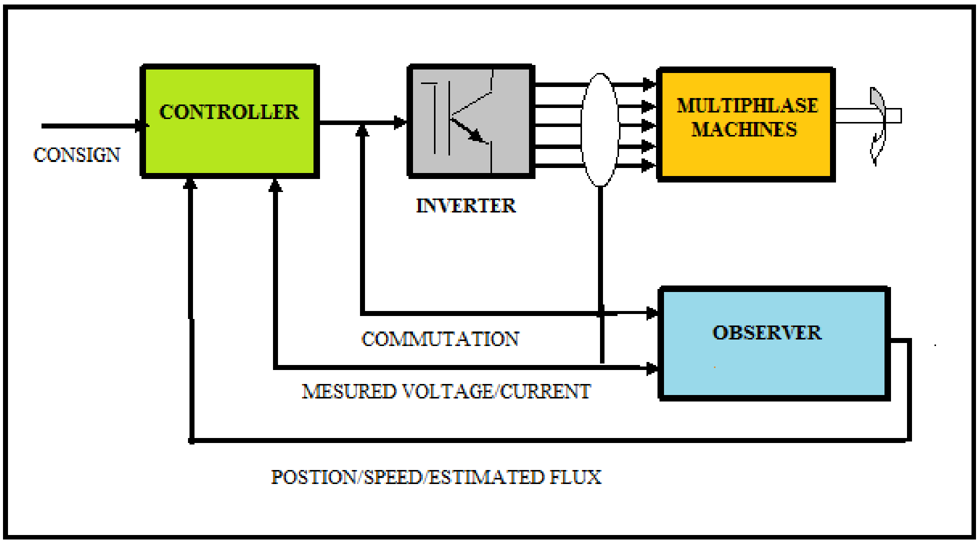

Figure (I.3): General structure of multiphase machines sensorless control

I.5.2. Multiphase machines

An electrical machine with more than three phases is called a multiphase machine. Since the machine is powered by a power converter, the number of phases it can have is theoretically limited only by the complexity of the system[32]. Multiphase systems were initially developed to increase power generation capacity by converting three-phase machines into six-phase machines, thereby lowering the current per phase without raising the voltage. without increasing the voltage. Indeed, that is possible when there are more than three phases, in addition the applications requiring a lot of power and current can effectively utilize this benefit. However, the investigation with some attempts of multiphase drives have been back to 1960s, but they gained significant interest due to advancements in power electronics, microcontrollers, and variable-speed drives in the 1990s for marine applications, where they were pioneered for both ship propulsion and power generation. The development of power electronics has made multiphase drives become more efficient affordable, and competitive alternative for wind high-power production ,vehicle electrification[33].The main challenge associated with multiphase machines is their complexity, because it have more phases than three-phase machines, which requires more complex control algorithms. However, the advantages of multiphase machines often outweigh the challenges.

I.5.2.1 Types of multiphase machines

In theory, three-phase and multiphase machines for variable-speed applications are identical in terms of design. Multiphase machines can be classified as either induction or synchronous. A synchronous machine might be stimulated by a permanent magnet, field winding, or reluctance. A permanent magnet synchronous machine with a trapezoidal flux distribution and a rectangular stator current supply, also referred to as a brushless DC machine, an exception to the rule that most three-phase machines are designed with a distributed stator winding that produces a nearly sinusoidal

MMF distribution and is supplied with sinusoidal currents. However, there are always going to be some spatial harmonics present since the spatial MMF distribution is never exactly sinusoidal. In this regard, multiphase machines have greater versatility. For all sorts of AC machines, a stator winding can be configured to provide a quasi-rectangular or near-sinusoidal MMF distribution by using concentrated or scattered windings. For a near-sinusoidal MMF distribution, more than one slot must be used for each pole in each phase. It gets increasingly challenging to achieve a near-sinusoidal MMF distribution as the number of phases rises [41].

Multiphase machines are classified also into two types based on the number of stator phases:' type 1' machines have a number of phases that is a multiple of three, while 'type 2' machines have a number of phases that is not a multiple of three. Even-numbered phase counts are rarely used, except when they are multiples of three [42].

1. **"Type 1" of multiphase machines:**

Table I.1: Multiphase machines (type 1) whose number of phases is a multiple of three.

Number of phases 'n'	Equivalant number of phases	Angular offset (α)	Schematic representation
3	3	$\pi/3$	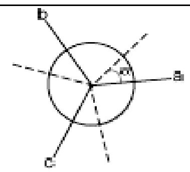
6	3	$\pi/3$	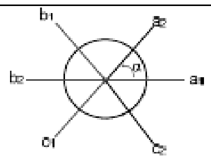
6	6	$\pi/6$	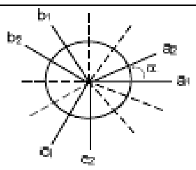
9	9	$\pi/9$	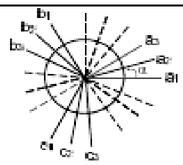
18	9	$\pi/9$	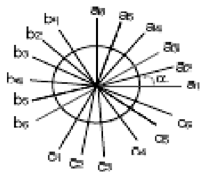

The multiphase machine of (type 1) are the machines whose number of phases stator ’n’ is a multiple of three, so that we can group them into ’m’ three-phase stars where the phase’s number n =3m (m =1.2.3….), these machines are also called “multi-star machines”.

Note that it is generally preferable in normal operation, to have many neutrals as stars, that is to say ‘m’ isolated neutrals. Table (I.1) gives details on some examples of multiphase machines ‘type 1’ or “multi-star machines”

However, for a specific number of phases, there can be several possible configurations depending on the angular offset between two adjacent coils (this corresponding to the offset between stars). Indeed, a double star machine (n = 6) whose stars are offset by ($\alpha = \pi/6$) has different characteristics from those of a machine whose stars are offset by $=\alpha/3$.

To differentiate the possible configurations an "equivalent number of phases" can be introduced, denoted $q_\alpha$which is defined by $q_\alpha = \pi/\alpha$.

2. **“Type 2” of multiphase machines:** are machines whose number of phase’s stator ‘n’ is an odd number. If α denotes the offset between two adjacent coils, the n phases are then regularly shifted by $2\pi/n=2\alpha$.the following table (I.2) presents some examples of ‘type 2’ multiphase machines:

Table (I.2): Multiphase machines (type 2) whose number of phases is an odd number of three.

Number of phases 'n'	equivalent number of phases'q_α'	Angular offset'α'	schematic representation
5	5	$\pi/5$	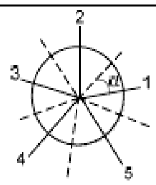
7	7	$\pi/7$	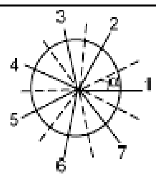
9	9	$\pi/9$	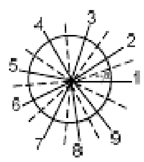

I.5.2.2 Advantages of multiphase machine counterpart of three phases

The number of phases in a multiphase machine can be any number greater than three. The most common phase counts are 5, 7, and 9, these machines constructed in a variety of ways, but the basic principles are the same as for three-phase machines. The stator of a multiphase machine has a number of slots, each slot containing a coil of wire. The coils are connected in a specific sequence to form the different phases, and the rotor of a multiphase machine can be either induction or synchronous. Induction rotors are simpler to construct, but synchronous rotors offer better performance. However, the multiphase drive systems provide the following benefits over the three-phase ones[32].

- **Higher efficiency:** Multiphase machines can have higher efficiency than three-phase machines due to the reduced harmonic content of their waveforms.
- **Higher power density**: Multiphase machines can have higher power density than three-phase machines due to their ability to use smaller conductors and stator windings.
- **Better torque control**: Multiphase machines have better torque control than three-phase machines due to their increased number of phases.
- **Lower noise and vibration:** Multiphase machines have lower noise and vibration than three-phase machines due to the reduced harmonic content of their waveforms.
- **Reduced harmonics:** Multiphase machines have reduced harmonics in their waveforms, which can improve the performance of power electronics systems.
- **Increased reliability:** Multiphase machines are more reliable than three-phase machines due to their reduced number of moving parts and their ability to operate even if one or more phases fail.

I.5.2.3. Applications of multiphase machine

Multiphase machines are used in a wide variety of applications, including:

- Electric vehicles: Multiphase machines are used in electric vehicles to achieve higher efficiency, power density, and torque control. This can lead to increased range, faster acceleration, and better overall performance.
- Hybrid electric vehicles: Multiphase machines are used in hybrid electric vehicles to improve fuel efficiency and reduce emissions.
- Aerospace propulsion: Multiphase machines are used in aerospace propulsion systems to achieve high efficiency, power density, and reliability. This can lead to reduced fuel consumption, increased thrust, and longer aircraft range.
- Ship propulsion: Multiphase machines are used in ship propulsion systems to achieve high efficiency, power density, and torque control. This can lead to reduced fuel consumption, increased speed, and better manoeuvrability.

- High-power industrial drives: Multiphase machines are used in high-power industrial drives to achieve high efficiency, power density, and torque control. This can lead to improved productivity, reduce energy consumption, and lower operating costs.

- Wind turbines: Multiphase machines are used in wind turbines to generate electricity efficiently and reliably

I.5.3. The converter topologies

To ensure variable speed operation of asynchronous machines, it is necessary to use a controllable variable frequency source. For this, the study of the behaviour of these machines when associated with DC/AC converters is very important for the development of controls which take into account all the problems linked to this power supply mode. Voltage inverters are an essential part of the drive system, they constitute an essential function of power electronics, and they are present in the most varied fields of application. The strong evolution of these converters has been based on the one hand, on the development of semiconductor components fully fast controllable, powerful, and robust[43].Inverters are classified based on the applied input source into two main categories:

I.5.3.1. Voltage Source Inverter (VSI)

VSIs operate with a stable DC voltage supply as their input that use power semiconductor devices like insulated gate bipolar transistors (IGBTs) or MOSFETs to switch the DC voltage on and off at high frequencies, they often use Pulse-Width Modulation (PWM) techniques to create a variable AC output voltage. By adjusting the PWM switching patterns, Voltage Source Inverters can produce high-quality sinusoidal AC output voltages suitable for a wide range of applications.

I.5.3.2. Current Source Inverter (CSI)

CSIs operate with a stable DC current source as their input, which can be provided by various sources such as a current-controlled power supply or energy storage systems, similar to VSIs, CSIs often use Pulse-Width Modulation (PWM) techniques to create a variable AC output current by controlling the width of pulses. That often use power semiconductor devices like thyristor. The main advantage of CSIs is their ability to control the output current, making them suitable for applications where precise current regulation is required.

I.5.3.3. Number of Voltage Level Classification

The output levels of an inverter can range from a minimum of two to more levels. Inverters can be categorized into two groups based on the number of output levels they possess.

I.5.3.3.1. Two-Level Inverter

In this category, the output voltage alternated between two output levels positive and negative with single-phase or multiple output phases. Multiphase inverters generate two or more output phases. However, the most common multiphase inverters include three-phase inverters, the two-level inverter circuit comprises input sources and a set of switches used to regulate current or voltage. In high-frequency, high-voltage applications, two-level inverters face restrictions due to switching losses and the constraints imposed by device ratings. Nonetheless, it is possible to enhance the switch ratings by employing combinations of switches in series and parallel configurations.

Two level inverters are not preferred due to their limited number of switches and supply, resulting in poor waveform quality and electromagnetic compatibility concerns, and their two levels, making multilevel inverters more practical [34].

I.5.3.3.2. Multilevel Inverter (MLI)

A multiphase inverter is an electric apparatus employed for transforming direct current (DC) into alternating current (AC) that features numerous output phases. In contrast to conventional single-phase inverters, which generate a solitary AC output, multiphase inverters produce two or more output phases. Among the prevalent forms of multiphase inverters are three-phase inverters, which yield three distinct output phases.

The benefits of multiphase inverters encompass enhancements in power quality, a decrease in harmonic distortion, and more seamless motor performance. They find extensive utilization in high-power demand applications like industrial motor drives, electric vehicle propulsion systems, and renewable energy converters. Multiphase inverters are especially advantageous in situations necessitating high torque, precise control, and efficient power conversion[44].

1.5.3.4. Types of Multilevel Inverters

There are several types of multilevel inverters, some common types can be mentioned as follow:

1.5.3.4.1. Diode Clamped Inverter (DCMI)

The diode-clamped inverter, as its name implies, employs diodes in conjunction with capacitors to generate a multilevel output voltage. In this configuration, diodes play a central role in rectification and also govern input source and output voltage regulation. One notable advantage of this inverter design is its need for fewer control switches. Consequently, it generates minimal harmonic distortions, resulting in comparatively reduced output voltage ripples when compared to traditional two-level inverters[45], figure (I.4) illustrates the schema of five-level diode clamp inverter.

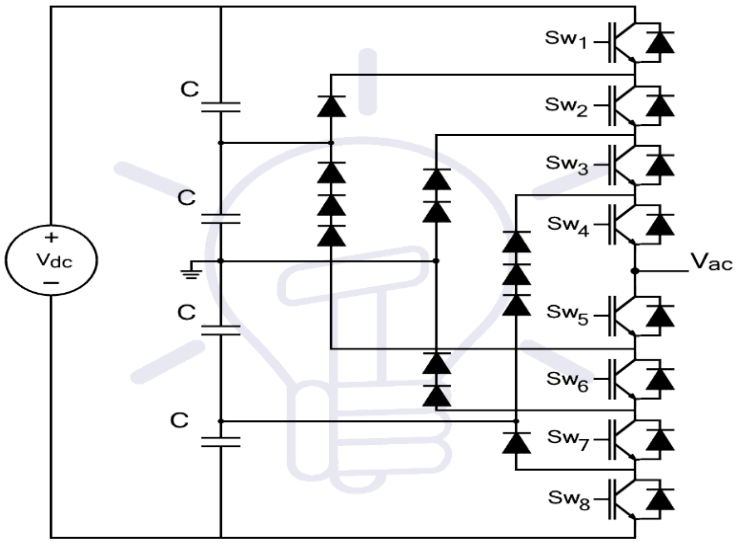

Figure (I.4): Schema of five-level diode clamp inverter.

The two most well-known variants are the 5-level and 9-level inverters based on their output voltage levels used in various types of the diode-clamped inverter, due to their advantages as they can be used for high voltage DC to AC line transmission, and a filter is unnecessary as the output waveform is close to a pure sinusoidal shape.

1.5.3.4.2. Flying Capacitor Inverter (FCMI)

In the configuration of a flying capacitor multilevel converter, the selection of switch states plays a crucial role in determining which capacitors influence the output voltage. The power circuit of a flying capacitor multilevel converter's phase leg for five-level variants can be observed in Figure (I.5). These converters find application in high-power industrial settings[46]. Expanding the converter to include more than five voltage levels is a straightforward process, similar to diode clamp converters. When all the lower switches are closed, the output leg voltage is held at the negative DC rail, and subsequently, the activation of upper switches contributes to the voltage from one of the capacitors. The main challenge of the flying capacitor topology is the need to balance the voltage levels of capacitors. In three-level converters, managing a single capacitor voltage simplifies control. However, as the number of levels increases, controlling the system becomes more complex due to the increasing number of clamping capacitors[33].

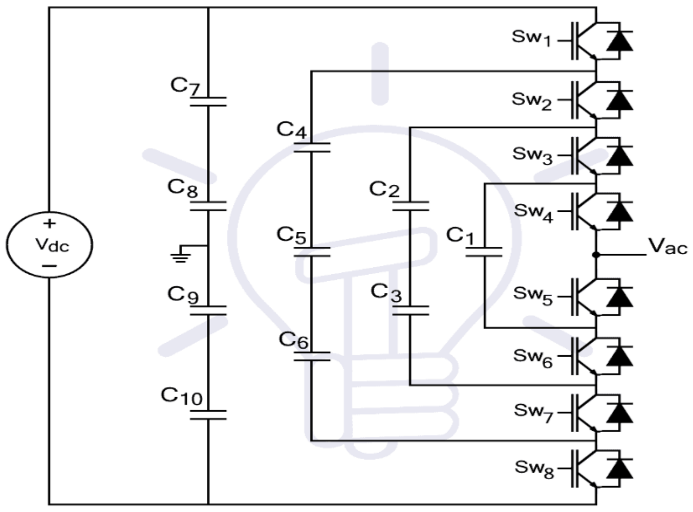

Figure (I.5): Schema of Five-level Flying capacitor inverter

1.5.3.4.3. Cascaded H-bridge Inverter

The power circuit diagrams of five-level H-bridge converters as multilevel inverters are displayed in Figure (I.6). The H-bridge converter was first developed in the 1990s for use in medium-voltage drive applications. A single-phase H-bridge converter can produce three different output voltages, and by connecting multiple H-bridge cells in a cascading manner, more than three voltage levels can be achieved. This approach is considered one of the most straightforward solutions for cascade converters, offering modularity that effectively lowers commissioning and maintenance costs. Additionally, it introduces some degree of fault tolerance [47]. The main disadvantage of cascade H-bridge converters is the need for each H-bridge cell to be equipped with an independent voltage source. For example, in scenarios such as a five-phase induction motor drive employing a full H-bridge converter, it becomes imperative to have five distinct DC power sources. This prerequisite leads to elevated expenses and contributes to the overall weight and energy losses within the drive system.

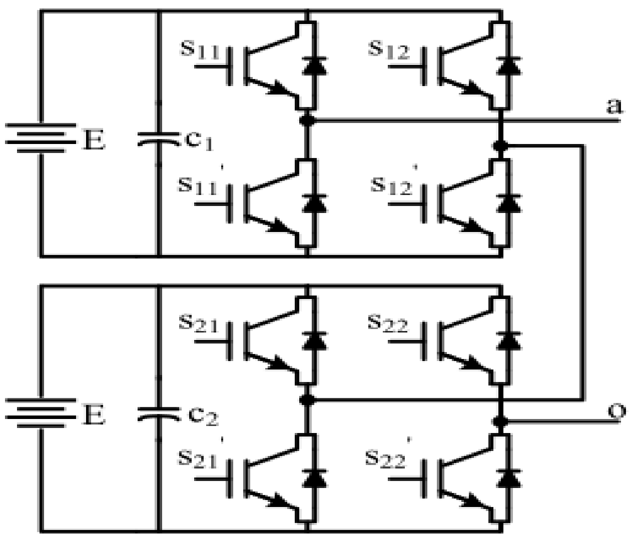

Figure (I.6): five level cascade H- bridge converter.

I.5.4. Multiphase drives control

The principles of regulating the speed of multiphase machines closely align with those used for three-phase machines, on the other hand the constant V/F control, which was once a primary approach, has diminished in importance. This shift is due to the fact that the expense of implementing advanced control algorithms is now quite minimal in comparison to the overall costs of acquiring multiphase power electronics and the multiphase machine itself, which are not widely available on the market. As a result, the focus has shifted towards emphasizing vector control and direct torque control (DTC) for speed regulation [48].The development of vector control, known as the field-oriented control, or FOC ,that transformed the regulation of multiphase machines, which allowed for the independent adjustment of torque and flux characteristics in multiphase machines due to involved controlling the elements of current or voltage vectors and translating machine variables into a rotating reference frame[35].

Over the years, numerous control techniques have been devised to improve the control of multiphase machines. These encompass direct torque control (DTC), model predictive control (MPC), sliding mode control (SMC), adaptive control, backstepping control and sensorless control which will be studied in next chapter 2 and 3 successively. The primary objective of these techniques is to enhance the dynamic response, efficiency, fault tolerance, and robustness of multiphase machine control.

In recent years, the use of multiphase machines has spread on various industries applications, where the control techniques were tailored to specific application requirements. The field continues to advance by exploring new control algorithms, such as a fault-tolerant strategies, advanced modulation techniques, and integration with emerging technologies like artificial intelligence and machine learning.

We will mention in the next two different methods of control that are most common used to the control of multiphase machines, field-oriented control and sliding mode controller. Also, the backstepping control detailed in the chapter three.

I.5.4.1. Field oriented control (FOC)

There are several types of vectors control but the rotor-flux oriented control (RFOC) system, which is based on numerous inner current control loops with an outside speed controller superimposed, is the most often used control strategy in multiphase drives. The number of independent 2D planes determines the number of current controllers, which is the subject of recent advancements. For a multiphase machine an n-phase drive with a single neutral point, it is necessary to have (n-1) current controllers. This is done to minimize the presence of low-order harmonic currents caused by asymmetry and inverter dead time, as well as to enhance the balance of current sharing among the windings[49].By employing this technique, it ensures the independent control of the rotor flux and electromagnetic torque. Additionally, the flux is regulated through the d1-current component, while the torque is controlled via the q1-current component. This is accomplished by aligning the flux with the d1-axis., the following figure (I.7) illustrate the principal of field-oriented control.

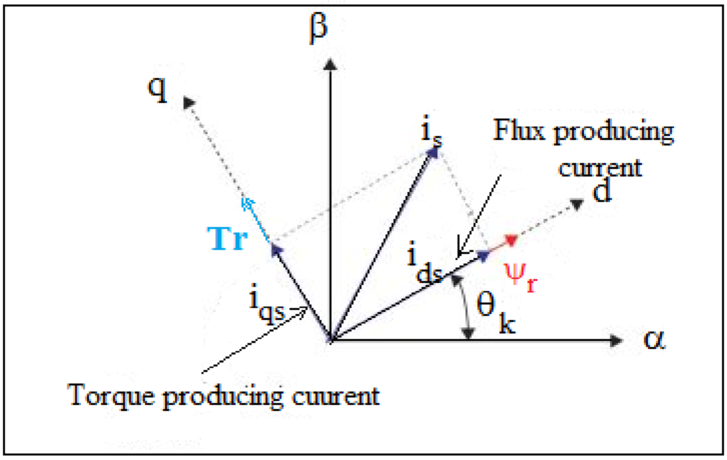

Figure (I.7): Decoupling of space vector currents into the (FOC)

To implement Field-Oriented Control (FOC) for multiphase machines, the following steps can be followed:

1-Develop a mathematical model of the multiphase machine either synchronous or asynchronous, considering its electrical, magnetic, and mechanical characteristics. This model should accurately represent the machine's behavior and dynamics.

2-Transform the multiphase currents from the stationary reference frame to a rotating reference frame, typically using Clarke and Park transformations. This allows for decoupled control of the torque and flux components.

3-Design a controller to regulate the flux component. This process involves generating a reference value for the d-axis current (Id) based on the desired flux level. The controller adjusts the d-axis current to maintain the desired flux, typically using a proportional-integral (PI) controller.

4-Design a controller to regulate the torque component with same component of speed. The speed regulation is achieved using a PI anti-windup controller. The output of this controller serves as the reference for the electromagnetic torque. This process involves generating a reference value for the q-axis current (Iq) based on the desired torque.

5- Determination the decoupling terms for achieving the complete independence between the d and q axes, this decoupling enables the formulation of simplified equations for the motor and control, thereby facilitating the calculation of the controller coefficients

6-Design current controllers to track the reference values of I_d and I_q. These controllers ensure accurate and responsive tracking of the desired currents, typically using PI controllers defined based on the motor's transfer functions, as follows:

I.5.4.1.1. PI speed controller

The output is the electromagnetic torque, the gains of PI speed controller can be calculated using the dynamic transfer function of speed closed loop.

I.5.4.1.2. PI controller of d-q axis current Loop

The parameters of PI currents controllers calculated using the electrical transfer function, where the comparison between the reference currents and the measured currents represents the input of the PI controller, and its output provides the reference voltages

-The following Figure fig (I.8) presents control scheme of the rotor flux-oriented control:

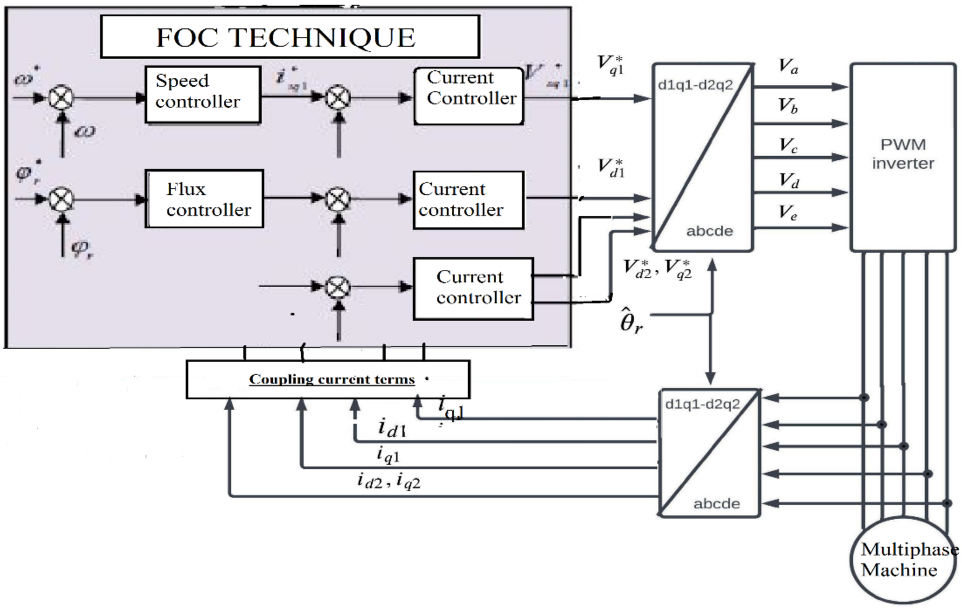

Figure (I.8): Field oriented Control of Multiphase Machines

I.5.4.2. Sliding mode controller (SMC)

The theory of Sliding Mode Control (SMC) was initially introduced by **Utkin** in 1977[50].Subsequently, there have been significant advancements in the theoretical understanding and practical applications of sliding mode controllers. Due to its exceptional robustness. Sliding Mode Control (SMC) is a robust control technique that can be applied to multiphase machine control. It is designed to ensure that the system's state trajectory follows a predefined sliding surface, regardless of uncertainties or disturbances. The objective of SMC is to make the system's state "slide" along this surface, providing robustness and stability in the control process for multiphase machines. However, one significant drawback of this control technique is the occurrence of chattering, which is caused by the discontinuous nature of the control action[51].

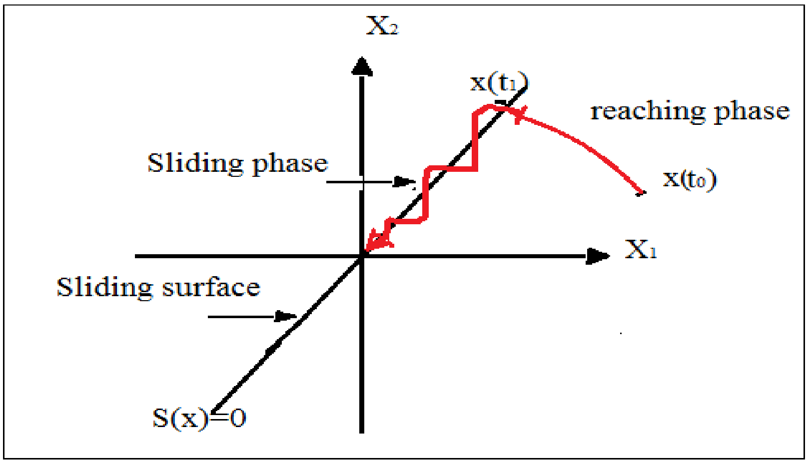

Figure (I.9): Principe of sliding mode control (Switching surface)

The structure of sliding mode control depends of the machine model formed in d-q frame, this model should capture the electrical and mechanical dynamics, as well as any uncertainties or disturbances in the system.

To apply Sliding Mode Control to multiphase machines, you would typically follow these steps:

a) Sliding Surface Design S(x): Determination of the desired sliding surface that represents the desired system behaviour. The sliding surface should be chosen based on the control objectives, such as torque control, speed control, or current control. The sliding surface should be designed to ensure stability and convergence of the system state. So, it depends of the state error e(x) which can be expressed using the following equation:

$$S(x)=\left(\frac{d}{dt}+\rho x\right)^{r-1}e(x) \qquad \text{(I.01)}$$

Where: ρ is a positive constant that interprets the bandwidth of desired control, and r is the relative degree.

b) Control Law Design: Design a control law that will drive the system state onto the sliding surface and maintain it there. This control law typically consists of two components: a reaching control and a sliding control

- Reaching Control: The reaching control component is responsible for driving the system's state trajectory towards the sliding surface. It ensures that the system reaches the sliding surface in finite. Which extracted from S(x)= 0.

- Sliding Control: Once the system reaches the sliding surface, the sliding control component keeps the system's state trajectory sliding along the surface, usually this control component is in the discontinuity function designed to reject uncertainties and disturbances, ensuring robustness.

c) Control Implementation: Implement the designed control law consists of combining the two controls, reaching and sliding. Implement the designed sliding mode controller involve adjusting Fine-tune the controller parameters to achieve the desired system performance, This can be achieved using a Lyapunov verification, through simulation studies or experimental testing.

d) Stability Analysis: Verifying that the surface is attractive and ensuring the system's sliding state trajectory remains on the surface. Also, stability analysis performed to ensure that the sliding mode control system is stable and robust. This analysis involves examining the Lyapunov

The main drawback of sliding mode control is the chattering caused by the rapid switching of the control signal between two values near the sliding surface. This phenomenon can result in high-frequency oscillations, causing adverse effects on the controlled system. Below are several strategies to alleviate chattering in sliding mode control[52].

- ✓ Use the super-twisting sliding control method.
- ✓ Combination of adaptive control with sliding mode controller.
- ✓ Using the integral of the sliding surface.
- ✓ Apply the continuous function instead of the discontinuity.

I.5.5. Observers and state estimators

The observer is the main component of sensorless control, termed also as state estimators that play a crucial role in control systems by predicting unmeasured states of a dynamic system using available measurements. Diverse observer types, including Luenberger observers, Kalman filters, Model Reference Adaptive System (MRAS) and sliding mode observers, utilize the system model and measured outputs to compute estimates of unmeasured states. These estimates are subsequently employed by the controller to generate control signals. Observers prove invaluable in situations where not all states of a system are directly measurable, facilitating feedback control based on estimated states. We will discuss two types of them, the first is Luenberger observers which based speed estimator, and the second is a MRAS based on reference model.

I.5.5.1. Luenberger observer

Typically, the parameters required to regulate a system are challenging to measure due to economic or technological constraints. In response to this issue, Luenberger explored the concept of observability to introduce his observer for linear systems.[53]The concept of the Luenberger observer emerged in control theory during the 1960s and has since made significant inroads into the field of motor drives. It aims to reconstruct the internal state variables within the system using input and output signal measurements. A typical observer operates by comparing the estimated states in the state model with the actual measured state signals. Initially the machine model is experimented in the stationary reference frame on state-space model utilized to form an observer, where the model is given by the following equation:

$$\begin{cases} \dot{X} = AX + BV_s \\ i_s = CX \end{cases} \qquad (I.02)$$

Where:

A is the state matrix of the observer is state vector, B is a control input matrix, Vs is input vector, C is output matrix; while the state of Luenberger observer is given by:

$$\begin{cases} \dot{\hat{X}} = \hat{A}X + BV_s + G(i_s - \hat{i}_s) \\ \hat{i}_s = C\hat{X} \end{cases} \qquad (I.03)$$

The selection of the coefficient gain matrix G is done meticulously to guarantee the stable operation and dynamic performance of the observer. The following figure (I.10) illustrates the diagram block of Luenberger observer.

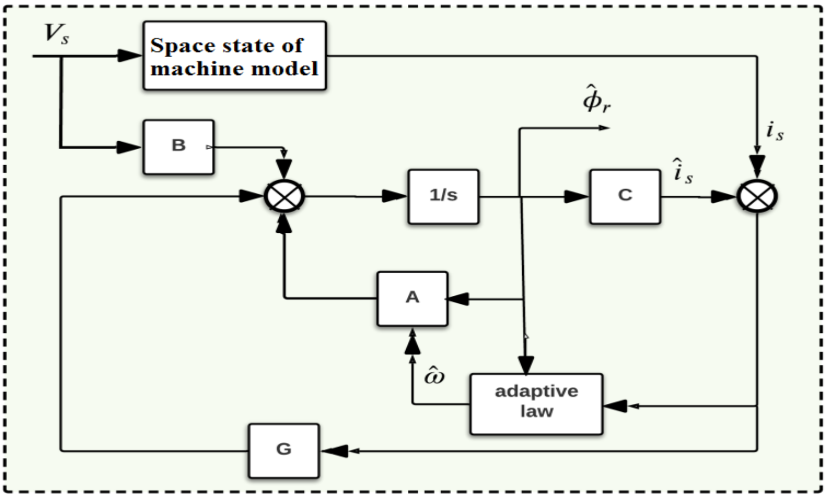

Figure (I.10): Schematic form of Luenberger observer technique

Nevertheless, in this type of observer, the gain matrix is computed using a pole placement method to deliberately position the poles of the observer. Subsequently, an adaptive controller is employed to compel the estimated states to align with the actual states by adjusting the unknown parameters, a design based on stability analysis. The primary drawback lies in the intricate nature of the Luenberger observer structure[33]. Additionally, there exists a challenge with parameter variation, leading to diminished accuracy in low-speed ranges or during regenerative modes. In order to achieve a full-order nonlinear speed observer.

I.5.5.2. Model Reference Adaptive System

One of the most effective closed-loop methods for estimating the rotor speed of sensorless control of multiphase machines drives is the model reference adaptive systems (MRAS) approach.

Tamai proposed a speed estimation technique based on MRAS in 1987. The MRAS method has the advantage of enhancing the noise rejection property, which helps to obtain unbiased rotor speed estimation. Figure (I.11) illustrates the schematic block of a MRAS-based speed estimator, which consists of three main components: a reference model, an adjustable model, and an adaptation mechanism. However, MRAS method minimizes the error between a reference model value and an adjustable model value. The Adaptive mechanism, which is based on Popov's stability criterion, is a favourable technique for estimating the speed and rotor resistance of the motor. The block "Reference Model" represents the dynamic models that contain the desired mathematical model of the motor with all unknown parameters, as shown in Equation (I.02), with the output system written on the form Y=CV.

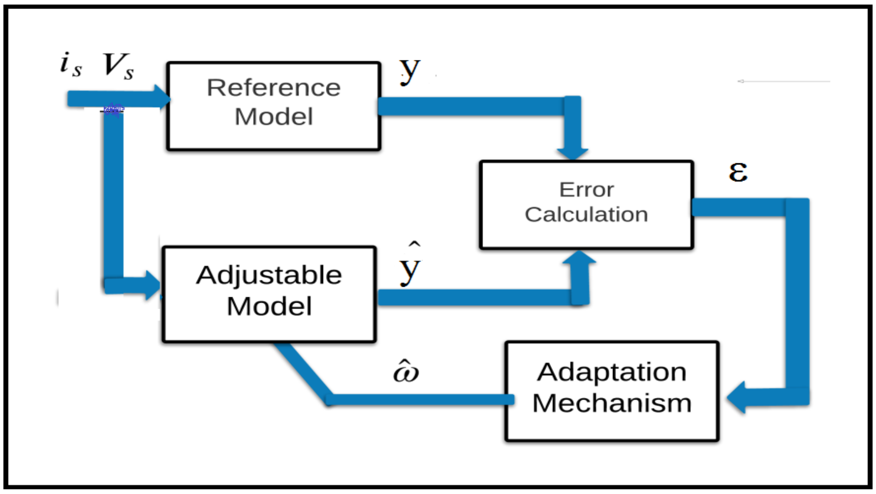

Figure (I.11): Schematic of speed estimation technique using MRAS

This system is adaptive, meaning that it modifies the control parameters based on the situation, using the "Adjustable Model" block shown in the previous figure, its model expressed in the following structure:

$$\begin{cases} \dot{\hat{X}} = \hat{A}\hat{X} + BU + \rho(y - \hat{y}) \\ \hat{y} = C\hat{X} \end{cases} \qquad \text{(I.04)}$$

A feedback control mechanism, typically a proportional-integral (PI) controller, is adequate to ensure the convergence of the adaptive model's dynamics to the reference model's dynamics.[54].The MRAS technique relies on the comparison of the outputs of two models that produce the same quantity using different methods. The output error of these models is used to drive an appropriate feedback control mechanism that generates the desired estimated quantity (usually the rotor speed). The MRAS-based speed estimator can be implemented in various forms, depending on the choice of the quantity for adaptation. Several MRAS structures have been proposed in the literature, such as MRAS based on rotor flux, back-EMF, reactive power, air-gap power, or artificial intelligence.

I.5.5.3. High-Frequency Injection Techniques

Most suggest several sensorless algorithms, including the machine model-based rotor angle estimator method. These methods provide dynamic performance similar to actual sensors but deteriorate as speed decreases due to inverter nonlinearity and variations in stator resistance.

At zero speed, the terminal stator voltage is zero, making these methods parameter sensitive and unable to operate at zero and low speeds. High-Frequency Injection method used mostly for MSAP drives to overcome the problem of sensorless control of electrical machines when stationary and at low speeds. HF signal injection methods are advantageous because they are independent of the rotation speed of the machine. These methods rely on saliency and use the anisotropic properties of the MSAP machine. The salience is mainly due to the geometry of the rotor, variations in the stator teeth, or saturation of the magnetic circuit. Since the inductance of the machine is a function of the rotor position due to salience, the rotor position can be deduced from the variation of this inductance[38].

Basically, the operating principle of these methods consists of injecting a high frequency signal (sinusoidal, rectangular, PWM signal, etc.) superimposed on the machine power signals. The signal recovered at the machine output contains information about the position of the rotor, provided that the machine presents salience ($L_d \neq L_q$)[39]. In this case, this signal is subjected to demodulation processing (using high-pass, pass-band, and low-pass filters) in order to extract the

The implementation of the method requires considering specific constraints when determining the amplitude and frequency of the high-frequency signal injected into the PMSM machine:

1-The signal frequency should not induce a skin effect on the machine winding and should steer clear of any interference with the frequency of PWM signals.

2-The signal frequency should be such that it does not induce a skin effect on the machine winding and avoids any interference with the frequency of PWM signals.

3-The signal's amplitude should prevent any rotor vibration when the machine is stationary. This implies that both the amplitude and frequency of the injected high-frequency signal should not induce the rotation or operation of the machine.

This method also can be implemented to the all-kinds of the frame (α-β) and (d-q), such as a sinusoidal or carrier signals or PWM however, the method used for d axis of (d-q) with carrier signal is the best choice car its simplicity and presents itself in its reduced calculation time, and its chain demodulation which does not require low pass filters. The principal of this method illustrated in the following figure (I.12).

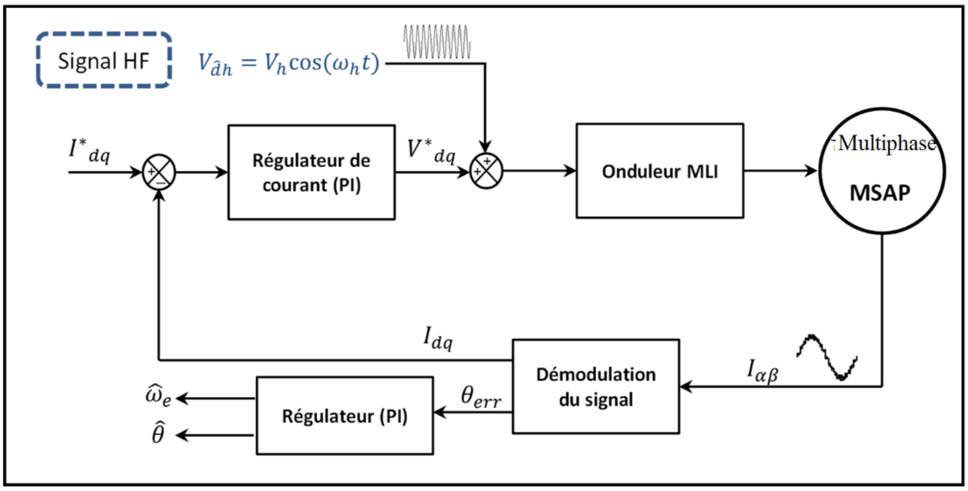

Figure (I.12): Principle of injecting sinusoidal signal at HF along the d-q axis

The techniques for introducing a high-frequency (HF) signal into the PMSM machine exhibit favourable attributes in terms of robustness and straightforward implementation. However, a critical aspect is the adjustment of filters within the demodulation chain processing the signal containing rotor information. This adjustment is delicate as the utilization of filters for demodulation introduces delays relative to the rotor system dynamics. Despite these merits, the primary drawbacks involve torque ripples and potential acoustic noise generated by the injected HF signal in the PMSM machine[40].

I.6. Estimation Algorithms for Sensorless Control

Several techniques are utilized in estimation algorithms for sensorless control, the majority of them to determine the position and speed of rotors in electric motors and others for the estimation of machine parameters.

I.6.1. Estimation of Rotor Position and Speed

Various techniques are employed to ascertain the position and speed of rotors in electric motors. These methods commonly integrate interpolation, filtering, and observers as fundamental components .A notable approach involves incorporating a pure integrator, a critical element that, despite its importance, may introduce inaccuracies in speed and position due to the absence of self-feedback [55]. The proposed algorithms are designed to be both descriptive and easily implementable for self-sensing operations in permanent magnet synchronous machines (PMSM) [56]. Additionally, there is ongoing exploration into a method that presents the PMSM motor model in a hypothetical reference frame oriented along an estimated rotor position [57]. In specific scenarios, a gradient approach is applied, utilizing an initial flux condition analyser to calculate the incorrect initial integral value for rotor flux compensation, ensuring stability in estimation[58]. Another enhanced method directly computes rotational speed based on stator electromotive force (EMF), utilizing speed as a reference for position estimation.

I.6.2. Estimation of Machine Parameters

The estimation of machine parameters is a crucial aspect of understanding and optimizing the performance of electric machines. Various methods and techniques are employed for this purpose, aiming to determine the key parameters that define the behaviour of the machine. One such approach involves the use of analytical methods, as demonstrated in studies that present novel techniques for estimating parameters like the mean life of electric power equipment based on failure data[59]. Additionally, advanced techniques such as Genetic Algorithms (GA) are applied for parameter identification in the context of electric motor condition monitoring [60]. These methods play a vital role in enhancing the understanding of machine dynamics, facilitating the development of efficient control strategies, and ensuring the reliability and longevity of electric machines in diverse applications.

I.7. Challenges and Limitations of Sensorless Techniques of multiphase machines

Sensorless methodologies offer numerous benefits, these enhance system reliability by removing sensors including cost reduction, thereby reducing overall system cost and complexity. Also, improving system dependability and eliminating potential points of failure. Sensorless control can improve dynamic performance, providing faster response compared to sensor-based control systems, especially in high-performance scenarios. Additionally, sensorless methodologies provide greater flexibility in machine design and integration, as they are not reliant on specific sensor hardware, allowing for more adaptable and versatile system configurations.

With all these advantages, it faces several challenges that may slow down progress in this field, of which we will mention the following:

1. Sensitivity to Parameter Variations: is a critical consideration in the sensorless control of multiphase machines. Since sensorless control relies on accurate estimation of machine parameters, any variations in these parameters can significantly impact the performance and reliability of the control system.[61] Some key factors contributing to sensitivity to parameter variations in sensorless control of multiphase machines include:
    - ✓ The accuracy of the mathematical model used for sensorless control.
    - ✓ Variations in machine parameters, such as inductance, resistance, and mutual inductance.
    - ✓ Changes in operating conditions, such as load torque, speed, and temperature, can introduce variations in machine parameters.
    - ✓ The non-ideal behaviour of power electronic components, such as voltage and current sensors and semi-conductors switch.

- ✓ Environmental factors, including temperature variations, humidity, and mechanical stresses, can impact the electrical and magnetic properties of the machine, leading to variations in parameters.

2. Initial Position Estimation: Determining the initial position of the rotor in sensorless control of electric machines is a crucial aspect of achieving accurate and reliable operation especially at standstill or low speeds[62].Several common approaches are used to determine the initial rotor position in sensorless control as Back-EMF Estimation and High-Frequency Signal Injection.
3. Robustness to Noise and Disturbances: Sensorless techniques may be susceptible to noise and disturbances, which can affect the accuracy of the estimated variables. The presence of noise and disturbances in the electrical signals used for sensorless control, such as voltage and current measurements, can degrade the accuracy of rotor position and speed estimation. Several factors contribute to this challenge similar to the parameter's variations, electrical noise and mechanical and load disturbances can be effect of sensorless control estimation.
4. Computational Complexity: The computational complexity of algorithms such as in the mathematical model complexity or Estimation Algorithms, can impact their real-time performance, responsiveness, and suitability for embedded systems. Several factors contribute to the computational complexity challenge in sensorless control.

I.8. Emerging trends and advancements in multiphase sensorless control

The growing need for high-performance, efficient, and dependable motor control systems in applications like electric vehicles, industrial automation, and renewable energy systems is Propelling the development of emerging trends and advancements in multiphase sensorless control. Within this field, several noteworthy trends and advancements are taking place. Utilizing advanced signal processing algorithms, such as Kalman filters, extended Kalman filters, as mentioned in [18] and [20] , and model-based observers as MRAS and Luenberger observers are noted in [54][63][64] and[53], to estimate the rotor position and speed of multiphase motors without the need for additional sensors. Some of the notable trends and advancements in this field include:

1. High-Frequency Injection Methods: Development of high-frequency injection-based sensorless control methods, which involve injecting high-frequency signals into the motor windings to facilitate accurate estimation of rotor position and speed.
2. Machine Learning and AI: Integration of machine learning and artificial intelligence techniques for sensorless control, enabling adaptive and self-learning control strategies that can improve the accuracy and robustness of multiphase motor control systems, cited in the research [65].

3. Fault-Tolerant Sensorless Control: Advancements in fault-tolerant sensorless control algorithms that can detect and compensate for faults or variations in motor parameters, enhancing the reliability and safety of multiphase motor control systems detailed in [66].
4. Sensorless Control for High-Speed Applications: Research and development efforts focused on sensorless control techniques tailored for high-speed multiphase motor applications, such as aerospace propulsion systems and high-speed industrial machinery as mentioned in the paper[51].
5. Integration with Power Electronics: Integration of sensorless control techniques with advanced power electronic converters and modulation strategies to achieve optimal performance and efficiency in multiphase motor drive systems.

Accordingly, a simple modelling, choosing a Multiphase Synchronous Motor (MSAP) over an induction machine can offer several advantages. MSAPs are known for their high efficiency, improved power density, and better controllability compared to traditional induction machines. Additionally, MSAPs exhibit a wider constant power speed range, making them suitable for applications requiring variable speed operation. Furthermore, MSAPs are inherently more fault-tolerant and have a simpler mechanical structure, leading to reduced maintenance requirements and increased reliability. These factors make MSAPs an attractive choice for applications such as electric vehicles, industrial machinery, and renewable energy systems where high efficiency[67], precise control, and reliability are paramount. From this standpoint, we will discuss in this research the study of the five-phase PMSM controlled in the presence of an observer.

I.9. Conclusion

This comprehensive review in this chapter discussed multiphase machines, whether synchronous or asynchronous, and their features and benefits, especially in modern industrial fields. As well as sensorless control methods and Multiphase drives control has been detailed, also the commonly used observers and state estimators has touched, especially for speed range and parameters variation. This led to provide us with the advantages of multiphase machines sensorless control. On the other hand, the majority of research in this field now deals with MSAP machines, typically exhibit higher efficiency due to reduced losses and improved utilization of magnetic materials. They also offer a higher power factor, which can lead to improved overall system efficiency and reduced reactive power requirements. Additionally, MSAP machines can provide better controllability, allowing for more precise torque and speed control, making them suitable for a wider range of applications. Overall, these advantages make multiphase MSAP machines an attractive choice for high-performance and energy-efficient industrial and automotive systems.

Therefore, we will discuss this type through a study conducted on the five-phase permanent magnet synchronous motor in the next chapter.

Chapter II.

Modeling of Five Phase Permanent

Magnet Synchronous Motor

II.1. Introduction

The increasing adoption of permanent magnet motors (PMSMs) in recent years is driven by their numerous benefits, including high efficiency, increased torque density, and enhanced controllability. These motors are widely used in electric vehicles, industrial automation, and renewable energy systems [67]. A thorough understanding of the description and modeling of PMSMs is essential for conducting a comprehensive performance analysis. The 5Ø-PMSM has garnered significant attention due to its advantages over traditional three-phase motors. To comprehend and evaluate the performance of these motors, it is essential to have a thorough understanding of their description and modeling. This chapter aims to provide a comprehensive overview of 5Ø-PMSM models, each with unique characteristics and applications. Furthermore, the associated with electronic converter plays a vital role in driving and controlling the 5Ø-PMSM. Therefore, this chapter will also delve into the modeling and control aspects of the converter, emphasizing its interaction with the motor and the overall system performance. Also, this chapter will present a simulation of the machine associated with inverter, the results extracted using MATLAB will be presented under different operate conditions.

II.2. Overview of Five Phase Permanent Magnet Synchronous Motor

The history of innovation in Five-Phase Permanent Magnet Synchronous Motors (5Ø-PMSMs) spans several decades, beginning with the development of three-phase induction motors in 1891. Progressing through early concepts and explorations in the late 20th century [68], the roots of 5Ø-PMSM innovation can be traced to the investigation of multiphase motor configurations. Early prototypes and simulations highlighted the advantages of these configurations over traditional three-phase systems. Researchers recognized the potential benefits of additional phases, such as improved torque density, reduced torque ripple, and enhanced fault tolerance. Between 2000 and 2010 [69], advancements in power electronics and computational tools enabled the practical realization of 5Ø-PMSMs. Inverters were developed to support various applications, including industrial automation, electric vehicles, and renewable energy systems. In recent years, research efforts have focused on optimizing machine design. The advent of advanced software, such as those associated with Industry 4.0 and digitalization, has introduced a new dimension to 5Ø-PMSM innovation.

II.3. Description of Five Phase Permanent Magnet Synchronous Motor

The five-phase permanent-magnet synchronous motor is a multi-phase electric motor composed like other types of motors, the fixed part is the stator which contains five sets of stator windings arranged around the stator core, these windings are carefully wound with insulated copper wire to ensure precise coil geometry and optimal electrical performance.

The stator windings are responsible for generating the rotating magnetic field, each phase is shifted from $\left(2\pi/5\right)$ with its previous phase, Moreover, the 5Ø-PMSM features a rotor that revolves within the stator, separated from it by an air gap. The rotor houses permanent magnets, specially designed to form the rotor poles. In the 5Ø-PMSM, permanent magnets made of **samarium-cobalt**, **medium**, **iron**, and **boron** are used for their higher permeability. However, the most widely used permanent magnet is **neodymium-iron-boron** due to its cost-effectiveness and availability[70], furthermore, the selection of the appropriate magnet is very important because that generates the magnetic field essential for motor operation.

II.4. Operating Principle of Five Phase Permanent Magnet Synchronous Motor

The 5Ø-PMSM is a type of synchronous motor that uses permanent magnets to create a rotating magnetic field, similar to the operation of three-phase synchronous motors. The motor's stator contains five-phase windings, spatially displaced by ($2\pi/5$) radians between two successive angles. These windings are arranged in a specific pattern to generate a magnetic field when five sinusoidal currents are applied to the stator windings. The magnetic field rotates at the supply frequency, meaning the electrical speed is equal to the synchronous speed [71]. According to Lorenz's law, electromagnetic forces are generated in the rotor. Permanent magnets inside the rotor produce their own magnetic field, forming magnetic poles. These poles are designed to be opposite to each other, creating the movement of the rotor at the same speed and frequency as the rotating field a motion known as synchronous motion which produces driving torque. This synchronization allows permanent magnets to generate a substantial air gap magnetic flux, enabling the design of highly efficient machines. These machines are valuable across various domains, from industrial applications to everyday life.

The following Figure (II.1) illustrates the interaction between the stator's magnetic field and the rotor's permanent magnet. In Figure (II.1a), current ‘ia’ flows through phase ‘a`, while phase ‘b’ carries no current. This generates a magnetic field along the axis of phase ‘a`. Subsequently, in Figure (II.1b), currents ‘ia’ and ‘ib’ flow through phases ‘a` and ‘b’, respectively, creating a combined magnetic field diagonally oriented between the two phases. In the configuration shown in Figure (II.1c), current ib flows through phase ‘b’, while phase ‘a` carries no current, indicating the beta phase. This shifts the magnetic field to align along the axis of phase ‘b’.

The sequence of current changes in the stator windings produces a rotating magnetic field, which interacts with the constant magnetic field of the rotor's permanent magnets. This interaction causes the rotor to turn synchronously with the rotating field, thereby converting electrical energy into mechanical motion

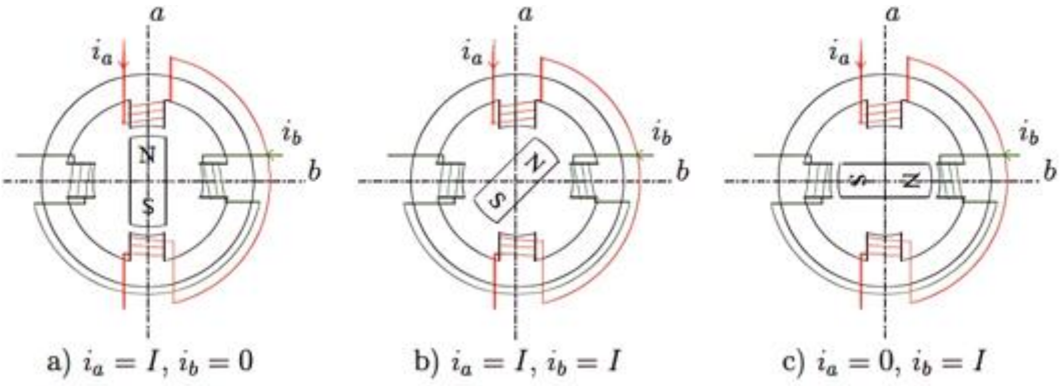

Figure (II.1): Principal of permanent magnet synchronous motor operating

II.5. Five Phase Permanent Magnet Synchronous Motor configuration

The 5Φ-PMSM configuration refers to a specific arrangement of Permanent Magnet Synchronous Motors (PMSM). There are several methods for configuring this machine such as:

II.5.1. Stator configuration

Several methods of connecting the stator windings in a 5Ø-PMSM provide varying electrical characteristics and operational advantages. Each method determines how the individual phase windings are interconnected to form the motor's electrical configuration. Below are the two most widely used methods, offering simplicity in inverter connections and supporting different control strategies for 5Ø-PMSM:

II.5.1.1. Star(Y) connection

The starting point of each phase winding in a star connection is connected to a common point, known as the star point or neutral point.as shown in Figure (II.2a), this kind of connection offers more advantages such as balanced voltage across each phase, making it suitable for applications with balanced loads. And it has a reduced line voltage that may be advantageous for certain voltage limitations requiring higher current levels in each winding, also it improves the fault tolerance, and if one phase winding fails the motor can continue operating with reduced performance[33].

II.5.1.2. Pentagon connection

In a pentagon connection which presented in figure (II,2b), each phase winding is connected in series with another phase winding, they form a closed-loop shape resembling a pentagon. This connection presents more benefits as it offers higher power density and torque output compared to a star connection. Moreover, the current through each phase winding in a pentagon connection is balanced, contributing to better load distribution, also this connection can lead to higher efficiency due to reduced winding currents. However, its line voltage is higher than in a star connection, which can impact certain applications and systems, and may lead to complete motor shutdown in case of a phase winding failure[67].

Consequently, the choice between star and pentagon connections for stator windings in a 5Ø-PMSM depends on the specific application requirements, load characteristics, and desired performance. The selection influences factors such as voltage distribution, current levels, and fault tolerance, all of which play a pivotal role in the motor's overall functionality and efficiency. The next figure (II.2) represents the stator winding configuration shown below:

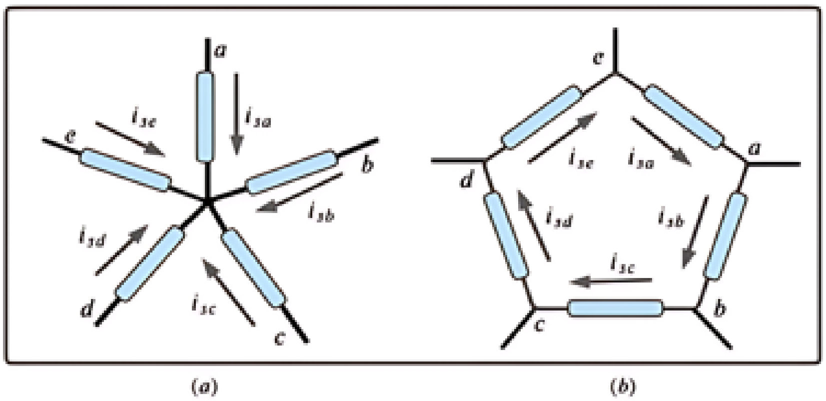

Figure (II.2): Different stator winding configurations (a) star and (b) pentagon

II.5.2. Rotor of Five Phase Permanent Magnet Synchronous Motor configuration

The rotor of a 5Ø-PMSM consists of permanent magnets made from ferromagnetic materials, which alternate between north and south poles. Various methods of configuring the rotor in a 5Ø-PMSM provide distinct advantages and influence the motor's performance and efficiency.

The rotor configuration directly affects how the permanent magnets interact with the stator's magnetic field to generate motion. Here are some commonly the used mounted methods:

II.5.2.1. Surface-Mounted Magnets

Permanent magnets are affixed to the surface of the rotor, facing outward, as shown in figure (II. 3A). This configuration provides easy access to the magnets for maintenance or replacement, also it allows for a high level of magnetic flux linkage between the rotor and stator, hence it provides big advantages of High magnetic flux density and enhanced cooling, this position increases aerodynamic drag, especially in high-speed applications.

II.5.2.2. Embedded Magnet Arrangement

As shown in figure (II.3B) the Magnets are arranged within a specific pattern, such as radial, skewed, or sinusoidal. This method aims to enhance efficiency and smoother operation due to improving the harmonics suppression with sinusoidal arrangement or reducing the cogging and torque ripple with skewed arrangement, but this method Complex manufacturing and assembly processes.

II.5.2.3. Interior-Mounted Magnets

In this case, the permanent magnets are embedded within slots or cavities in the rotor core, which covers the magnets, offering protection and streamlining the outer surface of the rotor, and reducing aerodynamic drag due to the smoother outer surface. However, this arrangement reduces the cooling efficiency of the permanent magnet. The following figure (II.3C) illustrates this method [72].

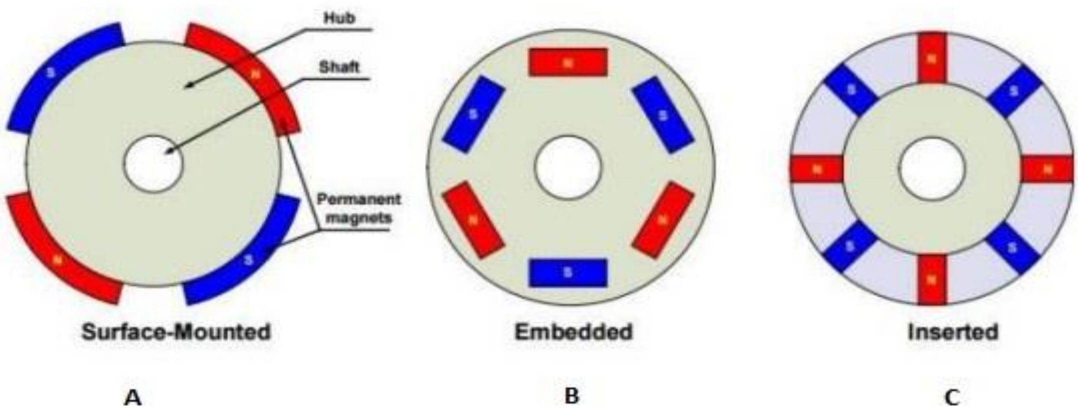

Figure (II.3): Different structure of 5Ø-PMSM rotor

Also, (5Ø-PMSMs) can be classified based on the rotor and magnet pole positions, as well as depending on the dimensions and arrangement of the permanent magnets. They are divided into two types: smooth or salient poles. In the case of surface-mounted magnets (Type A), where the magnet is glued to the surface with smooth poles, the quadrature axis inductance is equal to the direct axis inductance (L_q=L_d). In contrast, for the second type with salient poles, these inductances are not equal.

II.6. Caracteristques of 5Ø-PMSMs

II.6.1. Advantages of 5Ø-PMSMs

- **Higher Torque Density:** 5Ø-PMSMs offer higher torque output compared to traditional three-phase motors, making them ideal for applications where compact size and high torque are essential. [73].

- **Smooth Torque Generation:** The multiphase configuration of 5Ø-PMSMs results in smoother torque production, reducing torque ripple and improving overall system stability.

- **Enhanced Power Output:** Due to the additional phase windings, 5Ø-PMSMs can deliver higher power outputs, making them suitable for applications requiring high power density.

- **Efficiency:** The advanced control strategies and optimized winding configurations of 5Ø-PMSMs contribute to high efficiency, leading to energy savings and reduced operating costs.

- **Flexibility in Control:** The extra phases enable finer control of torque and speed, allowing for better precision and adaptability to varying load conditions[32].
- **Fault Tolerance:** The multi-phase design provides inherent fault tolerance, allowing the motor to continue functioning even if one phase is compromised.
- **Reduced Cogging:** Innovative rotor designs and magnet arrangements can significantly reduce cogging effects, resulting in smoother operation and improved motion quality.
- **Variable Speed Operation:** 5Ø-PMSMs can operate over a wide range of speeds, offering flexibility in applications that require variable speeds.
- **Wide Application Range:** These motors find applications in various fields, including robotics, electric vehicles, industrial automation, and renewable energy systems[48].

II.6.2. Disadvantages of 5Ø-PMSMs

- **Complex Control Algorithms:** The control algorithms for 5Ø-PMSMs are more intricate than those for three-phase motors, requiring advanced knowledge and expertise for implementation[74].
- **Higher Manufacturing Costs:** The design complexity and additional phase windings can lead to higher manufacturing costs compared to traditional three-phase motors.
- **Limited Availability**: 5Ø-PMSMs may have limited availability compared to their three-phase counterparts, making them less accessible in certain markets.
- **Control Complexity:** While the extra phases offer control flexibility, they can also make the control system more complex, potentially requiring specialized hardware and software[74][75].
- **Maintenance and Repairs:** In the case of maintenance or repairs, the multi-phase design might lead to more involved procedures compared to simpler motor configurations.
- **Learning Curve:** Engineers and technicians who are familiar with three-phase systems may need to learn new concepts and techniques when working with 5Ø-PMSMs.
- **Integration Challenges:** Integrating these machines into existing systems may require modifications and adaptations, adding complexity to the integration process.
- **Specific Applications:** While versatile, 5Ø-PMSMs may be more suited to specific applications that benefit from their unique characteristics, limiting their use in some scenarios.

II.7. Modeling of Five Phase Permanent Magnet Synchronous Motor

The modeling of a Five-Phase Permanent Magnet Synchronous Motor (5Ø-PMSM) is a pivotal methodology that plays a crucial role in understanding, analysing, and optimizing the performance characteristics and behaviour of the motor. It helps to create an accurate virtual representation of the motor, capturing its electrical, magnetic, and mechanical interactions. This involves formulating mathematical equations that describe the motor's dynamics, considering factors such as electromagnetic fields, torque generation, and control responses[70].

The inherent complexity of multiphase systems, including 5Ø-PMSMs, can make detailed modeling ungainly and computationally intensive. To avoid this drawback, several simplifications have been proposed to help manage this complexity and facilitate a more tractable analysis.

II.7.1. Simplified assumption

Simplifying the mathematical model of Five-Phase Permanent Magnet Synchronous Motor involves making certain assumptions and applying principal conditions. The magnetic circuit refers to the path of magnetic flux created by the permanent magnets in the rotor[76]. Here are the principal conditions commonly used to simplify the mathematical model:

1. Linear Magnetic Characteristics: The first principal condition assumes that the magnetic characteristics of the permanent magnets are linear within the operating range. This allows us to model the magnets' behaviour using a linear relationship between magnetic flux and magneto motive force (MMF).

2. Uniform Air Gap: It is assumed that the air gap between the rotor and stator is uniform, resulting in a constant air gap length. This simplification eliminates variations in magnetic flux density due to non-uniformity in the air gap.

3. No Magnetic Saturation: The model assumes that the magnetic materials in the motor, such as the stator and rotor cores, do not exhibit magnetic saturation. This simplifies the calculation of magnetic flux density and reduces the complexity of the model.

4. Negligible Iron Losses: Iron losses, including hysteresis and eddy current losses, are assumed to be negligible. While these losses can affect motor performance, neglecting them simplifies the model without significantly compromising accuracy.

5. No Leakage Flux: Leakage flux, which occurs when magnetic flux does not pass through the desired path, is disregarded in the simplified model. This assumption assumes that most of the magnetic flux follows the intended path.

6. Negligible Radial Magnetic Flux: It is assumed that the radial magnetic flux, which flows along the radial direction of the motor, is negligible compared to the axial magnetic flux.

This simplification reduces the complexity of the model while retaining sufficient accuracy for many applications.

By applying these principal conditions, the mathematical model of the magnet circuit in the 5Φ-PMSM can be simplified, making it more tractable for analysis, control design, and optimization. However, it is important to note that these assumptions may not hold in all operating conditions, and more complex models may be necessary for highly accurate simulations or specialized applications

II.7.2. Mathematical model of the 5Ø-PMSM in natural frame

Modelling a Five-Phase Permanent Magnet Synchronous Motor in its original frame involves developing equations that describe the motor's behaviour using the inherent properties of its phases and components. The following equations, which are expressed in terms of space vectors describe the dynamic behaviour of 5Ø-PMSM in (a,b,c,d,e) frame.

II.7.2.1. Voltages equations

As known a 5Ø-PMSM has a permanent magnet in its rotor which can be noted as a constant flux value, While the stator contains a windings coil, its voltage equations describe the electrical behaviour can be expressed according to Faraday’s law as follows[73]:

$$[V_s]=[R_s][I_s]+\frac{d[\phi_s]}{dt} \qquad \text{(II.01)}$$

The following definitions represent the voltages, the currents, and the flux linkages used in the previous equation:

$$[V_s]=\begin{pmatrix} V_a \\ V_b \\ V_c \\ V_d \\ V_e \end{pmatrix};[I_s]=\begin{pmatrix} I_a \\ I_b \\ I_c \\ I_d \\ I_e \end{pmatrix} and\, [\varphi_s]=\begin{pmatrix} \varphi_a \\ \varphi_b \\ \varphi_c \\ \varphi_d \\ \varphi_e \end{pmatrix} \qquad \text{(II.02)}$$

The notifications (Abcde): designed to the stator phase indices, and [R_s] is the stator resistance matrix with considering of the 5Ø -PMSM is a perfect symmetrical machine, so: $R_a=R_b=R_c=R_d=R_e=R_s$, such as the stator resistance matrix was written by:

$$[R_s]=\begin{bmatrix} R_s & 0 & 0 & 0 & 0 \\ 0 & R_s & 0 & 0 & 0 \\ 0 & 0 & R_s & 0 & 0 \\ 0 & 0 & 0 & R_s & 0 \\ 0 & 0 & 0 & 0 & R_s \end{bmatrix} \qquad \text{(II.03)}$$

II.7.2.2. Flux linkage equations

The total flux linkages in the air gap generated by stator inductances and the combined magnetic flux generated by the permanent magnets passing through the stator windings[70], which can be defined by the following expression:

$$[\varphi_s]=[\varphi_{ss}]+[\varphi_m]=[L_s][I_s]+[\varphi_m] \qquad \text{(II.04)}$$

Where:

$[\varphi_m]$: Matrix Vector of the flux created by the permanent magnets through the stator windings can be expressed it as:

$$[\varphi_m]=|\varphi_m|\begin{bmatrix}\cos(\theta)\\ \cos(\theta-2\pi/5)\\ \cos(\theta-4\pi/5)\\ \cos(\theta-6\pi/5)\\ \cos(\theta-8\pi/5)\end{bmatrix} \qquad \text{(II.05)}$$

And θ is the electrical angle of the rotor, $|\varphi_m|$ is the flux amplitude of permanent magnet.

$[L_s]$:is the total stator inductance matrix involving the proper and mutual matrix of its windings, then can be written it as:

$$[L_s]=[L_{s0}]+[L_{s1}] \qquad \text{(II.06)}$$

With:

$[L_{s0}]$: is the proper inductances matrix of stator windings, and:

$[L_{s1}]$: The mutual inductances matrix of stator windings.

From (2) in the simplified hypotheses, where the air gap has a fixed width, that assumes to accept the constant value of proper and mutual inductances, which also are independent of rotor position, it can be write:

$$[L_{s0}]=\begin{bmatrix}L_s&0&0&0&0\\0&L_s&0&0&0\\0&0&L_s&0&0\\0&0&0&L_s&0\\0&0&0&0&L_s\end{bmatrix} \qquad \text{(II.07)}$$

The mutual inductances matrix of stator windings is computed as:

$$\left[L_{s1}\right]=L_m\begin{bmatrix} 1 & \cos(2\pi/5) & \cos(4\pi/5) & \cos(6\pi/5) & \cos(8\pi/5) \\ \cos(8\pi/5) & 1 & \cos(2\pi/5) & \cos(4\pi/5) & \cos(6\pi/5) \\ \cos(6\pi/5) & \cos(8\pi/5) & 1 & \cos(2\pi/5) & \cos(4\pi/5) \\ \cos(4\pi/5) & \cos(6\pi/5) & \cos(8\pi/5) & 1 & \cos(2\pi/5) \\ \cos(2\pi/5) & \cos(4\pi/5) & \cos(6\pi/5) & \cos(8\pi/5) & 1 \end{bmatrix} \qquad \text{(II.08)}$$

Where L_m: is the main stator inductance and L_S its linkage inductance.

II.7.2.3. Mechanical equations of 5P-PMSM

The mechanical model of a Five-Phase Permanent Magnet Synchronous Motor describes the motor's rotational dynamics and its interaction with external loads. This model provides insights into how the motor's electromagnetic behaviour translates into mechanical motion[67]. The fundamental equation of the mechanical model is based on Newton's second law of motion expressed as follow:

$$J\frac{d\Omega}{dt}=T_{em}-T_L-F\Omega \qquad \text{(II.09)}$$

Where:

J : is inertia moment of the motor and load combined.

F : is the friction coefficient

T_{em} : is the net torque generated by the electromagnetic interaction of the motor's phases.

T_L : is the external load torque acting on the motor.

Ω : is the rotor speed, as well can be write $\Omega.P=w$, with w is the electrical speed, and P is pair of pol number.

II.7.2.4. Electromagnetic torque of the 5Ø-PMSM

Generally, the electromagnetic torque delivered by the 5Ø-PMSM obtained from the derivative of the mechanical energy to the electrical position of the rotor, is given by the following expression:

$$T_{em}=\frac{dW}{d\theta_r}=\frac{P}{2}\left[I_s\right]^T\left[\frac{d\left[L_s\right]}{d\theta}\right]\left[I_s\right] \qquad \text{(II.10)}$$

Where:

W:is the mechanical energy delivered by rotor, and $\left[I_s\right]^T$ is the transposed matrix of stator current.

II.7.3. Nonlinear model of 5Ø-PMSM

The model of (5Ø -PMSM) in original frame depend of the rotor position which depend of the time too, this coupling makes a nonlinearity of model, from equations (II.01),(II.03), and (II.06), can be rewritten the electrical equation as the following form:

$$[V_s]=[R_s][I_s]+\frac{d\left[[L_{s0}]+[L_{s1}]\right]}{dt}[I_s]+\frac{d}{dt}[\varphi_m] \qquad \text{(II .11)}$$

The mutual inductances between the stator and rotor windings depend on the rotor position, making the voltage equations depend on the time. This makes the model unsuitable for numerical simulation and control. To eliminate the varying time of coefficients, the stator and rotor equations can be referred to as a common frame using the vector space decomposition technique. It leads to relations independent of the angle θ and to a reduction of the order of the machine equations. The transformation best known by electrical technicians is that of Park and Clark.

II.7.4. Park and Clark transformation

The Park`s transformation also known as the d-q transformation, is a mathematical technique used to simplify the analysis and control of electrical machines, like the Five-Phase Permanent Magnet Synchronous Motor (5Ø -PMSM),this transformation consist of change the referential frame from real five-phase reference into a fictitious two-phase reference has a perpendicular axes, consequently the representation of own variables(voltage, current and flux) of stator and rotor in new reference independent of the angle θ removing time-varying variables[77], and simplify the differential equations characterizing the behaviour of the motor, the proposed park`s transformation matrix applied to 5Ø-PMSM described as follow:

$$[T(\theta_{co})]=K\begin{bmatrix} \cos\theta_{co} & \cos(\theta_{co}-\frac{2\pi}{5}) & \cos(\theta_{co}-\frac{4\pi}{5}) & \cos(\theta_{co}+\frac{4\pi}{5}) & \cos(\theta_{co}+\frac{2\pi}{5}) \\ \sin\theta_{co} & \sin(\theta_{co}-\frac{2\pi}{5}) & \sin(\theta_{co}-\frac{4\pi}{5}) & \sin(\theta_{co}+\frac{4\pi}{5}) & \sin(\theta_{co}+\frac{2\pi}{5}) \\ \cos\theta_{co} & \cos(\theta_{co}+\frac{4\pi}{5}) & \cos(\theta_{co}-\frac{2\pi}{5}) & \cos(\theta_{co}+\frac{2\pi}{5}) & \cos(\theta_{co}-\frac{4\pi}{5}) \\ \sin\theta_{co} & \sin(\theta_{co}+\frac{4\pi}{5}) & \sin(\theta_{co}-\frac{2\pi}{5}) & \sin(\theta_{co}+\frac{2\pi}{5}) & \sin(\theta_{co}-\frac{4\pi}{5}) \\ \frac{1}{2} & \frac{1}{2} & \frac{1}{2} & \frac{1}{2} & \frac{1}{2} \end{bmatrix} \qquad \text{(II.12)}$$

Where θ_{co} is the angle between the a-axis of referential frame and the d1-axis of the arbitrary frame, and K is a constant factor depend of the power transformation from the original frame to the new reference frame, such as K has two values:

- $K = \frac{2}{5}$: For the transformation preserving of amplitude.
- $K = \sqrt{\frac{2}{5}}$: For the transformation preserving the power.

Through Park's transformation, which is related to the angle coordinate, there are three important choices the new reference frame can be setting, depending on the position is the orientation speed. It is as follows:

II.7.5. Stator reference frame

Also is called also stationary reference frame and its indices $(\alpha \quad \beta)$, this system of axes is immobile relative to the stator, where $\theta_{co} = 0 \Rightarrow w_{co} = 0$.

The voltage in this system varies as a function of time in sinusoidal magnitudes, which can be represented by the following method:

$$\left[X_{\alpha 1 \beta 1 \alpha 2 \beta 2}\right] = \left[T\left(\theta_{co} = 0\right)\right]\left[X_{abcde}\right] \qquad \text{(II.13)}$$

The inverse Park transform is compatible to return to five-phase variables, it is defined by:

$$\left[X_{abcde}\right] = \left[T\left(\theta_{co} = 0\right)\right]^{-1}\left[X_{\alpha 1 \beta 1 \alpha 2 \beta 2}\right] \qquad \text{(II.14)}$$

II.7.6. Rotor reference frame

This system of axes is attached to the rotor and rotates at its electrical speed, corresponding to its indices (d q). where $w_{co} = w$ *and* $\theta_{co} = \theta$ .Also the system is used to study the transient processes in the machine therefore is suitable from the control. The representation of variables of machine are extracted by:

$$\begin{cases} \left[X_{d1q1d2q2}\right] = \left[T\left(\theta_{co} = \theta\right)\right]\left[X_{abcde}\right] \\ \left[X_{abcde}\right] = \left[T\left(\theta_{co} = \theta\right)\right]^{-1}\left[X_{d1q1d2q2}\right] \end{cases} \qquad \text{(II.15)}$$

II.7.7. Synchronous reference frame

It symbolizes par (U V), this system is rotated with the speed of the electromagnetic field, created by the stator windings, where the coordinate speed of this reference is the synchronous speed $w_{co} = w_s \Rightarrow \theta_{co} = \theta_s$.

Figure (II.4) illustrates the schematic representation of different reference frames of 5P-PMSM, these three references frames mentioned, most researchers in the control machine field used in their literature, either the stator reference frame (α_1,β_1, α_2,β_2)or rotor reference frame (d_1,q_1,d_2,q_2), which we will list below considering that the machines have smooth poles.

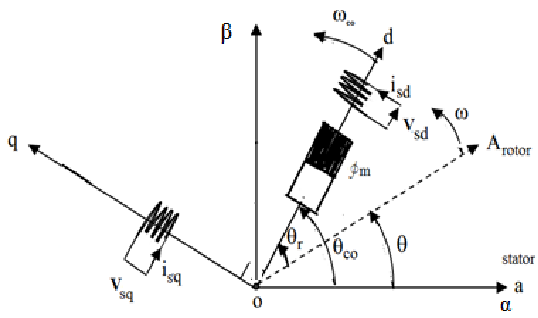

Figure (II.4): Different references frames of representation the5Ø-PMSM

II.8. Dynamic model of 5Ø-PMSM (in a stationary frame (α, β))

The choice of this reference frame is appropriate to apply for the application of observation techniques, this modeling of 5Ø-PMSM expressed in a stationary frame (α_1,β_1,α_2,β_2) can be determined from the mathematical model of natural frame[78], transformed by Park's matrix for (θ_{co} = 0), or from the transformation of dynamic model variables, voltage, courant and flux expressed in (d1,q1,d2,q2) multiplied of a transformation matrix such as:

$$\left[X_{d1q1d2q2}\right]=\left[T\left(\theta\right)\right]^{-1}\left[X_{\alpha1\beta1\alpha2\beta2}\right] \qquad \text{(II.15)}$$

Where the matrix [T]expressed in following form:

$$T(\theta)=\begin{bmatrix} \cos(\theta) & \sin(\theta) & 0 & 0 \\ -\sin(\theta) & \cos(\theta) & 0 & 0 \\ 0 & 0 & 1 & 0 \\ 0 & 0 & 0 & 1 \end{bmatrix} \qquad \text{(II.16)}$$

The final dynamic model of 5Ø-PMSM in (α1,β1,α2,β2) frame written as follow:

$$\begin{cases} V_{\alpha1}=R_s I_{\alpha1}+L_{\alpha1}\dfrac{dI_{\alpha1}}{dt}-w\,\varphi_m \sin\theta \\ V_{\beta1}=R_s I_{\beta1}+L_{\beta1}\dfrac{dI_{\beta1}}{dt}+w\,\varphi_m \cos\theta \\ V_{\alpha2}=R_s I_{\alpha2}+L_l\dfrac{dI_{\alpha2}}{dt} \\ V_{\beta2}=R_s I_{\beta2}+L_l\dfrac{dI_{\beta2}}{dt} \\ J\dfrac{d\Omega}{dt}=T_{em}-T_L-F\Omega \\ T_{em}=\dfrac{5}{2}P\varphi_m(I_{\beta1}\cos\theta-I_{\alpha1}\sin\theta) \end{cases} \qquad \text{(II.17)}$$

II.9. Dynamic model of 5Ø-PMSM in rotating frame (d-q)

The choice of this reference frame is preferable to using for the application of machine control techniques, the representation of the 5Ø-PMSM in (d1,q1,d2,q2) frame extracted from the multiplication between stator voltage equations (II.01) with Park's transformation matrix (II.10), which is turned by the electrical speed w_{co}=w, gives the model in the following form:

II.9.1. Electrical equation

$$\begin{cases} V_{d1} = R_s I_{d1} + \dfrac{d\varphi_{d1}}{dt} - w\varphi_{q1} \\ V_{q1} = R_s I_{q1} + \dfrac{d\varphi_{q1}}{dt} + w\varphi_{d1} \\ V_{d2} = R_s I_{d2} + \dfrac{d\varphi_{d2}}{dt} \\ V_{q2} = R_s I_{q2} + \dfrac{d\varphi_{q2}}{dt} \\ V_0 = R_s I_0 + \dfrac{d\varphi_0}{dt} \end{cases} \qquad \text{(II.18)}$$

Where the fifth row of the previous equation (II.18) represents the zero-sequence component that can be removed.

II.9.2. Flux linkage equation

For representation of stator flux linkage by using the projection of its component in (d1,q1,d2,q2) frame, only direct coordinate exists, with this consideration, the flux linkage equations can be expressed as follows:

$$\begin{cases} \varphi_{d1} = L_d I_{d1} + \varphi_m \\ \varphi_{q1} = L_q I_{q1} \\ \varphi_{d2} = L_l I_{d2} \\ \varphi_{q2} = L_l I_{q2} \end{cases} \qquad \text{(II.19)}$$

With:

L_l :is the inductance of secondary frame (d_2,q_2).

II.9.3. Mechanical Equation

The mechanical equation of 5Ø-PMSM is mentioned in (II.09) which defined by Newton law's, It is the same expression, except for the expression of the electromagnetic torque in the (d1,q1,d2,q2) frame is modified as given in the following equation:

$$T_{em} = \frac{5}{2} P(\varphi_{d1} I_{q1} - \varphi_{q1} I_{d1}) \qquad \text{(II.20)}$$

By setting equation (2.13) in (2.14) can be write the mechanical equation as follow:

$$\begin{cases} J\dfrac{d\Omega}{dt} = T_{em} - T_L - F\Omega \\ T_{em} = \dfrac{5}{2}P(\varphi_m I_{q1} + (L_d - L_q)I_{q1}I_{d1}) \end{cases} \tag{II.21}$$

The final dynamic model of 5Ø-PMSM in (d1,q1,d2,q2) frame defined by the combination of the stator voltage and current equations, flux and mechanical equation, as follow:

$$\begin{cases} V_{d1} = R_s I_{d1} + L_{d1}\dfrac{dI_{d1}}{dt} + wL_{q1}I_{q1} \\ V_{q1} = R_s I_{q1} + L_{q1}\dfrac{dI_{q1}}{dt} + wL_{d1}I_{d1} + w\varphi_m \\ V_{d2} = R_s I_{d2} + L_{d2}\dfrac{dI_{d2}}{dt} \\ V_{q2} = R_s I_{q2} + L_{q2}\dfrac{dI_{q2}}{dt} \\ J\dfrac{d\Omega}{dt} = T_{em} - T_L - F\Omega \\ T_{em} = \dfrac{5}{2}P(\varphi_m I_{q1} + (L_{d1} - L_{q1})I_{q1}I_{d1}) \end{cases} \tag{II.22}$$

II.10. The state space model of a (5Ø-PMSM)

Representing the machine model in state space simplifies the system by organizing it into a form with a controllable component, particularly focusing on torque, position, or machine speed. Considering that the pole of the machine is smoother, then Lq1=Ld1, this model is represented in the following form [13]:

$$\begin{cases} \dfrac{dX}{dt} = [A]X + [B]U + [E]D \\ Y = [C]X \end{cases} \tag{II.23}$$

Where: X represent the state vector of the system, Y is the output vector, U indicate the control vector, and D is the disturbance input of system, [A] is the system (or state) matrix, [B] is the input matrix, [C] represent the output matrix, and [E] represent the disturbance input matrix.

Consequently, the equation (II.22) can be rewritten as follows:

$$\begin{cases} \dfrac{dI_{d1}}{dt} = \dfrac{1}{L_{d1}}V_{d1} - \dfrac{R_s}{L_{d1}}I_{d1} + P\Omega\dfrac{L_{q1}}{L_{d1}}I_{q1} \\ \dfrac{dI_{q1}}{dt} = \dfrac{1}{L_{q1}}V_{q1} - \dfrac{R_s}{L_{q1}}I_{q1} - P\Omega\dfrac{L_{d1}}{L_{q1}}I_{d1} - P\Omega\dfrac{\varphi_m}{L_{q1}} \\ \dfrac{dI_{d2}}{dt} = \dfrac{1}{L_{d2}}V_{d2} - \dfrac{R_s}{L_{d2}}I_{d2} \\ \dfrac{dI_{q2}}{dt} = \dfrac{1}{L_{q2}}V_{q2} - \dfrac{R_s}{L_{q2}}I_{q2} \\ \dfrac{d\Omega}{dt} = \dfrac{T_{em}}{J} - \dfrac{T_l}{J} - \dfrac{F}{J}\Omega \\ T_{em} = \dfrac{5}{2}P\varphi_m I_{q1} \end{cases} \tag{II.24}$$

The general form of state space model based on setting input-output model, which is depending of the state vector choices, the model of 5Ø-PMSM in the reference frame linked to the rotor the components of the inputs vector are the machine voltages $V_{d1q1d2q2}$, and the outputs vector are the stator currents $I_{d1q1d2q2}$.Though the model of state space of 5Ø-PMSM looks like in (II.24) detailed as follow:

$X = \begin{bmatrix} I_{d1} & I_{q1} & I_{d2} & I_{q2} & \Omega \end{bmatrix}^T$,$U = \begin{bmatrix} V_{d1} & V_{q1} & V_{d2} & V_{q2} \end{bmatrix}$,$D = \begin{bmatrix} 0 & 0 & 0 & 0 & T_l \end{bmatrix}$ and:

$$[A] = \begin{bmatrix} -\dfrac{R_s}{L_1} & \dfrac{P\Omega L_{q1}}{L_{di}} & 0 & 0 & 0 \\ \dfrac{-P\Omega L_{d1}}{L_1} & -\dfrac{R_s}{L_1} & 0 & 0 & \dfrac{P\varphi_m}{L_1} \\ 0 & 0 & -\dfrac{R_s}{L_2} & 0 & 0 \\ 0 & 0 & 0 & -\dfrac{R_s}{L_2} & 0 \\ 0 & \dfrac{5P\varphi_m}{2} & 0 & 0 & \dfrac{-F}{J} \end{bmatrix} \text{And,} [B] = \begin{bmatrix} \dfrac{1}{L_p} & 0 & 0 & 0 \\ 0 & \dfrac{1}{L_p} & 0 & 0 \\ 0 & 0 & \dfrac{1}{L_s} & 0 \\ 0 & 0 & 0 & \dfrac{1}{L_s} \\ 0 & 0 & 0 & 0 \end{bmatrix}, [E] = \begin{bmatrix} 0 \\ 0 \\ 0 \\ 0 \\ \dfrac{-F}{J} \end{bmatrix} \tag{II.25}$$

The output Y is selected component to control it as a torque, the output matrix in this case:

$$[C] = \begin{bmatrix} 0 & \dfrac{5P\varphi_m}{2} & 0 & 0 \end{bmatrix} \tag{II.26}$$

II.11. Mathematical model of 5Ø-PMSM considering harmonic subspace

The influence of the third order current harmonic cannot be overlooked in a five-phase permanent magnet synchronous motor [79], The stator is distributed with the full-pitch winding. So, while building the mathematical model of the motor, each harmonic space must be considered. For fifth and above harmonics have less effect on the motor, so, only the fundamental and third harmonic subspaces are considered. By dual-plane rotation transformation, the fundamental and third-harmonic subspace equations are, respectively, projected into the rotary coordinate systems (d1,q1,d3,q3). Here, it should be noted that the fundamental and third-harmonic space rotation speeds are not synchronized, namely $w_1 = w$ is not equal to $w_3 = 3w$.

The decoupled model of 5Ø-PMSM projected into the coordinate (d1,q1, d3q3) with third harmonic can be extracted by using the matrix of the following transformation:

$$T(\theta) = \begin{bmatrix} \cos(\theta) & \sin(\theta) & 0 & 0 & 0 \\ -\sin(\theta) & \cos(\theta) & 0 & 0 & 0 \\ 0 & 0 & \cos(3\theta) & \sin(3\theta) & 0 \\ 0 & 0 & -\sin(3\theta) & \cos(3\theta) & 0 \\ 0 & 0 & 0 & 0 & 1 \end{bmatrix} \tag{II.27}$$

However, we can write the model with third harmonic in (α1, β1, α2, β2) frame also, while we are satisfied by the used model form in next chapters for d1–q1, d3–q3 frame defined as follows:

$$\begin{cases} \dfrac{dI_{d1}}{dt} = \dfrac{1}{L_{d1}} V_{d1} - \dfrac{R_s}{L_{d1}} I_{d1} + w \dfrac{L_{q1}}{L_{d1}} I_{q1} \\ \dfrac{dI_{q1}}{dt} = \dfrac{1}{L_{q1}} V_{q1} - \dfrac{R_s}{L_{q1}} I_{q1} - w \dfrac{L_{d1}}{L_{q1}} I_{d1} - w \dfrac{\varphi_m}{L_{q1}} \\ \dfrac{dI_{d2}}{dt} = \dfrac{1}{L_{d2}} V_{d2} - \dfrac{R_s}{L_{d2}} I_{d2} + 3w\, L_{q2} I_{q2} \\ \dfrac{dI_{q2}}{dt} = \dfrac{1}{L_{q2}} V_{q2} - \dfrac{R_s}{L_{q2}} I_{q2} - 3w\, L_{d2} I_{d2} \\ \dfrac{d\Omega}{dt} = \dfrac{T_{em}}{J} - \dfrac{T_l}{J} - \dfrac{F}{J}\Omega \\ T_{em} = \dfrac{5}{2} P[\varphi_m I_{q1} + (L_{d1} - L_{q1}) I_{d1} I_{q1}] \end{cases} \tag{II.28}$$

II.12. Association inverter-(5Ø-PMSM)

Generally, an inverter is typically utilized to operate the 5Ø-PMSM by converting DC power to AC power with the proper phase changes. This machine, which is renowned for its rapid dynamic response, short moment of inertia, high torque-to-inertia ratio, good low-speed performance, and accurate phase control, needs the inverter's assistance to operate efficiently. Compared to a conventional 3-phase motor, a 5-phase motor requires more complex control algorithms and power electronics, which are often handled by the inverter. This makes controlling a 5-phase motor more difficult[80].

II.12.1. Description of five phase inverter

To achieve the control of speed or position of the 5Ø-PMSM, it is necessary to use a voltage inverter to supply power to the machine, The inverter is a static converter capable of transforming electrical energy from a direct voltage source into alternating electrical energy[81]. The main structure of the inverter contains ten power switches, which can be referred to as controllable semiconductors. like Transistors or IGBT linked with antiparallel diodes making five legs, in the operating mode of inverter only one semiconductors of the same leg can be closed so in the state “on” to avoid the source short circuit, the next figure (II.5) illustrate the VSI inverter scheme supply the 5Φ-PMSM.

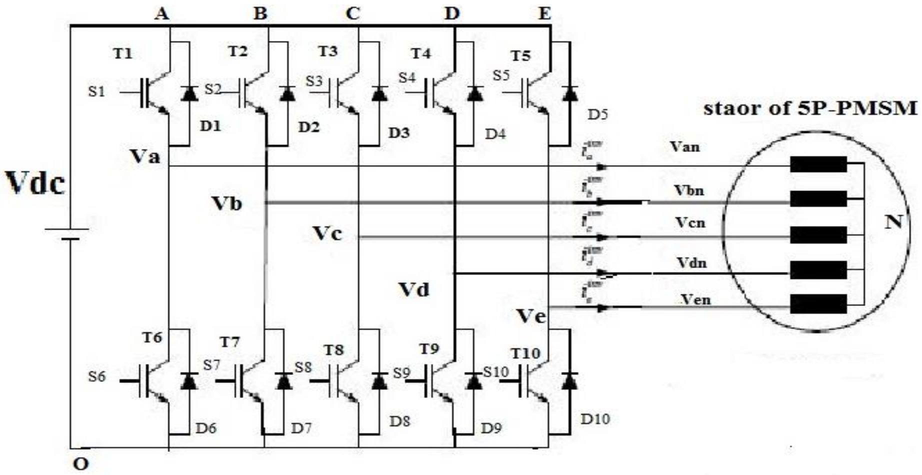

Figure (II.5): Five-phase two-level inverter

Additionally, the continuity of current circulation in the opposite direction is ensured by parallel switching diodes. These network switches are connected in parallel to a direct voltage source of constant value. By a sequence of opening and closing these switches, the desired operation is achieved, the power inverter switches the currents or the voltages of the five phases in order to obtain a five-phase power supply system of voltage and current has adjustable amplitude and frequency, where:

V_{dc}: is the DC-link source of constant value, (T_1,T_2……. T_{10}) are ten symmetrical controllable semiconductors. (D_1,D_2……. D_{10}) are ten symmetrical protective diodes.

II.12.2. Five-phase voltage source inverters (VSI)

In the set inverter-machine, calculating the output voltage of a Five-Phase Voltage Source Inverter (VSI) involves understanding the phase relationships and modulation techniques used to generate the desired voltage waveform. To simplify the modeling mechanism of the inverter, some hypotheses are considered.[82]:

- The 5Φ-PMSM is equilibrium coupled in star-coupled with isolated neutral.
- The voltage drops across the switches is negligible
- The switching of controllable semiconductors is instantaneous.

- The DC source is a perfect voltage continue and constant does not change value.

Also, to define a relationship between the phase voltage and the closing and opening states of the inverter switches as follow:

S_i=0 if when switch number `i' is open, and S_i=1 if it is closed, with i = (1, 2, 3, 4, 5).

The voltages between each leg of inverter and the neutral point (N) are defined by the following relationships:

$$\begin{cases} V_{AO} = V_{AN} + V_{NO} = S_1 V_{dc} \\ V_{BO} = V_{BN} + V_{NO} = S_2 V_{dc} \\ V_{CO} = V_{CN} + V_{NO} = S_3 V_{dc} \\ V_{DO} = V_{DN} + V_{NO} = S_4 V_{dc} \\ V_{EO} = V_{EN} + V_{NO} = S_5 V_{dc} \end{cases} \quad \text{(II.29)}$$

Knowing that V_{dc} is the direct voltage of the inverter, V_{NO} is the voltage between the neutral of the machine and the neutral of the source, and V_{AN} is phase voltage of machine. Equation (II.29) can be rewritten as:

$$\begin{cases} V_{AN} = V_{AO} - V_{NO} \\ V_{BN} = V_{BO} - V_{NO} \\ V_{CN} = V_{CO} - V_{NO} \\ V_{DN} = V_{DO} - V_{NO} \\ V_{EN} = V_{EO} - V_{NO} \end{cases} \quad \text{(II.30)}$$

According to previous equation, either the equilibrium of machine, we can write the following:

$$V_{NO} = \frac{V_{AO} + V_{BO} + V_{CO} + V_{DO} + V_{EO}}{5} \quad \text{(II.31)}$$

By setting (II25) and (II.27) in (II.26) can be obtain the phase output voltage of inverter as follow:

$$\begin{bmatrix} V_{AN} \\ V_{BN} \\ V_{CN} \\ V_{DN} \\ V_{EN} \end{bmatrix} = \frac{V_{dc}}{5} \begin{bmatrix} 4 & -1 & -1 & -1 & -1 \\ -1 & 4 & -1 & -1 & -1 \\ -1 & -1 & 4 & -1 & -1 \\ -1 & -1 & -1 & 4 & -1 \\ -1 & -1 & -1 & -1 & 4 \end{bmatrix} \begin{bmatrix} S_1 \\ S_2 \\ S_3 \\ S_4 \\ S_5 \end{bmatrix} \quad \text{(II.32)}$$

II.13. Techniques of inverter control

Controlling a Five-Phase Permanent Magnet Synchronous Motor (5Φ-PMSM) using an inverter involves various techniques to achieve desired performance characteristics, when the calculating the output voltage of a Five-Phase Voltage Source Inverter (VSI) indispensable of understanding the phase relationships and modulation techniques used to generate the desired voltage waveform[49], The choice of modulation technique may vary based on the specific application and the motor's requirements to generate the switching signals for the semiconductor devices of the inverter. Commonly used techniques include:

- ✓ Space Vector Modulation (SVM).
- ✓ Pulse Width Modulation (PWM)

II.13.1. Space vector Modulation (SVM) techniques

SVM is a widely used technique for Five-Phase Inverters. It's an extension of the three-phase SVM to five phases, which optimizes the switching states of the inverter to generate voltage vectors that closely approximate the desired reference vector[83]. The output voltage of the inverter is represented as a space vector in a two-dimensional complex plane, typically referred to as the (α1,β1,α2,β2) plane. It has a twenty-two voltage vectors presented in the following figure (II.6), two of them are inactive and the twenty others are active voltage vectors.

Additionally, the output voltage of inverter can be expressed in (α1, β1, α2, β2) frame based on the five -phase output voltage of inverter in original frame as follow:

$$\begin{cases} V_{\alpha 1\beta 1} = \dfrac{2}{5}(V_a + aV_b + a^2V_c + a^3V_d + a^4V_e) \\ V_{\alpha 2\beta 2} = \dfrac{2}{5}(V_a + a^2V_b + a^4V_c + a^6V_d + a^8V_e) \end{cases} \tag{II.33}$$

Where: $a = e^{(j2\pi/5)}$.

The control system defines a reference voltage vector Vref in the (α1, β1, α2, β2) frame, which represents the desired voltage magnitude and phase angle based on the control objectives, the SVM algorithm identifies the sector in which the reference voltage vector lies, there are ten possible sectors, each defined by specific voltage vector combinations, within each sector K, SVM calculate the switching times of individual vector as follow:

$$\begin{cases} T_s V_{ref} = t_{lk}V_{lk} + t_{mk}V_{mk} + t_{l(k+1)}V_{l(k+1)} + t_{m(k+1)}V_{m(k+1)} \\ T_s = t_{lk} + t_{mk} + t_{l(k+1)} + t_{m(k+1)} \end{cases} \tag{II.34}$$

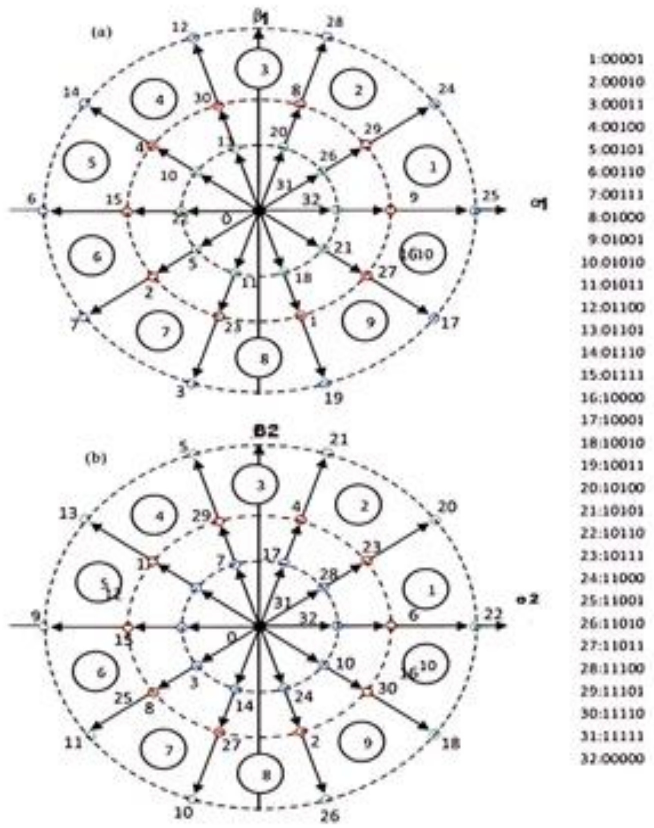

Figure (II.6): The voltages of space vector, switching states and sectors of five phase inverter in (α1, β1, α2, β2) frame.

Where: T_s :is the sampling time (period), $V_{mk}, t_{mk}, V_{lk}, t_{lk}$: are the middle vectors, switching time of middle vector, large vectors and switching time respectively of sector number k. as well as:

$$\begin{cases} t_{mk} = \dfrac{0.276\left|V_{ref}\right|\sin(k\pi/5-\theta)}{\left|V_{mk}\right|\sin(\pi/5)}T_s \\ t_{m(k+1)} = \dfrac{0.276\left|V_{ref}\right|\sin(\theta-(k-1)\pi/5)}{\left|V_{mk}\right|\sin(\pi/5)}T_s \\ t_{lk} = \dfrac{0.276\left|V_{ref}\right|\sin(k\pi/5-\theta)}{\left|V_{lk}\right|\sin(\pi/5)}T_s \\ t_{l(k+1)} = \dfrac{0.276\left|V_{ref}\right|\sin(\theta-(k-1)\pi/5)}{\left|V_{lk}\right|\sin(\pi/5)}T_s \end{cases} \tag{II.35}$$

The time off zero vector can be calculated by:

$$t_0 = T_s - t_{mk} - t_{m(k+1)} - t_{lk} - t_{l(k+1)} \tag{II.36}$$

And θ is the angle between the reference voltage and the coordinate α1.

II.13.2. The pulse width Modulation (PWM) technique

The PWM technique remains an attractive choice for many applications. It allows for precise control of inverter output voltage by varying the width of pulses while maintaining a constant frequency. This technique is widely used in various motor drives, voltage regulation, and uninterruptible power supplies. Its straightforward implementation and minimal computational demands make it a preferred choice when high computational resources are not available. The principle of PWM involves determining the switching times by using the intersections between the reference modulated signal (as the output of the control part), with a triangular carrier periodic function. In order for the energy supplied to the motor and its load to primarily depend on the modulating signal, the frequency of a PWM signal needs to be significantly greater than that of the modulating signal, or fundamental frequency[84].

Pulse Width Modulation (PWM) is a technique used to regulate the power supplied to a load without changing the voltage level. To control the output voltage of the inverter, either Single Pulse Width Modulation or Multiple Pulse Width Modulation techniques can be applied. The desired output voltage is achieved by adjusting the number of pulses and their widths. Some examples of PWM approaches are as follows:

II.13.2.1. Sinusoidal Pulse Width Modulation

This technique used to control inverter output in AC power systems. It modulates pulse width based on the intersection points of a reference sine wave and a high-frequency carrier wave, typically triangular or sawtooth, to generate a sinusoidal output.

II.13.2.2. Hysteresis Band Pulse Width Modulation

This method adjusts the pulse width based on the discrepancy between the output signal and the reference signal. The pulse width is modified in accordance with the comparison of the error with a hysteresis band [85].

II.13.2.3. Trail Edge Pulse Width Modulation

In this method, the modulation is based on the trailing edge (or falling edge) of the carrier signal rather than the leading edge (or rising edge) as in traditional PWM techniques.

II.13.2.4. Lead Edge Pulse Width Modulation:

This method maintains the leading edge fixed while modulating the trailing edge of the signal[86].

II.13.2.5. Pulse Center Two Edge Modulation

In this method, the edges remain fixed · while the pulse center is modified.

The technique of PWM-based switching power converters is commonly used and has several types with more advantages, such as:

- Simple to control and put into effect and implemented.
- There is no decrease in linearity or drifting due to age and temperature changes.

- ❖ Compatible and in line with the digital microprocessors of today.
- ❖ Reduced loss of power.
- ❖ Makes previously unavailable linear amplitude control over the output voltage/current possible

II.14. Simulation and result

In the simulation part, we will use the Matlab-Simulink software to validate the block diagram of the 5Φ-PMSAP associated with inverter, where the used parameters are presented in the appendix (Annex A).

II.14.1. Simulation of Inverter Control

The design of a two-level inverter, which contains ten semiconductors, is illustrated in the next figure (II.7) using Matlab-Simulink, that contains five voltage sources signals compared to triangular signal of repeating sequence block, the comparison output result multiplying of constant value which represents the DC source.

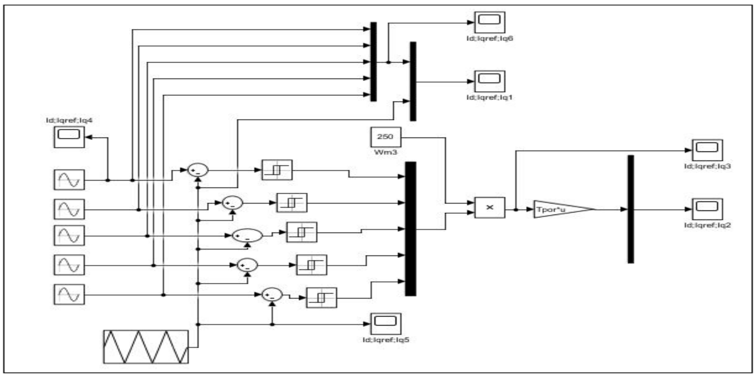

Figure (II.7): Simulation Scheme of five phase inverter control

The Figure (II.8) represents the comparison of input and triangular signals in part a), and inverter output signals in b) as follow:

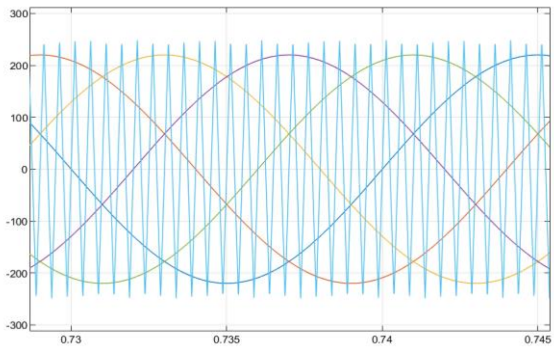

a) Sinusoidal Pulse Width Modulation

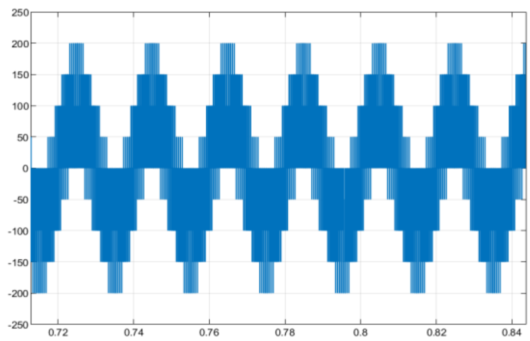

b) single phase output of 5Φ-inverter

Figure (II.8): Simulation results of five phase inverter control

II.14.2. Open loop simulation of 5P-PMSM

To simulate a Five-Phase Permanent Magnet Synchronous Motor (5Φ-PMSM) with an inverter, the following block as shown in Figure (II.9) is implemented in the MATLAB Simulink,

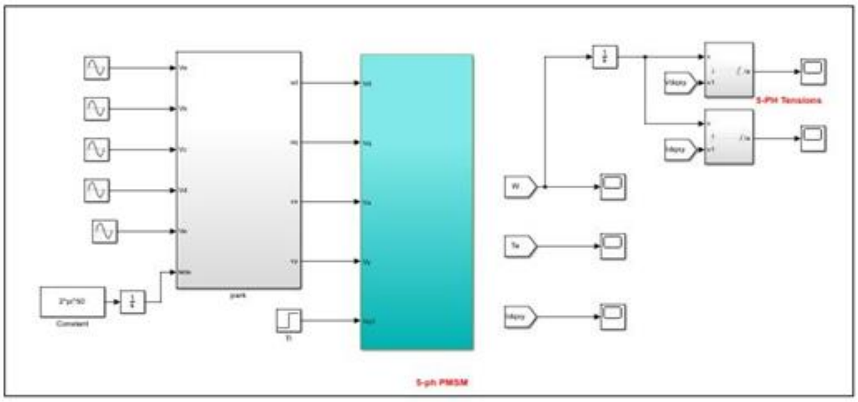

Figure (II.9): Simulation block of 5Φ-PMSM with inverter

The results of the 5Φ-PMSM simulation integrated with an inverter, under conditions with nominal parameters and without load torque (TL = 0), are shown in the figure (II.10.) .The successive results (a,b,c,d) represent the speed, electromagnetic torque, phase currents, and quadratic current..

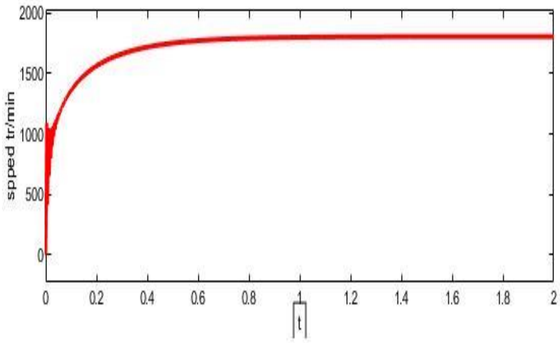

a)

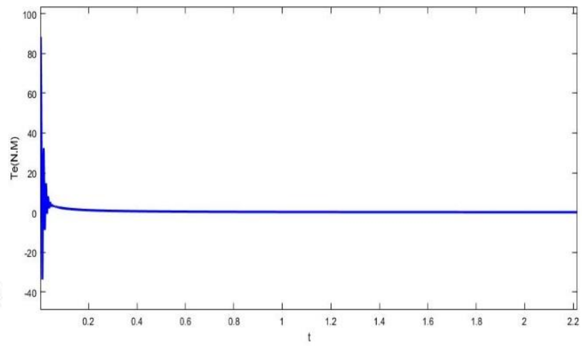

b)

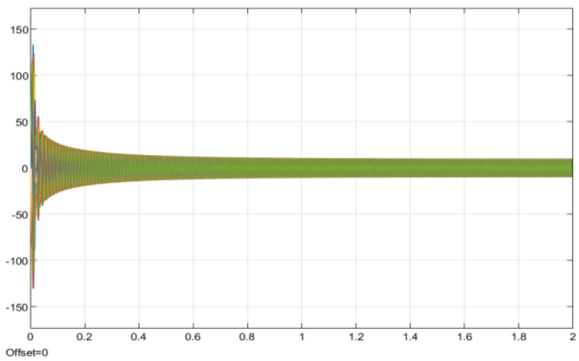

C)

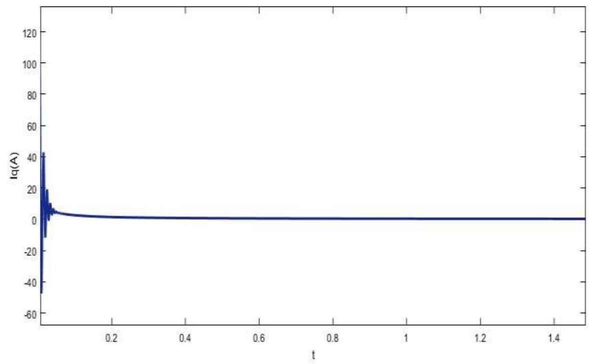

d)

Figure(II.10) : Simulation results of 5Φ-PMSM associed with inverter

Based on these results, the output of the inverter for a single phase, illustrated in Figure (II.8), section 'b,' is in the form of a sine wave, which is considered an acceptable input for the 5Φ-PMSM phases. Additionally, the simulation results shown in Figure (II.10), obtained from MATLAB Simulink software, confirm the motor operates correctly under nominal conditions.

II.15. Conclusion

This chapter covered the fundamentals of the 5Φ-PMSM, including its configuration, principal operation, and advantages. Additionally, to simplify the modeling process, the comprehensive modeling of five-phase permanent magnet synchronous motors was explored within three distinct reference frames, taking into account the modeling of the 5Φ-PMSM with harmonic subspace. The detailed analysis included the development and integration of an inverter system, highlighting its critical role in motor control. Simulations were carried out under open-loop conditions to assess the performance of the 5Φ-PMSM. The simulation results confirmed that the motor operates efficiently and reliably under nominal conditions, meeting the expected performance criteria. This validates the viability and robustness of the developed models and control strategies for practical applications. In the next chapter, the control of this type of machine will be explored using nonlinear backstepping control.

Chapter III.

Backstepping Control of Five Phases Permanent Magnet Synchronous Motor

III.1. Introduction

In recent years, the demand for highly efficient and reliable motor control systems has surged, driven by advancements in industrial automation, electric vehicles, and renewable energy applications. Among various motor types, the Permanent Magnet Synchronous Motor (PMSM) has emerged as a prominent choice due to its superior performance characteristics, including high efficiency, high power density, and precise control capabilities[87]. The advent of multi-phase motor configurations, particularly the 5Φ-PMSM, further enhances these attributes, offering additional degrees of freedom and improved fault tolerance.

Numerous control techniques have been extensively employed to regulate AC motors, one of which is field orientation control, which permits a decoupling of the torque and flux to achieve autonomous control of the torque and flux, similar to DC motors [88].However, the Performance of these controls is affected by changes in the motor parameters, particularly the motor resistances, which are affected by temperature and the magnetizing inductance's saturation. However, the PI controller's performance is effectively constrained since it ignores the relationship between the inner and outer control loops. As a result, there is a great deal of interest in creating so-called nonlinear control, which aims to address this issue[89]. The successful application of modern mathematical tools played an important role in the development of non-linear control, which contributed to the emergence of two significant nonlinear control systems that have been developed in recent decades are sliding mode control and backstepping control.

This chapter explores the advanced control technique called backstepping control, which is designed with the 5Φ-PMSM in mind. A recursive, Lyapunov-based design process called backstepping control builds control rules methodically to guarantee system stability and reliable operation, Lyapunov-based design methodology that systematically constructs control laws ensuring system stability and robust performance. Moreover, the implementation of backstepping control of 5Φ-PMSM under different operating conditions such as variable load torque, open fault phase and speed reverse operation has been verified by MATLAB Simulink.

This chapter begins with an overview of the fundamental principles of nonlinear backstepping control and the inherent advantages of this approach. In addition, Lyapunov's stability theorem is discussed, and MATLAB is used to extract simulation results to verify the effectiveness and performance of the proposed control, which has been completed.

III.2. History and innovation of backstepping control

The backstepping control technique dates back to the late 1980s and early 1990s, as the primary idea behind this control method was developed in response to the need for control strategies capable of managing highly nonlinear and uncertain systems [90]. In fact, the concept of backstepping control was first introduced in 1989 by **Ioannis Kanelakopoulos**, **Petar V. Kokotovic**, and Andrey S. Morse in their landmark research titled: 'Systematic Design of Adaptive Controllers for Feedback Linearizable Systems'. They proposed a systematic design approach that breaks down the control challenge into several simpler sub-problems. The core idea of this method is based on recursive design, where each stage focuses on stabilizing and tracking a particular subsystem of the overall system control systems community. It was seen as a potentially successful approach for managing highly nonlinear and complex systems, which are common in a variety of engineering applications.

Over the years, researchers have continued to refine and improve the backstepping control strategy. Various modifications and extensions have been proposed to address specific challenge and improve the performance of the technique. These include adaptative backstepping control, robust backstepping control, and backstepping control with neural networks.[91]. To guarantee stability and convergence features, a number of stability analysis techniques, including Lyapunov-based analysis, were incorporated into the backstepping control framework.

III.3. Principal of backstepping control

The principle of the backstepping control strategy is a control design technique used to stabilize nonlinear systems. It involves breaking down the control problem into multiple smaller subsystems and designing controllers for each subsystem to achieve stability. This control strategy works by introducing a series of virtual control inputs that are used to stabilize the system. These virtual inputs are then combined with the actual control inputs to achieve the desired system behavior. The main idea behind backstepping control is to design a Lyapunov function for each subsystem that guarantees stability[92].The Lyapunov function is a mathematical function that measures the energy of system and ensures that it decreases over time. By designing Lyapunov functions for each subsystem, the overall stability of the system can be achieved. Although there is no specific theoretical for determining the proper Lyapunov function for the given system, in the majority of control it is dependent primarily on the control designer's experience and intuition. This might be viewed as the biggest significant disadvantage of employing the Lyapunov function with the suggested controller. Nonetheless the backstepping control strategy is particularly useful for controlling complex nonlinear systems where traditional control may not be effective.it allows for the design of controllers that can handle uncertainties[93].

III.4. Stability by Lyapunov theory

Lyapunov stability analysis is a mathematical approach used to decide the steadiness of equilibrium factors in a dynamic machine, it is a powerful mathematical principle used in the discipline of coping with concepts and dynamical structures to investigate and expect the stability of systems and control concepts, physics, engineering, and different fields to assess the behaviour of structures through the years. This idea was named after the Russian mathematician Aleksandr Lyapunov, who developed this concept in the overdue nineteenth century.

In current years this Theory of stability has ended up a totally crucial tool for the manipulation of nonlinear structures, its miles used to analyse the stableness of closed-loop systems. Furthermore, the principle of this technique is based on the concept of power in a machine, which in a physical gadget is an advantageous exact characteristic, it remains constant if the machine is conservative, and it decreases if the device is dissipative. In both instances, we are able to say that the gadget is stable. On the other hand, the device is stated to be unstable if its energy will increase. This method includes reading the variations of a function (representative of the power of the device) alongside the trajectory of the system [94].

For that, the nonlinear system with equilibrium point x_0 is considered:

$$\begin{cases} \dot{x} = f(x,u) \\ f(x_0) = 0 \end{cases} \qquad \text{(III.01)}$$

An equilibrium point x_0 a state where the system does not change over time $f(x_0,u)=0$,in control system design to ensure that a controlled system behaves as desired around an equilibrium point, this means that any small perturbation from the equilibrium point will result in the system eventually returning to that point. The choice of Lyapunov function V(x) must be positive and realize its derivative a negative, then:

$$\begin{cases} layuponov \quad function\ V(x) > 0 \\ \dot{V}(x) = \dfrac{\partial V}{\partial x}\dot{x} = \dfrac{\partial V}{\partial x} f(x,u) < 0 \end{cases} \qquad \text{(III.02)}$$

Where: ‘x’ is the state vector, and ‘u’ is the control vector.

III.5. Overview of Backstepping Control

Backstepping control first appeared in the early 1990s as a result of researchers investigating new control techniques to address complex and nonlinear systems. Initially, it was developed as an extension of the sliding mode control approach. This method enables the control of nonlinear systems by breaking them down into a series of simpler subsystems. Furthermore. One of the key advantages of backstepping control is its ability to handle uncertainties and disturbances in the system, which has drawn significant attention since its proposal. It has been extensively used to address control issues in the field of aerospace engineering[33].

The literature on backstepping control for five-phase Permanent Magnet Synchronous Motors highlights several advancements and methodologies aimed at enhancing performance and stability. Various studies focus on the synthesis and application of backstepping control strategies.

For instance, one research discusses the speed control strategy for a 5Φ-PMSM drive, showcasing the effectiveness of backstepping in improving motor performance like in [95]speed tracking the reference with error is near to zero. Another study integrates sliding mode observers with sensorless backstepping control, further addressing the need for robust speed control in the absence of sensors [13],the author use MRAS observer for parameters estimation. To realize more different improved backstepping some authors use integral surface error [14] another study integrates sliding mode observers with sensorless backstepping control some in the literature , further addressing the need for robust speed control in the absence of sensors[96]. In terms of adaptive control, the integration of artificial techniques, such as the use of neural networks for adaptive backstepping control, highlights the adaptability of this method in handling nonlinearities and uncertainties. in[97].

Additionally, research emphasizes the advantages of nonlinear adaptive backstepping control in managing parametric variations and achieving precise speed tracking[98] . Collectively, these studies demonstrate that backstepping control is a highly effective strategy for managing the complexities and ensuring the robust performance of 5Φ-PMSM systems.

On the other hand, like sliding mode observers, new research explores the backstepping observer. These observers extend the backstepping design approach to not only stabilize systems but also estimate unmeasured states. Additionally, observer backstepping has been applied in flight control, presenting a new framework for nonlinear flight control design.[99].

III.6. Backstepping control theory

Consider the following second-order system, which has a differential equation of the form:

$$\begin{cases} \dot{x}_1 = f(x_1) + x_2 \\ \dot{x}_2 = u \end{cases} \qquad \text{(III.03)}$$

It is assumed that the output of the system is desired to follow the reference signal in order for the recursive process of backstepping control to be described and the stability of the system to be analysed. Next, the defined sign of the function V(x) is sought, and the system is operated in two steps:[100]

III.6.1. First step

To create the first scalar function of Lyapunov for a system with such an equation (III,03) as follow:

$$V_1 = \frac{1}{2} z_1^2 \tag{III.04}$$

Where Z_1 represents the tracking error described in the following form:

$$z_1 = x_1^* - x_1 \tag{III.05}$$

With x_1^* is the desired reference output.

For guarantee the stability of the system and ensure the negativity of Lyapunov function (III.04) must be make derivation of V_1which written on the next equation as follow:

$$\dot{V}_1 = \dot{z}_1 \, z_1 \tag{III.06}$$

The derivative of error equation (III.05) is:

$$\dot{z}_1 = \dot{x}_1^* - \dot{x}_1 = \dot{x}_1^* - f(x_1) - x_2 \tag{III.07}$$

Setting the equation (III.07) in (III.06) gives us the following:

$$\dot{V}_1 = z_1(\dot{x}_1^* - \dot{x}_1) = z_1(\dot{x}_1^* - f(x_1) - x_2) \tag{III.08}$$

To ensure the negation of the Lyapunov function derivative and to realize the stability condition, introducing a positive constant k_1 such that:

$$\dot{V}_1 = z_1(\dot{x}_1^* + k_1 z_1 - k_1 z_1 - f(x_1) - x_2) = -k_1 z_1^2 + (\dot{x}_1^* + k_1 z_1 - f(x_1) - x_2) \tag{III.09}$$

For guarantee $\dot{V}_1 < 0$ must be the virtual command determined for assure the condition $(\dot{x}_1^* + k_1 z_1 - f(x_1) - x_{c2}) = 0$. So that realize $\dot{V}_1 = -k_1 z_1^2 < 0$; consequently, the virtual control is written in the following expression:

$$x_{c2} = \dot{x}_1^* + k_1 z_1 - f(x_1) \tag{III.10}$$

III.6.2. Second step

In the second step, the new error Z_2 are defined from the previous virtual control that considered as a new reference variable as follow:

$$z_2 = x_2^* - x_2 = k_1 z_1 + \dot{x}_1^* - f(x_1) - x_2 = k_1 z_1 + \dot{z}_1 \qquad \text{(III.11)}$$

The derivative of this error calculated from the previous equation (III.11) equal:

$$\begin{aligned} \dot{z}_2 &= \dot{x}_2^* - \dot{x}_2 = k_1 \dot{z}_1 + \ddot{x}_1^* - \dot{f}(x_1) - \dot{x}_2 \\ \dot{z}_2 &= k_1 \dot{z}_1 + \ddot{x}_1^* - \dot{f}(x_1) - u \end{aligned} \qquad \text{(III.12)}$$

The Lyapunov function V_2 can be written in to take account the global error as follow:

$$V_2 = \frac{1}{2} z_1^2 + \frac{1}{2} z_2^2 \qquad \text{(III.13)}$$

The derivative of the second Lyapunov function V_2 is:

$$\begin{aligned} \dot{V}_2 &= z_1 \dot{z}_1 + z_2 \dot{z}_2 = z_1 (z_2 - k_1 z_1) + z_2 (k_1 \dot{z}_1 + \ddot{x}_1^* - f(x_1) - u) \\ &= -k_1 z_1^2 + z_2 (z_1 + k_1 z_2 - k_1^2 z_1 + \ddot{x}_1^* - f(x_1) - u) \end{aligned} \qquad \text{(III.14)}$$

To ensure the negative of the derivative of the Lyapunov function we defined a positive k_2 that realizes the following condition:

$$\dot{V}_2 = -k_1 z_1^2 - k_2 z_2^2 < 0 \qquad \text{(III.15)}$$

By matching the two equations (III.13) and (III.14) the command Udefined as follow:

$$\begin{aligned} u &= z_1 + k_1 z_2 - k_1^2 z_1 + \ddot{x}_1^* - f(x_1) + k_2 z_2 \\ &= (k_1 + k_2) z_2 + (1 - k_1^2) z_1 + \ddot{x}_1^* - f(x_1) \end{aligned} \qquad \text{(III.16)}$$

The values of the positive constants k1 and k2 play a crucial role in shaping the system's response. Selecting the appropriate control gains for backstepping control requires a blend of theoretical principles and creative intuition. This process demands a solid understanding of control theory, deep knowledge of the specific system, and a readiness to experiment. The goal is to strike a balance between stability and performance, ensuring the system operates as desired across different scenarios

III.7. The Backstepping control of 5Φ-PMSM

The fundamental idea of backstepping control is to reduce the complicated nonlinear system to an equivalent form in order one cascade subsystems [101]. And using the Lyapunov approach offers stability of system. The corresponding nonlinear model of 5Φ-PMSM drive with consideration for the third harmonic mentioned above in previous chapter can be rewritten in a rotating reference frame ($d1-q1-d2-q2$) as follow:

$$\begin{cases} \dfrac{di_{d1}}{dt} = d_1 + \dfrac{V_{d1}}{L_s} \\ \dfrac{di_{q1}}{dt} = d_2 + \dfrac{V_{q1}}{L_s} \\ \dfrac{di_{d2}}{dt} = d_3 + \dfrac{V_{d2}}{L_{ls}} \\ \dfrac{di_{q2}}{dt} = d_4 + \dfrac{V_{q2}}{L_{ls}} \end{cases} \qquad \text{(III.17)}$$

And the mechanical equation expressed in next form as:

$$\begin{cases} T_{em} = K\varphi_f P i_{q1} \\ \dfrac{d\Omega}{dt} = d_5 \end{cases} \qquad \text{(III.18)}$$

Where $K = \sqrt{5/2}$ .also:

$$\begin{cases} d_1 = -\dfrac{R_s}{L_s} i_{d1} + \omega\, i_{q1} \\ d_2 = -\dfrac{R_s}{L_s} i_{q1} - \omega\, i_{d1} - \dfrac{\varphi_m}{L_s}\omega \\ d_3 = -\dfrac{R_s}{L_{ls}} i_{d2} + 3\omega\, i_{q2} \\ d_4 = -\dfrac{R_s}{L_{ls}} i_{q2} - 3\omega\, i_{d2} \\ d_5 = \dfrac{T_{em}}{J} - \dfrac{T_L}{J} - \dfrac{F\Omega}{J} \end{cases} \qquad \text{(III.19)}$$

Figure (III.1): displays the block diagram of the proposed backstepping strategy of 5Φ-PMSM drive. The presented backstepping algorithm in this paper is synthesized in two phases.

III.7.1. Calculation of the reference currents

The speed controller should track the trajectory for input reference at this initial stage. Consequently, the speed error and its derivative are shown as:

$$\begin{cases} z_1 = \omega^* - \omega \\ \dot{z}_1 = \dot{\omega}^* - \dot{\omega} \end{cases} \qquad \text{(III.20)}$$

The derivative of speed error can be established as:

$$\dot{z}_1 = \dot{\omega}^* - d_5 \tag{III.21}$$

The first Lyapunov function related with speed error is established to check the tracking performances as:

$$V_1 = \frac{1}{2} z_1^2 \tag{III.22}$$

Based on (III.21), the derivative of system (III.22) is computed as follows:

$$\dot{V}_1 = z_1 \left(\dot{\omega}^* - d_5 \right) \tag{III.23}$$

Thus, the system (III.23) can be rewritten as:

$$\dot{V}_1 = z_1 \left(\dot{\omega}^* - d_5 \right) = -c_1 z_1^2 \tag{III.24}$$

Where, $c_1 > 0$ and the derivative of speed error gives:

$$\dot{z}_1 = \dot{\omega}^* - \dot{\omega} = -c_1 z_1 \tag{III.25}$$

The i_{q1} component contributes to developed torque, while the i_{d1}, i_{d2}, i_{q2} components contribute to the power losses . Then the references currents can be described as:

$$\begin{cases} i_{d1}^* = 0 \\ i_{q1}^* = \left(\dot{\omega}^* + \dfrac{T_L}{J} + \dfrac{B\omega}{J} + c_1 z_1 \right) / \left(\dfrac{K\varphi_m P}{J} \right) \\ i_{d2}^* = 0 \\ i_{q2}^* = 0 \end{cases} \tag{III.26}$$

III.7.2. Calculation of the reference voltages

Obtaining the reference voltages based on the preceding phase is the aim of this phase., where the current errors are derived as follows:

$$\begin{cases} z_2 = i_{d1}^* - i_{d1} \\ z_3 = i_{q1}^* - i_{q1} \\ z_4 = i_{d2}^* - i_{d2} \\ z_5 = i_{q2}^* - i_{q2} \end{cases} \tag{III.27}$$

Hence, their derivative is expressed as follows:

$$\begin{cases} \dot{z}_2 = \dot{i}_{d1}^* - \dot{i}_{d1} \\ \dot{z}_3 = \dot{i}_{q1}^* - \dot{i}_{q1} \\ \dot{z}_4 = \dot{i}_{d2}^* - \dot{i}_{d2} \\ \dot{z}_5 = \dot{i}_{q2}^* - \dot{i}_{q2} \end{cases} \tag{III.28}$$

Using the system (III.26), the current errors are given as follows:

$$\begin{cases} z_2 = -i_{d1} \\ z_3 = \left(\dot{\omega}^* + \frac{T_L}{J} + \frac{B\omega}{J} + c_1 z_1 \right) / \left(\frac{K\varphi_m P}{J} \right) - i_{q1} \\ z_4 = -i_{d2} \\ z_5 = -i_{q2} \end{cases} \tag{III.29}$$

Considering (III.25), the system expressed in (III.26) can be obtained as:

$$\dot{z}_1 = \frac{K\varphi_m P \ z_3}{J} - c_1 z_1 \tag{III.30}$$

By setting (III.17) in the system (III.28), one obtains:

$$\begin{cases} \dot{z}_2 = \dot{i}_{d1}^* - d_1 - \frac{V_{d1}}{L_s} \\ \dot{z}_3 = \dot{i}_{q1}^* - d_2 - \frac{V_{q1}}{L_s} \\ \dot{z}_4 = \dot{i}_{d2}^* - d_3 - \frac{V_{d2}}{L_{ls}} \\ \dot{z}_5 = \dot{i}_{q2}^* - d_4 - \frac{V_{q2}}{L_{ls}} \end{cases} \tag{III.31}$$

Therefore, to prove the overall stability of the studied control algorithm, a new Lyapunov function is defined as:

$$V_2 = \frac{z_1^2 + z_2^2 + z_3^2 + z_4^2 + z_5^2}{2} \tag{III.32}$$

The derivative of the system (III.32) becomes:

$$\begin{aligned}\dot{V}_2 &= -c_1 z_1^2 - c_2 z_2^2 - c_3 z_3^2 - c_4 z_4^2 - c_4 z_5^2 \\ &+ z_2\left(c_2 z_2 + \dot{i}_{d1}^* - d_1 - \frac{V_{d1}}{L_s}\right) \\ &+ z_3\left(c_3 z_3 + K\varphi_f n_p z_1 + \dot{i}_{q1}^* - d_2 - \frac{V_{q1}}{L_s}\right) \\ &+ z_4\left(c_4 z_4 + \dot{i}_{d2}^* - d_3 - \frac{V_{d2}}{L_{ls}}\right) \\ &+ z_5\left(c_4 z_5 + \dot{i}_{q2}^* - d_4 - \frac{V_{q2}}{L_{ls}}\right)\end{aligned} \tag{III.33}$$

Consequently, if the variables within parentheses in the same expression are equal to zero, the derivative of the overall Lyapunov function (III.33) is negative.

$$\begin{cases} c_2 z_2 + \dot{i}_{d1}^* - d_1 - \dfrac{V_{d1}}{L_s} = 0 \\ c_3 z_3 + K\varphi_f n_p z_1 + \dot{i}_{q1}^* - d_2 - \dfrac{V_{q1}}{L_s} = 0 \\ c_4 z_4 + \dot{i}_{d2}^* - d_3 - \dfrac{V_{d2}}{L_{ls}} = 0 \\ c_4 z_5 + \dot{i}_{q2}^* - d_4 - \dfrac{V_{q2}}{L_{ls}} = 0 \end{cases} \tag{III.34}$$

Finally, the reference voltages are obtained as:

$$\begin{cases} V_{d1}^* = L_s\left(c_2 z_2 + \dot{i}_{d1}^* - d_1\right) \\ V_{q1}^* = L_s\left(c_3 z_3 + k\varphi_m P\ z_1 + \dot{i}_{q1}^* - d_2\right) \\ V_{d2}^* = L_{ls}\left(c_4 z_4 + \dot{i}_{d2}^* - d_3\right) \\ V_{q2}^* = L_{ls}\left(c_4 z_5 + \dot{i}_{q2}^* - d_4\right) \end{cases} \tag{III.35}$$

Where: c1, c2, c3, and c4 are that have been employed in our suggested control are positive and have been selected to meet the enhanced requirements of the suggested backstepping control, including a quicker dynamic of the rotor speed and stator currents, with minimum overshoot. Where by their precise value selection will enhance the closed loop's dynamic and hence ensure the regulated system's stability. In this chapter, the values of these parameters that have been selected from multiple simulation sessions where fitting the optimal dynamic demand of the rotor speed and stator current served as the primary selection criterion.

Indeed, Tuning the gains for backstepping control can be complex, particularly in nonlinear multi-systems, where improper tuning can lead to instability or suboptimal performance [102].This process often involves trial and error or empirical methods to achieve the desired performance. Several researchers to solve this problem have made several suggestions for sports methods such as numerical algorithms, which is what we will address in the next chapter.

III.8. Simulation and results of Backstepping control of 5P-PMSM

The backstepping control strategy for a five-phase Permanent Magnet Synchronous Motor (5Φ-PMSM) implemented in Matlab Simulink illustrated in next figure (III.1). The speed controller generates the reference current $Iq1ref$ based on the reference speed $Wref$, it aims to adjust the motor speed to match the desired speed, whereas There are three current controllers, each responsible for regulating different components of the current:

-The first current controller uses $Iq1ref$ to generate the reference voltage $Vq1ref$.

-The second and third current controllers regulate $Id1ref$, $Iq2ref$ and $Id2ref$ respectively to produce the corresponding reference voltages $Vd1ref$, $Vq2ref$ and $Vd2ref$.

Additionally, the generated reference voltages are transformed from the ($d1$,$q1$,$d2$,$q2$)frame to the (a,b,c,d,e) frame, which matches the motor's physical, the 5Φ-PMSM is the load, which receives the input from the inverter and operates according to the control signals to achieve the desired speed and performance.However, the motor's position θ and current feedback are continuously monitored and sent back to the control system to adjust the control signals dynamically.

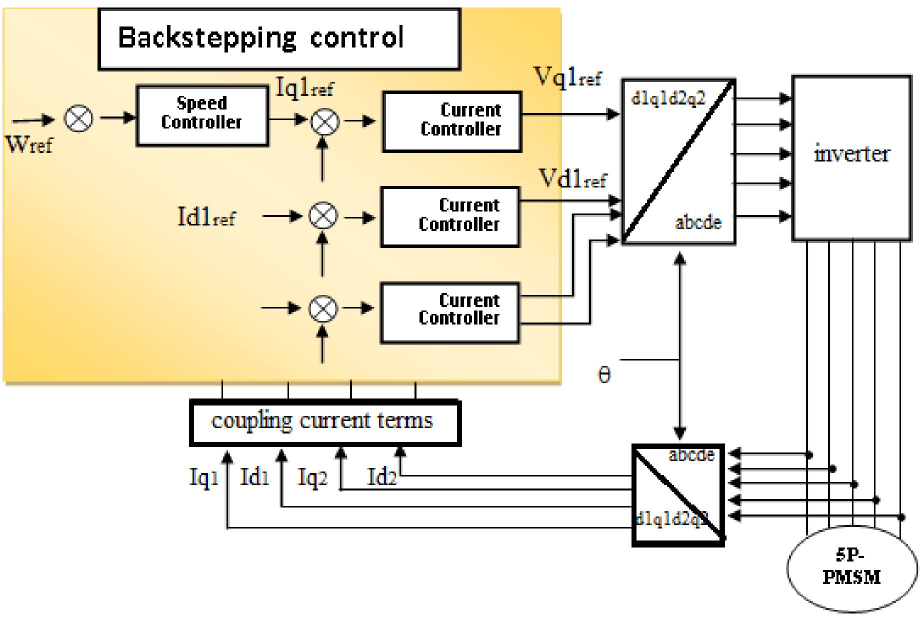

Figure (III.1): Backstepping control of 5P-PMSM Scheme.

In order to verify and assess the benefits of the non-linear backstepping control described in this chapter for guaranteeing the control performance, MALAB simulation results are offered in order to evaluate the backstepping control's dynamic performance under various operating circumstances, including load application, reversal speed, open phase fault, and startup.

III.8.1. Performance under high-speed operation

This test is done using MATLAB Simulink, where the 5Φ-PMSM under study is run at a high speed while maintaining a consistent torque under load. The findings of the nonlinear backstepping simulation and experiment using a MATLB-SIMULINK are displayed in fig (III.02). The reference speed that is being used has two phases. The first phase lasts for 0.03 seconds and varies linearly from zero to the steady state value of 150 rad/s. the second phase displays the steady state speed, the disturbance load equal 3N.m is a fixed value applied in 0.2s. The real and reference rotor speeds for the suggested backstepping control of the motor under study are displayed in Figure (III.2a). It is noted that the reference rotor speed of 150 rad/s is exactly followed by the actual rotor speed, which is attained fastly and responds quickly. So, the speed error which represents the instantaneous difference between the reference speed and the real rotor speed, is shown in Figure (III.2b),But it is somewhat not accurate compared to the results obtained in the following references[23], [95]. There is Unneglected speed error. Also, the electromagnetic torque of the motor under study is displayed in Figure (III.2c). In addition, the electromagnetic torque results show high dynamic and acceptable torque ripples, confirming the Backstepping control's ability to reduce overshoot and its resilience to load torque variations. The direct and quadratic current components are shown in Figure (III.2d) where the response of the quadratic and direct current components clearly demonstrates good decoupling, So, through the Figure (III.2e) displays the stator currents in the stationary reference frame. At first, these currents are not equal because of circuit inductance. When the conditions are stable, the stator currents show a balanced sinusoidal pattern. As the load torque goes up during load placement, the current amplitude goes up as well. The rotor position is shown in Figure (III.2f), It fluctuates between 2π rad and zero. It is evident that the function is periodic; but, because of the acceleration phenomenon that occurs during the start-up (between 0 and 0.03 seconds), the period gets shorter as the rotor speed increases until it reaches a constant value at steady state.

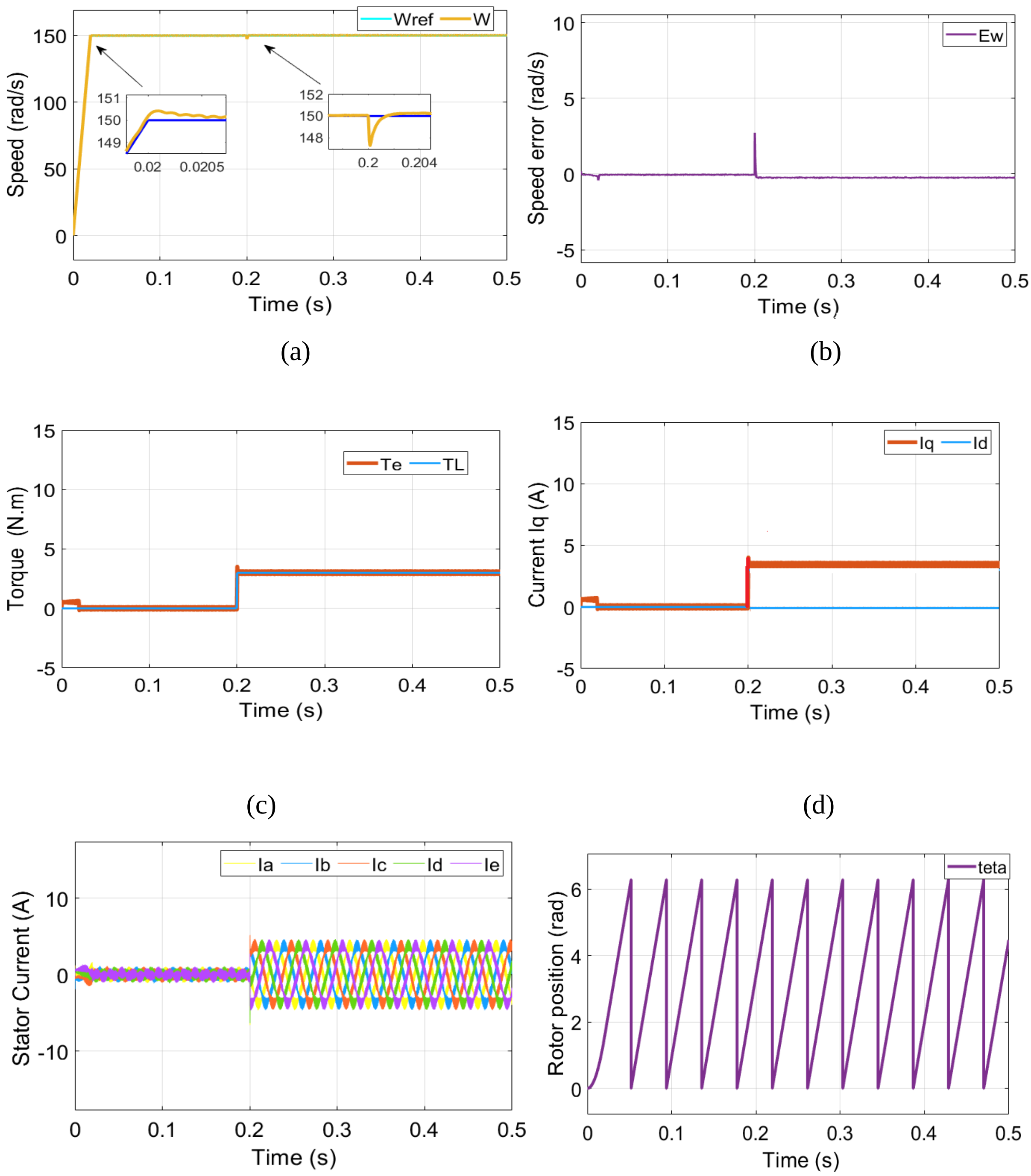

(a) (b)

(c) (d)

(e) (f)

Figure (III.2): Simulation results of proposed Backstepping control 5P-PMSMunder high-speed operation

.

III.8.2. Performance under reversal speed operation

It is important to test the proposed Backstepping control with a speed sensor while the motor is running at a reverse speed and a steady load torque equal 3 Nm is applied for 0.2 seconds. This will show how well the proposed Backstepping control works. Therefore, the reference speed changes in two steps, from 0 to 150 rad/sec and from 150 rad/s to -150 rad/s, as shown in Figure (III.3a). A reverse speed test was also done.

For the motor that was studied, Figure (III.3a) shows the reference speed and the real rotor speed for the suggested backstepping control. The rotor speed stays close to the reference number and doesn't go too fast or too slow. As shown in Figure (III.3b), the speed difference quickly goes to zero whenever the reference speed changes quickly. This result shows that the Backstepping control works perfectly, even when the speed is reversed, But it is not optimal compared to several other results.[23],[95].However, it is easy to see in Figure (III.3c) that the electromagnetic torque created by the motor follows the load torque profile along the reference speed profile. Although it is absent and then quickly returns to the load value at the moment of velocity reversal and this proves the effectiveness of the backstepping control. Since the torque is originally related to the current Iq, then result obtained in the figure (III.3d) is similar to the figure (III.3c). In addition, figure (III.3e) shows that the five-phase stator currents have sinusoidal patterns when the speed is reversed. However, the current increases when the load charge is applied in t=0.2 s, as well as has null at the moment of velocity reversal, this shows the validity of the results. Also, figure (III.3f) shows the position of the rotor, which changes from sinusoidal, which had an acceleration phenomenon that occurs during the start-up (between 0 and 0.03 seconds), but There's a change in the direction of the fluctuation at t=o.25 s due of the reverse speed.

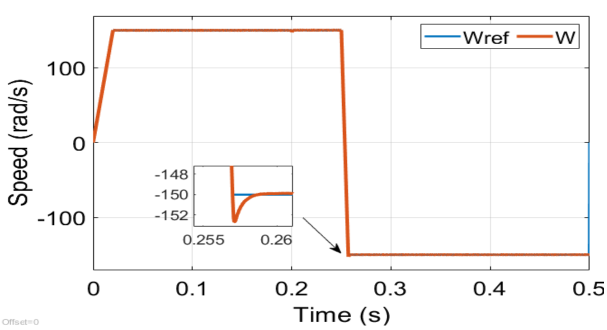

a)

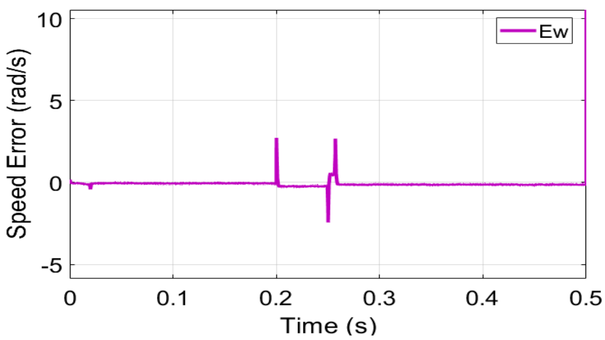

b)

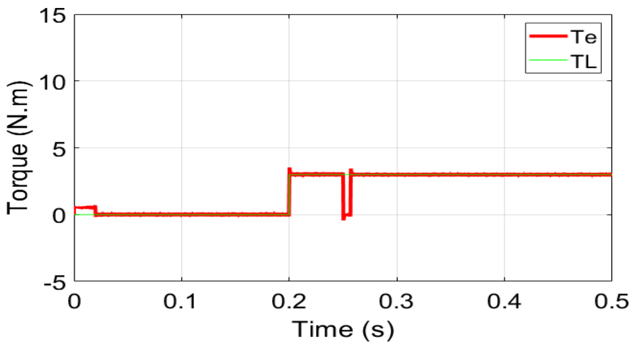

c)

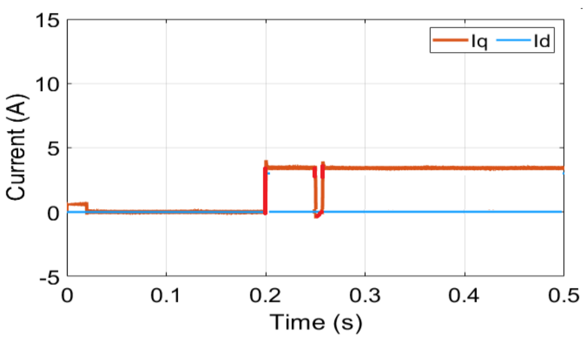

d)

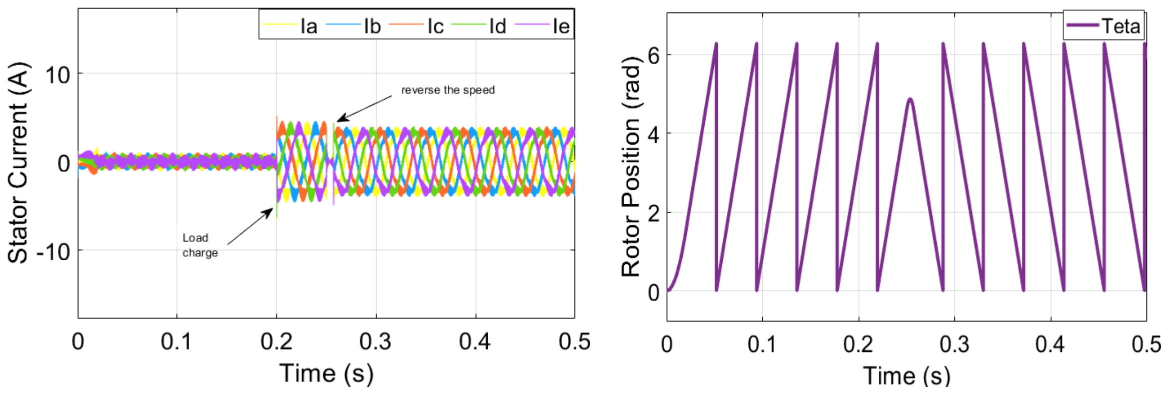

e) f)

Figure (III.3): Simulation results of proposed Backstepping control 5P-PMSM under reversal speed

III.8.3. Performance under open phase fault

The purpose of this test is to study the control performance when there is an opening of one or two phases. It is an indication of a fault that occurred in the motor during its operation. Where the load torque equal 3 Nm is delivered at time t=0.25s under the same preceding circumstances. The reference speed changes in two steps, from 0 to 150 rad/sec and from 150 rad/s to -150 rad/s, as shown in Figure (III.4a). The speed during open fault phase has several fluctuations, but it does not affect the performance of the control, that also shown in the figure (III,4b) which represent the speed error. The figures (III,4c) and (III, ad) indicate the torque and Iq current respectively have a title perturbation abandonable, whereasthe stator currents in the stationary reference frame shown in figure (III.4e). The motor operates under normal conditions till o,2s, with balanced currents in all five phases. The currents are stable and synchronized, indicating normal motor operation. So, at 0.2 seconds, a load is applied to the motor. This introduces a transient response in the stator currents, which then stabilize at a higher amplitude reflecting the increased load. Around 0.3 seconds, the motor undergoes a speed reversal. After that, at 0.4 seconds, an open-phase fault occurs, the remaining currents show increased oscillations and imbalances as the system tries to compensate for the loss of one phase. This results in distorted current waveforms indicating the fault. furthermore, the figure (III.4f) illustrates the rotor position in the reverse speed with fault event at 0.4 seconds, following this result, the rotor position waveform shows a marked deviation from its previous periodic pattern.

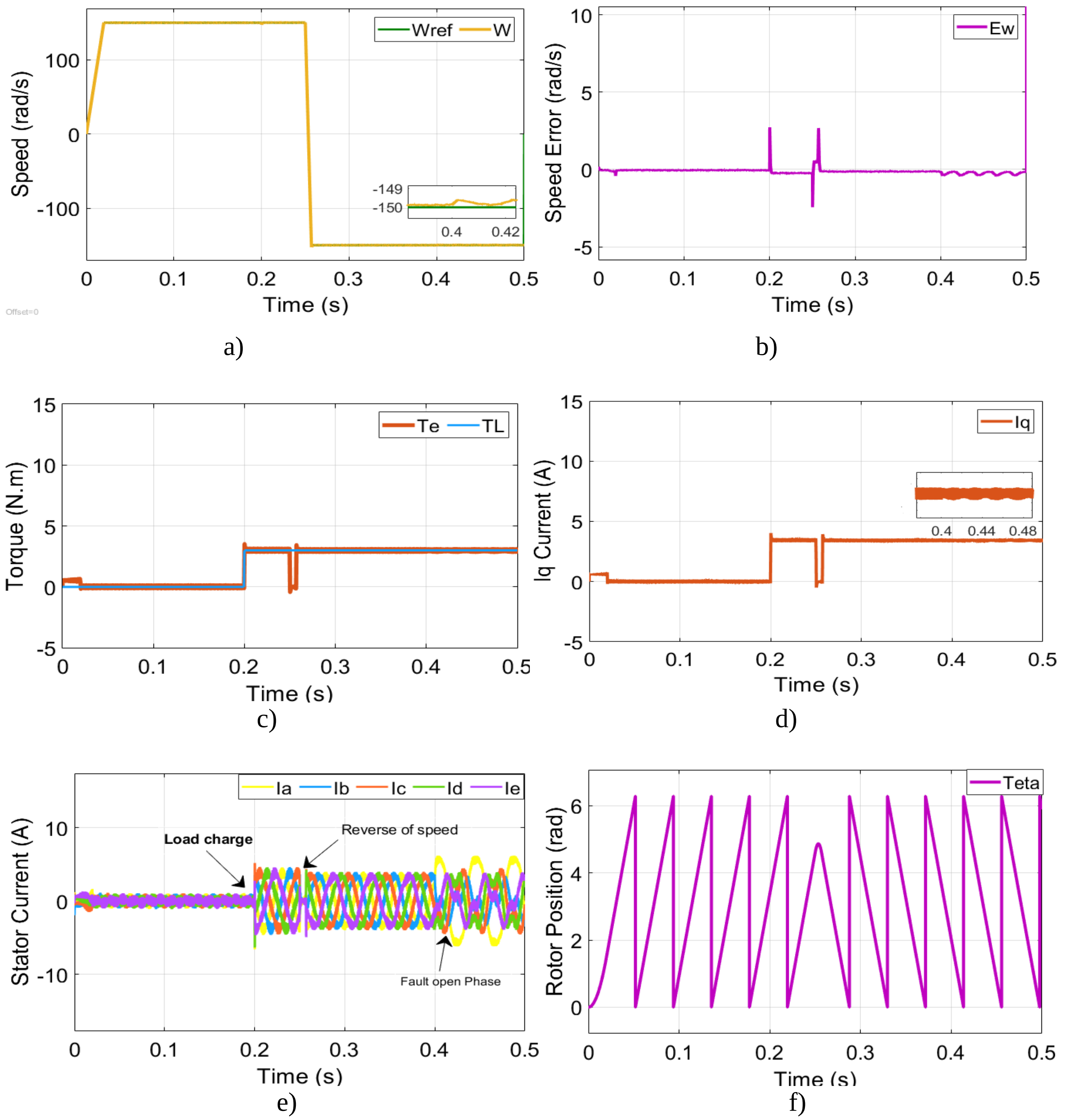

Figure (III.4): Simulation results of proposed Backstepping control 5P-PMSMunder open phase fault

In addition, these parameters that have been selected from multiple simulation sessions are:

Table III.1. Gains of backstepping controller

*c*1	*c*2	*c*3	*c*4
11000	500	500	5000

III.9. Conclusion

This chapter has provided a comprehensive overview of the backstepping control approach applied to a five-phase permanent magnet synchronous motor (5Φ-PMSM). The theoretical foundations of backstepping control were meticulously outlined, followed by a detailed application to the 5Φ-PMSM system. Through the use of MATLAB Simulink, the efficacy of this control strategy was rigorously tested under various conditions. The simulation results demonstrated the robust performance of the backstepping control in managing load torque variations, reversing motor speed, and handling fault conditions such as an open-phase fault. Each test underscored the ability of the backstepping controller to maintain stability, and ensure good performance despite the introduction of disturbances and faults. But these results were not optimal because the selection of backstepping gains was experimental, for solving this problem we will integrate genetic algorithms to improve control performance and obtain optimum performance. The promising results from these tests pave the way for further enhancements. The next chapter will delve into integrating a Sliding Mode Observer (SMO) with the optimized backstepping control. This addition aims to improve the system's fault tolerance and observer accuracy, thereby augmenting the overall control performance of the 5Φ-PMSM.

Chapter IV.

Optimized Sensorless Control of Five-Phases Permanent Magnet Synchronous Motor using Genetic Algorithm

IV.1. Introduction

In the proposed backstepping control, the design of control gains can lead to instability and poor performance,this makes precise tuning crucial for effective control.Setting the right gains is imptortant for achieving set performance measures like settling time and overshoot[103]. These issues highlight the importance of employing more advanced optimization methods. like the Artificial Technique algorithms. Previous studies have demonstrated the effectiveness of stochastic search methods, such as genetic algorithms, in generating the appropriate gains. Furthermore,a detailed assessment of the control algorithms' performance under different circumstances by implementing sensorless control in a closed-loop configuration becomes essential ,for estimate a crucial parameters such as motor speed and position,The use of real-time estimator also gives more efficiency and credibility to this control.

This chapter focuses on how to use Genetic Algorithms (GA) to enhance backstepping control and how to implement a Sliding Mode Observer (SMO) to enable sensorless control [104]. The primary objective is to improve the performance and reliability of 5Φ-PMSM drives across a range of operating conditions. Real-time estimation was performed using the OPAL-RT OP4500 platform to verify that the proposed control strategies were effective. In addition, several rigorous tests, such as load torque variations, robustness assessments, and industry trajectory evaluations, were conducted to assess how well the system performed under various conditions. The results demonstrate that the optimized backstepping control and the sensorless method using SMO maintain high performance and stability, even when motor settings change. The significance of these benefits underscores the applicability of the proposed methods in real-world industrial environments.

IV.2. optimized the backstepping control with Genetic algorithms

IV.2.1. History of Genetic algorithms

- **Early Development (1950s–1960s):** Holland introduced genetic algorithms in the 1950s and 1960s during his research on adaptable systems, establishing the foundation for this field. His concept involved using simplified models of natural evolution to address optimization and search problems [105]
- **Formalization (1970s):** Holland and his associates created the fundamental ideas of genetic algorithms during the 1970s, and he later formalized them in his seminal work "Adaptation in Natural and Artificial Systems" (1975). Genetic algorithms can now be applied to a wide range of problem areas thanks to this groundbreaking study. Holland developed the foundational concepts of genetic algorithms in the 1970s, later formalizing them in his influential work "Adaptation in Natural and Artificial Systems" (1975). This seminal research laid the

groundwork for the application of genetic algorithms across diverse problem areas, enabling their widespread use in solving complex problems [106].

- **Widespread Adoption (1990s):** Genetic algorithms saw a boom in popularity and use in the 1990s in a number of disciplines, including engineering, machine learning, artificial intelligence, and optimization. More advanced genetic algorithms were developed and used into useful applications during this time [107].
- **Sustained Progress (2000s–present):** Since the 2000s, academics have been investigating hybridization, parallelization, and the application of genetic algorithms to progressively complicated real-world situations, leading to further evolution of these algorithms. They are still widely used as an optimization and problem-solving tool today [108]

IV.2.2. Basic terms in genetic algorithms

- **Chromosomes**: String of genes serve as the foundational components used in constructing solutions through processes such as genetic mutation and crossover. A chromosome is configured to contain solution-relevant data, with the binary string format being the most commonly utilized method of encoding[109].
- **Population (Generation):** It refers to the set of chromosomes which represents a group of potential solutions to the optimization problem. Each solution is represented by a chromosome within the population, and the entire population constitutes a generation.
- **Objective Function:** called also a (cost function, optimization criterion, or fitness function, this function is the one the optimization algorithm seeks to optimize to find the best possible solution.
- **Reproduction:** This is the stage where chromosomes are combined. Reproduction in genetic algorithms refers to the process of generating offspring from parent individuals. This process involves two main operators: mutation and crossover. Mutation introduces random changes in the genetic information of an individual, ensuring diversity within the population[110].

These well-known terms in the field of genetic algorithms, which are represented in the figure below Figure (IV.1): are considered a major formation in the algorithm engineering to find the optimal solution.

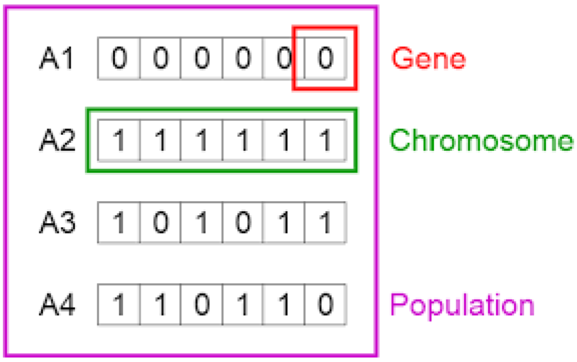

Figure (IV.1): Basic terms of Genetic Algorithm

IV.2.3. Definition of Genetic Algorithm

As a category of evolutionary algorithms, genetic algorithms use natural evolutionary processes and genetic concepts to address optimization problems. These algorithms emulate the mechanisms found in biological systems, such as natural selection, reproduction, and genetic variation. By iteratively generating and refining candidate solutions through operations like selection, crossover, and mutation, genetic algorithms strive to iteratively improve solution quality[111]. They operate on a population of potential solutions, mimicking the concept of a gene pool in biological evolution. Through successive generations, genetic algorithms evolve towards increasingly optimal solutions .This iterative process allows genetic algorithms to efficiently explore solution spaces and adapt to complex problem domains, making them versatile tools in optimization and problem-solving tasks across various fields [112].

IV.2.4. Applications of Genetic Algorithm

Genetic algorithms can be used in various fields, such as:

- Solving complex numerical optimization problems, including those with discontinuous functions.
- Processing images, like aligning satellite photos or identifying suspects.
- Optimizing schedules, designs, and controlling industrial systems.
- Training neural networks.
- Managing systems that change over time, such as production lines or nuclear power plants, because the population can adapt to evolving conditions.
- Optimizing different types of networks, including cable networks, optical Fiber networks, and infrastructure for water or gas distribution.

IV.2.5. Description the Structure of Genetic Algorithms

In the genetic algorithm, in order to facilitate problem solving, genetic algorithms are built upon the many principle’s phases. The first step is to create a starting community that will change over time. These groups represent potential solutions to a given problem. They are sometimes called people or chromosomes, and they can be made at random. This makes it possible for more variety.in this phase, the task does not involve discovering a definitive solution. The key is to discover a sufficient number of solutions that are capable of effectively addressing the problem. The greater the diversity of the initial population, the higher the likelihood of devising optimal solutions.[111], [113].

IV.2.5.1. Fitness function evaluation

The next phase refers to the fitness function, or the fitness criteria are applied at each stage to the population in order to evaluate which part of the population should be picked for future computations or to determine when the algorithm should be stopped.[114]

Applying genetic operators on individuals assessed by a certain fitness function enables the exploration of the solution space in order to find an extremum. Usually, the genetic algorithm is implemented by following these steps:

- Evaluate the fitness function for every member in the population.
- Generate a new population by applying procedures such as proportional selection, crossover, and mutation to individuals whose fitness function has recently been assessed.
- Eliminate the previous population and proceed to replicate the identical procedures with the new population.

The fitness function in genetic algorithms is application-specific and varies based on the application's requirements. It evaluates the quality of a hypothesis, sets a fitness threshold, determines the mutation rate, the size of the population, the fraction of population to be replaced, and the mutation rate. The design of the fitness function is crucial for optimal performance. The algorithm must be iterated multiple times for non-trivial problems. Fitness functions can be mutable or constant[111], [114].

Nowadays, several fitness functions are used in different sectors:

- ✓ Single variable single argument
- ✓ Multiple variable single arguments
- ✓ Multiple variables multiple arguments
- ✓ Vectorization of Fitness Function:

IV.2.5.2. Individual coding and decoding operations

To address a problem using Genetic Algorithms (GAs), encoding the parameters is an essential first step. Each gene within the genetic encoding corresponds to an optimization variable Xi, and a chromosome comprises a set of genes. An individual encompasses one or more chromosomes, and a population comprises a group of individuals.

Typically, in Genetic Algorithms, the parameters of the objective function are encoded, commonly using binary representation. The codes derived from this encoding are then utilized in lieu of the parameters themselves. Binary encoding, utilizing 0 and 1, is frequently adopted to represent variables. For instance, a gene might be represented as a long integer (32 bits). Binary encoding offers the advantage of facilitating the representation of various object types, including real numbers, integers, Boolean values, and character strings. The transition from one representation to another necessitates the application of encoding and decoding functions.[115], [116] .

For example: coding and decoding the number 150 are:

$$150 \Longleftrightarrow \mathbf{1\ 0\ 0\ 1\ 0\ 1\ 1\ 0}$$

IV.2.5.3. Selection of Individuals for Reproduction

Selection is the stage where individuals from the current population are chosen to contribute to the formation of the next generation. This selection is primarily determined by the fitness scores associated with each individual. Those with higher fitness values have a greater probability of being selected for reproduction, thereby passing on their genetic information to the subsequent generation.[113], [117].

The Selection of Individuals can be divided in different Methods:

IV.2.5.3.1. Lottery Wheel Selection

In this method, that called also of Roulette Wheel Selection, each individual is assigned a probability of being selected based on its fitness value. Individuals with higher fitness values have a greater chance of being selected. The selection process is analogous to a roulette wheel, where each individual is represented by a slice of the wheel proportional to its fitness value, each individual's probability of selection is computed as follows:[114].[118]

$$P_{seli} = fi / P_{fi} \qquad \text{(IV.01)}$$

After that, an array with each individual's cumulative probability is constructed. To find an array entry with a higher value for each random integer, n random numbers are created between 0 and P_{fi} As a result, people are chosen based on their chances of being chosen.

IV.2.5.3.2. Rank Selection

In rank selection, the population is first sorted based on the fitness values of the chromosomes. Each chromosome is then assigned a rank corresponding to its position in the sorted order. The chromosome with the lowest fitness gets rank 1, the next one rank 2, and so on, until the chromosome with the highest fitness, which receives rank N (where N is the total number of chromosomes in the population)[118].

The selection process for chromosomes based on rank is similar to roulette wheel selection, but the probabilities are determined by the ranks rather than the actual fitness values. This method ensures that all chromosomes have a non-zero chance of being selected. However, it can lead to slower convergence towards the optimal solution. This is because the best chromosomes do not have a significantly higher probability of selection compared to the worst ones, as the difference in their ranks is relatively small.[119].

IV.2.5.3.3. Steady-State Selection

This approach does not represent a specific method for selecting parent chromosomes. Instead, the central concept is that a substantial portion of the population can carry over to the next generation. The genetic algorithm operates in the following manner:

In each generation, a subset of chromosomes with the highest fitness values is chosen to produce offspring chromosomes. Subsequently, the chromosomes with the poorest performance are eliminated from the population and replaced by the newly created offspring. The remaining chromosomes, which constitute the majority of the population, are carried forward to the next generation.[120].

IV.2.5.3.4. Tournament Selection

In this method, a group of individuals (typically two or more) is randomly selected from the population, and the individual with the highest fitness value is chosen as a parent. This process is repeated until the desired number of parents is selected. Tournament selection can be further classified into deterministic and probabilistic variants [121], for example:

In a population of *N* chromosomes, *N* pairs of chromosomes are formed. In the parameters of the genetic algorithm, a probability of victory for the stronger chromosome is determined. This probability represents the chance that the better chromosome in each pair will be selected. This probability should be high (between 70% and 100%). From these *N* pairs, *N* individuals are selected for reproduction.[122].

IV.2.5.3.5. Elitism

Elitism is not a standalone selection method but is frequently combined with other selection techniques. In this approach, the individuals with the highest fitness from the current generation are directly transferred to the next generation, ensuring that the best solutions obtained so far are not lost during the evolutionary process [117]. During the process of generating a new population, there is a high risk of losing the best chromosomes after the crossover and mutation operations. To mitigate this issue, the elitism method is employed. It involves directly copying one or more of the fittest chromosomes into the new generation. Subsequently, the remaining individuals in the population are generated using the standard reproduction algorithm. This approach significantly enhances the performance of genetic algorithms as it ensures that the best solutions discovered so far are preserved [123].

Other methods that we have not detailed, such as the method: Stochastic Universal Sampling (SUS), Truncation Selection and Fitness Scaling. Generally, the choice of selection method depends on various factors, such as the problem domain, the fitness landscape, and the desired balance between exploration and exploitation. Different selection methods can be combined or modified to suit the specific requirements of the problem at hand [113],. Additionally, adaptive or dynamic selection methods that adjust the selection pressure during the evolutionary process can also be employed.

IV.2.5.4. Genetic Recombination

In the context of genetic recombination, two primary operators are identified: crossover and mutation, these two operators serve as the driving force behind the advancement and progress achieved by genetic algorithms.

IV.2.5.4.1. Crossover

Crossover, a natural characteristic of DNA, serves as an analogy for how crossover operations are executed in genetic algorithms. When two individuals (parents) are used, they give rise to two new individuals (children), who inherit specific traits from each parent [118].

In genetic algorithms, crossover selects genetic information from the parent individuals to create new ones. This process involves combining genes from both parents, resulting in children that share attributes from each. The crossover probability indicates the likelihood of crossover operations being applied during the genetic algorithm [124].

- Without crossover, the offspring are identical to their parents.
- When crossover occurs, the children are made up of components from each of their parents.
- When the probability is zero0%, the next generation exactly replicates the previous one.
- With a probability of 100%, all offspring are produced via crossover.

Crossover is used to make sure that the new chromosomes inherit the best elements from the old ones, which can lead to improved chromosomes. Nonetheless, it's crucial that a portion of the current population carries over into the new generation.

There are two types of crossovers:

IV.2.5.4.1.1. Single-Point Crossover

A crossover point is chosen randomly for every pair (see Figure IV.2).

A crossover point is chosen along the string of the parent organism. All data located after that point in the organism's string is exchanged between the two parent organisms. The strings exhibit Positional Bias, the crossover takes place at the binary level, not at the gene level, and it may intersect within a gene's sequence.

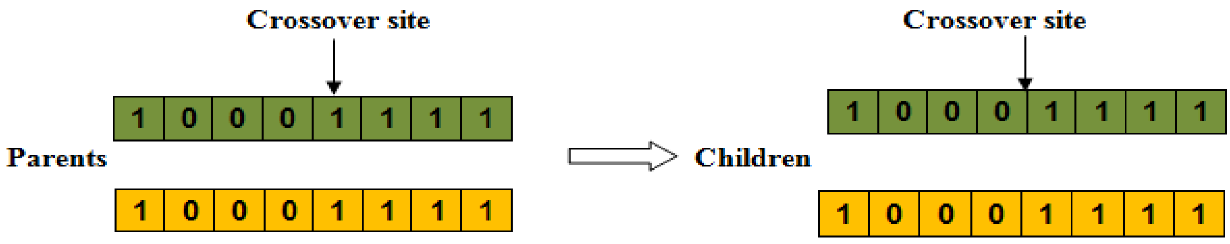

Figure (IV.2): Single-point crossover representation

IV.2.5.4.1.2. Multipoint Crossover

Unlike single-point crossover, multipoint crossover involves utilizing more than one pivot point. This amplifies the degree of disturbance to the original parent chromosomes. As illustrated in Figure (IV.3), genetic material between two designated crossover points, situated to the right of an even (or odd) number of pivot points, is exchanged to generate two distinct offspring individuals.[125].

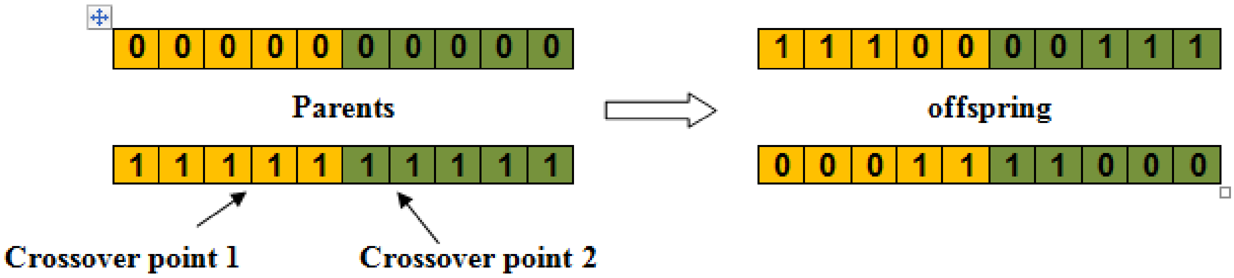

Figure (IV.3): Multipoint crossover representation

IV.2.5.4.1.3. Uniform Crossover

Uniform crossover that represented in Figure (IV.4) ensures consistency in blending the bits from both parents. This process involves swapping bits between the parents to incorporate them into the offspring, achieved by selecting a uniform random real number ranging from 0 to 1. This method chooses the two parents for crossover, producing two child offspring each comprising 'n' genes selected from both parents uniformly. The selection of genes for the first child from either the first or second parent is determined by a random real number.[126].

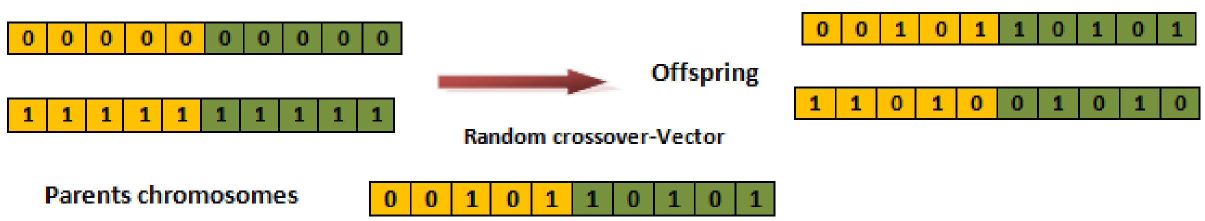

Figure (IV.4): Uniform crossover representation

IV.2.5.4.2. Mutation

The effectiveness of our genetic algorithms is influenced by the quantity of genes (variables) within a chromosome that are permitted to undergo mutation. Traditionally, mutation has been viewed as a peripheral operator, yet it imbues genetic algorithms with the property of ergodicity, meaning all points within the search space can be reached. This operator serves a dual purpose:

- ✓ It facilitates local exploration by making small changes to solutions, allowing for a fine-tuned search in the nearby regions of the search space.
- ✓ It enables the algorithm to escape from local optima or areas where the search has become trapped by introducing larger, more disruptive modifications to the solutions[127].

This long-range search capability helps the algorithm explore distant regions of the search space, preventing it from becoming stuck indefinitely. Mutation creates "copying errors" that lead to the formation of a new individual, one that did not previously exist. This process aims to keep the genetic algorithm from converging to local function extremes and facilitates the creation of unique elements. If mutation results in a less fit individual, that individual is usually discarded. The mutation probability indicates how often the genes in a chromosome are subject to mutation noted by P_{mut}.

- If mutation does not occur, the offspring is added to the new population without any modifications.
- If mutation occurs, a segment of the chromosome is altered.

The mutation approach principle of Algorithm Genetic is depicted in Figure (IV.5) below.

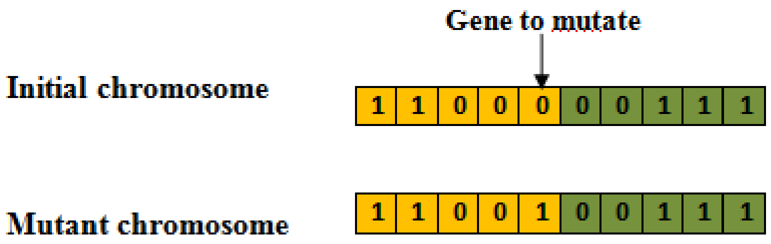

Figure (IV.5): Principal of mutation method in GA

Different types of mutation operators exist, such as:

IV.2.5.4.2.1. Bit Flip Mutation

A single bit in the chromosome is flipped from 0 to 1 or vice versa.

IV.2.5.4.2.2. Random Resetting Mutation

A random gene within the chromosome is replaced with a random value.

IV.2.5.4.2.3. Swap Mutation

Two genes within the chromosome are swapped.

IV.2.5.4.2.4. Scramble Mutation

A subset of genes within the chromosome is randomly shuffled.

IV.2.5.4.2.5. Inversion Mutation

A subset of genes is reversed, creating an inversion in the genetic sequence.

The choice of mutation operator and its rate (frequency of mutation) affects the algorithm's balance between exploration and exploitation, impacting its efficiency and convergence behaviour[128].

However, genetic algorithm (GA) is a metaheuristic optimization algorithm inspired by the process of natural selection and genetics. It is used to find optimal or near-optimal solutions to complex problems by mimicking the principles of biological evolution. Here are the basics of a genetic algorithm summarized in the next figure (IV.6):

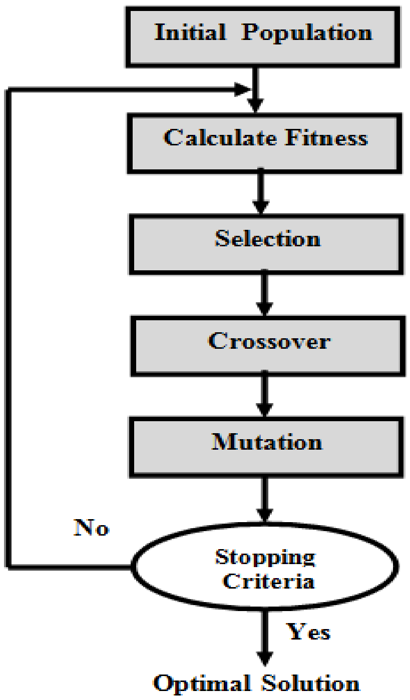

Figure (IV.6): Basic of genetic algorithm steps

IV.2.6. Selecting the Parameters for a Genetic Algorithm

To start a genetic algorithm, you need to set certain parameters, including the population size, mutation and crossover rates, and the number of generations. There is no exact formula for determining the ideal values for these parameters, making it a tuning issue that must be customized for each specific problem. This task is a major component of the experimenter's role. In research, the specification of these parameters can differ widely from one application to another. The parameters under consideration include population size, the number of generations, and the likelihood of reproduction[129][130]

IV.2.6.1. Population Size

A good population size should be big enough to ensure adequate genetic diversity, helping the algorithm explore the search space thoroughly and avoid being stuck in local optima. However, it shouldn't be excessively large to avoid creating unnecessary computational load, individuals numbers must be is considered a good starting point for most problems[131].

The complexity of the problem, the size of the search space, the desired rate of convergence, and the available computer resources are some of the factors that affect the population size decision. Starting with a small population size and adjusting it based on the genetic algorithm's observed success is a popular strategy.[132].

IV.2.6.2. Number of Generations

The number of generations is a value that the experimenter must set, based on the characteristics of the function being optimized and the number of its variables. When the function has a lot of variables, it usually requires a larger population in the search space, which leads to the need for more generations to reach an optimal solution. The challenge is to achieve convergence within a fewer number of generations.[133].

IV.2.6.3. Probability of Genetic Operators

Determining the mutation probability (P_{mut}) and crossover probability (P_{cross}) is a complex nonlinear optimization problem. These probabilities are influenced by the characteristics of the objective function and might require experimental tuning to get right.

Typically, a high crossover probability is chosen to encourage genetic recombination and speed up convergence toward the best solutions. A low mutation probability is preferred to minimize interference with the results from crossover. Despite being low, this mutation rate helps prevent premature convergence and allows exploration of new areas in the search space.[134].

IV.2.6.4. Termination Criterion

As with any iterative algorithm, it's crucial to establish a termination criterion. This can be defined in several ways[135], such as:

- Ending the algorithm once a satisfactory solution is achieved.
- Stopping if there's no improvement over a specific number of generations.
- Halting when a set number of generations has been reached.

In more detail, the steps these algorithms follow can be outlined in a flowchart, like the one shown in next Figure (4.7).

IV.2.7. Tuning of Genetic Algorithm Parameters

Optimizing a genetic algorithm's performance involves carefully adjusting various parameters. The way these parameters are tuned significantly influences how quickly the genetic algorithm converges on a solution and the quality of the results it produces. However, there are no definitive rules for setting the ideal parameter values for a genetic algorithm. These values are typically determined through trial-and-error and empirical testing.[136], some key considerations when tuning a genetic algorithm's parameters include:

- The probability of crossover plays a key role in determining how quickly a genetic algorithm converges. A higher crossover probability tends to increase the recombination of individuals, but it also raises the chances of getting stuck in a local optimum. Generally, typical crossover probabilities fall within the range of 0.6 to 0.95.

- The mutation probability should be lower than the crossover probability to prevent the algorithm's evolution from being overly disrupted. If this value is too high, the algorithm can become akin to a random search, but if it's too low, it might struggle to escape local optima. Generally, the typical range for this parameter is between 0.001 and 0.2.[137] .

IV.2.8. Optimization Problem Solved by Genetic Algorithms

Genetic algorithms (GA) are a powerful optimization approach inspired by the principles of natural selection and genetics, they are designed to solve complex optimization problems by iteratively evolving a population of solutions through processes such as selection, crossover, and mutation. Where the goal is to find the best solution among many possibilities.GA is used for a variety of optimization problems, including:

- Genetic algorithms can optimize complex mathematical functions to find global optima, overcoming issues like local minima and discontinuities [138].
- GA can solve problems like the traveling salesman problem or scheduling, where a large number of possible configurations exist [139].
- GA can optimize parameters in machine learning tasks, aiding in finding the best configurations for models [140].
- GA can be used to optimize control systems that need to adapt to changing conditions over time [112].

IV.3. Implementation the Genetic Algorithm for optimizing the Backstepping control

Genetic algorithms (GAs) are powerful stochastic global search techniques inspired by the principles of natural selection and genetics. They are designed to find optimal or near-optimal solutions to complex optimization problems across various fields. These algorithms are particularly effective in solving problems where traditional methods struggle due to large search spaces, non-linearity, or the presence of multiple local optima. Their versatility enables their application in diverse domains such as management for resource allocation, economics for financial modeling, industrial processes for scheduling or design optimization, and even scientific research. By balancing exploration and exploitation of the search space[15]. GAs provides robust and flexible tools for tackling challenging optimization tasks Figure (IV.7) shows flowchart of GA.

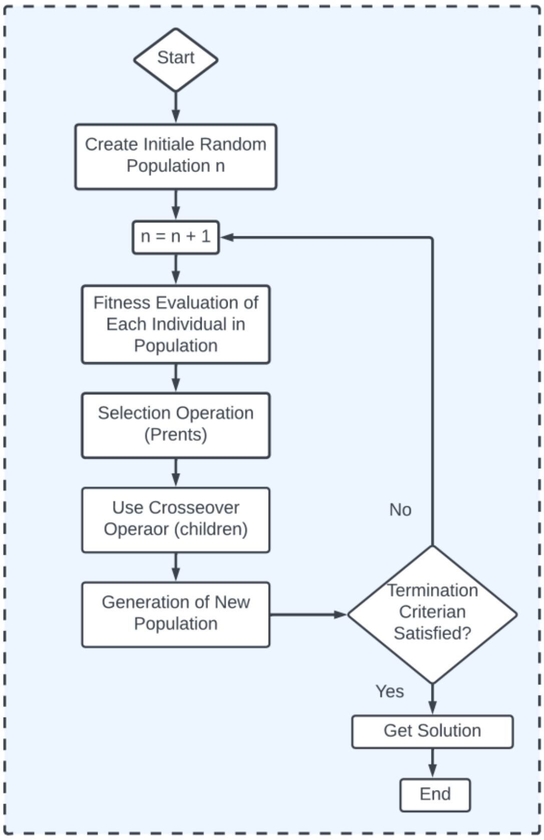

Figure (IV.7): Flowchart of standard GA.

The choice of control gains is the main issue with the Backstepping control[18]. In order to address this difficulty, it seems necessary to employ stochastic optimization approaches. Consequently, this work proposes the use of a genetic algorithm to solve the discrete model of the dynamical system equations. In this work, the proposed Genetic Algorithms (GAs) are built based on five crucial stages:

IV.3.1. Chromosome design

As shown in Figure (IV.8), the genes that will build the chromosomes are the control gains.

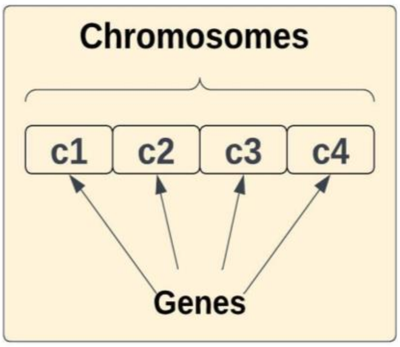

Figure (IV.8). Chromosome structure.

IV.3.2. Encoding

A decimal coding is chosen in this work for its simplicity over binary coding, as well as because the control gains take a decimal number value.

IV.3.3. Selection function

A selection algorithm is used that combines the threshold and the tournament of two competitors with a selection probability $P_s = 0.8$ .where:

- ✓ **Threshold Selection:** This approach establishes a minimal level of fitness (threshold) that candidates must fulfil in order to be considered for selection. Only those whose level of fitness is higher than this cutoff are taken into consideration for the following phase[141].
- ✓ **Selection of the Tournament:** Using this method, a tournament, or subset of people, is selected at random from the general population. A crossover is made up of the best person (the one with the highest fitness) in this subset. Regarding the phrase "tournament of two competitors," it denotes a competition wherein only two participants participate, and the winner is determined based on fitness level[142].

This gives the selection process an additional probabilistic component. There is a chance attached to selection, which can add some randomness and preserve genetic variety within the population, as opposed to always choosing the greatest player in the competition.

IV.3.4. Genetic operator

a linear discrete crossing of the parent is performed, resulting in three possible children (F_1, F_2, F_3) as:

$$\begin{cases} F_1 = 0.5\left(P_1 + P_2\right) \\ F_2 = 1.5P_1 - 0.5P_2 \\ F_3 = -0.5P_1 + 1.5P_2 \end{cases} \tag{IV.02}$$

With P1 and P2 are selection probability of two competitors (parents).

After evaluating the three children and verifying for constraints, the two better children are chosen and considered descendants.

IV.3.5. Mutation operator

The Gaussian mutation offers valuable advantages by providing precise control over the level of diversity introduced during the mutation. This process enhances diversity among the population by incorporating a randomly generated value from a Gaussian (normal) distribution into each element of an individual's vector. it arbitrary inclusion facilitate exploring the range of possibilities and promote convergence in optimization issues. Initially, we apply more intense mutations to explore a wider range of possibilities, reserving milder mutations for later stages to refine solutions.

[143] , in this case a Gaussian mutation is used with a variable percentage of children, which decreases linearly. A distance restriction is also set on mutation magnitude, which lowers as the number of generations' increases.

Moreover, the following constraints must be considered:

- Parameters ($c1, c2, c3, c4$) defined intervals
- Physical limitations of 5Φ-PMSM drive in terms of stator voltages, currents, and torque.

The objective function is computed by considering the numerous characteristics that characterize the intended performance. We considered the time responses, overshoots, dynamic errors and of the current and rotor speed of 5Φ-PMSM drive. The fitness is the total of these characteristics, which must be reduced by the genetic algorithm as:

$$\Gamma = \Delta\omega + \Delta i + \Delta T_{r\omega} + \Delta T_{ri} + D(\omega) + D(i) \qquad \text{(IV.03)}$$

where, $\Delta\omega$ and Δi are the relative errors of speed and current. $\Delta T_{r\omega}$ and ΔT_{ri} are the time response errors of speed and current. $D(\omega)$, $D(i)$ are the overshoots of speed and current. The following figures (IV.9) represent a block diagram used in the context of optimizing the control of a 5Φ-PMSM.

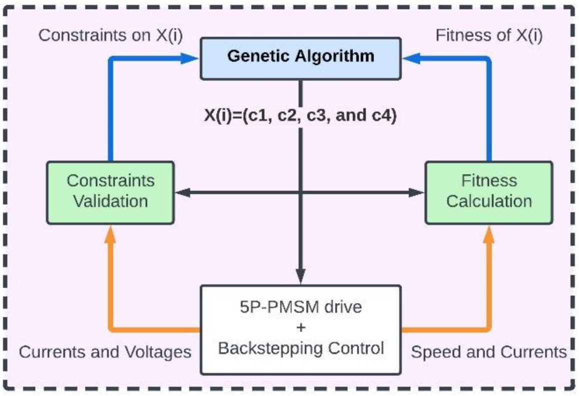

Figure (IV.9). Bloc diagram of the gain's determination algorithm.

Finally, the backstepping controller gains based on AG are selected in Table IV.1.

Table IV.1. Gains of backstepping controller

$c1$	$c2$	$c3$	$c4$
6000	4000	2500	800

To thoroughly examine and ensure the performance and reliability of a control system, particularly in applications where precision and stability are critical, obtaining accurate speed values for a five-phase Permanent Magnet Synchronous Motor is essential for evaluating the effectiveness of improved control systems. A detailed assessment of the control algorithms' performance under different circumstances is made possible by the accurate measurement of speed. Furthermore, implementing sensorless control in a closed-loop configuration becomes essential. Sensorless control techniques utilize advanced algorithms to estimate crucial parameters such as motor speed and position without the need for physical sensors. For sensorless control in various industrial application, Sliding Mode Observers are powerful tools in control systems engineering, particularly for systems requiring robust performance in the presence of uncertainties and disturbances. By leveraging the principles of sliding mode control, SMOs offer precise and reliable state estimation[144], [145], making them suitable for a variety of complex and nonlinear applications. In the next part, sensorless control of optimized backstepping control of 5Φ-PMSM is investigated with real-time implementation

IV.4. Sensorless of the System control using Slide model observer

With an excellent grasp of motor speed facilitates the identification of potential inefficiencies or opportunities for control plan improvement. By comparing expected and actual performance, it is possible to fine-tune control parameters and enhance efficiency, stability, and responsiveness even further. When reliable speed data is unavailable, it becomes more challenging to design and assess robust control systems for complex applications, which reduces the effectiveness of optimization techniques. Accurate speed measurement plays a crucial role in helping 5Φ-PMSM systems assess and refine their optimal control strategies[146]. It follows that selecting an observer model is crucial. Since we discussed in chapter 1, there are numerous models. And because of the Sliding Mode Observer's (SMO) numerous benefits, we have been selected on the sensorless control mechanism.

IV.4.1. Slide model observer

A Sliding Mode Observer (SMO) is a type of state observer used primarily in control systems to estimate the state of a dynamic system. It is particularly useful for systems with non-linearity and uncertainties. The core idea behind a sliding mode observer is to force the estimation error dynamics to "slide" along a predefined surface, ensuring robustness to model inaccuracies and external disturbances. Here’s an overview of the key concepts and features of SMO:

IV.4.1.1. Overview of SMO

The idea of sliding mode control (SMC) first appeared in the 1950s and 1960s as to handle the control of nonlinear systems by changing their dynamics through discontinuous control actions, this prepared the way for sliding mode observers to be developed. Whereas, in the latter half of the 20th century, SMO formalisation and application started to gain up, in order to create observers that could estimate system states in the face of disruptions and model uncertainty, researchers concentrated on taking use of the inherent robustness of sliding mode approaches. Early SMO applications were mostly in electrical engineering, namely in motor control. In sensorless motor control applications, like Permanent Magnet Synchronous Motors (PMSMs), SMOs were used to estimate rotor position and speed[147]. Over the years, SMOs have been able to estimate states and velocities in mechanical systems with more precision and less chattering thanks to developments like the creation of second-order sliding mode algorithms, such as the super-twisting algorithm [148].and adaptative control method.

Today, the SMOs are now widely employed in many different industries, including as the automotive, aerospace, and robotics sectors. Because of their resilience to model uncertainties and outside disruptions, they are incorporated into contemporary control systems and offer dependable state estimates in real-time applications.

IV.4.1.2. Structure General of SMO

The basic form of a sliding mode Observer depends on the system model, which typically involves adding a discontinuous term to the observer's dynamics to enforce sliding mode behaviour. The following figure (IV.10) illustrate the main structure of sliding mode observer:

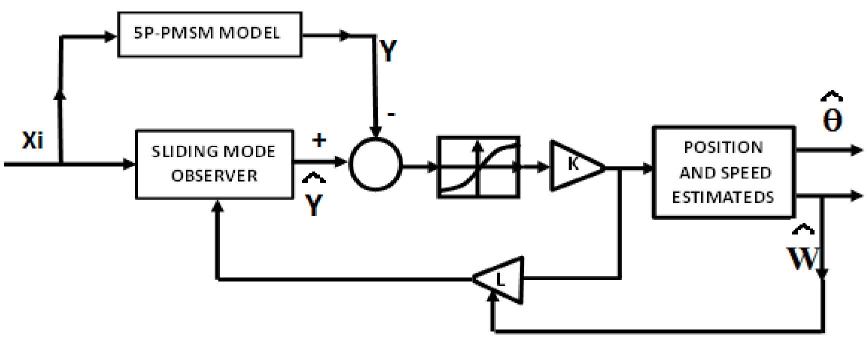

Fig (IV.10): The basic form of a sliding mode Observer

Here's a main structured to designing of SMO:

IV.4.1.2.1. Define the System Model

Establish the system you wish to observe first. This is often provided by a collection of linear state-space equations:

$$\begin{cases} \dot{x} = Ax + Bu + w \\ y = Cx + v \end{cases} \qquad \text{(IV.04)}$$

Where: x is the state vector of system, u is the control input, and y is the output measurement.

A, B, C are the system matrix and w, v are process and measurement noise, respectively.

IV.4.1.2.2. Design the Observer Structure

A sliding mode observer model can be described as follows:

$$\begin{cases} \dot{\hat{x}} = A\hat{x} + Bu + L(y - \hat{y}) + H(s) \\ \hat{y} = C\hat{x} \end{cases} \quad \text{(IV.05)}$$

$\hat{x}, \hat{y}$ are the estimated state variable and output vectors of observer respectively, H(s) is the discontinuity term as signum function `K sign (s)´ and `L´ is an observer gain.

IV.4.1.2.3. Define the Sliding Surface

Typically, the sliding surface *s* is defined in terms of the estimation error:

$$s = (y - \hat{y}) = C(x - \hat{x}) \quad \text{(IV.06)}$$

IV.4.1.2.4. Calculate the Observer Gain *L*

Usually, the observer gains L and K are chosen to guarantee the dynamics of the estimate error stability. Methods like calculating a linear matrix inequality (LMI) [149], placing poles can be used for this issue. Lyapunov stability approach too and adaptive sliding mode observer method.

IV.4.1.2. Different types of SMO

Conventional sliding mode observer principles, which estimate rotor position by observing the back-EMF (electromotive force) of the motor, often suffer from chattering, a high-frequency oscillation that can affect performance[150]. Several methods have emerged to improve upon the basic SMO, including:

IV.4.1.2.1. Novel SMO

These techniques frequently use sophisticated filters or algorithms to streamline the estimating process and produce more dependable results[151].

IV.4.1.2.2. PLL-based SMO

Combining SMO with Phase-Locked Loop (PLL) helps enhance rotor position estimation. By assisting in the synchronisation of the estimated and actual signals, the PLL lowers estimation errors and speeds up response times[152].

IV.4.1.2.3. Extended Sliding Mode Observer

These observers are developed for nonlinear systems; to address nonlinearities in the dynamics of the system, they expand the concepts of sliding mode observation to Handles nonlinear system dynamics using extended state-space representations. The disadvantage of this type is more complex analysis and design.

IV.4.1.2.4. High-Order Sliding Mode Observer (HOSMO)

The design involves making a sliding mode surface with higher-order dynamics that converges in finite time and is stable even when parameters change or there are outside disturbances.[153]So, it eliminates the chattering phenomenon observed in classical SMOs. In real applications, they offer improved performance and more smoother control activities. Among them a Super-Twisting Observer.

IV.4.1.2.5. Adaptive Sliding Mode Observer (ASMO)

An adaptive sliding mode observer (ASMO) is crafted to estimate system states while accommodating variations in system dynamics and disturbances. This observer integrates the robustness of sliding mode control with adaptive methods to effectively manage parameter uncertainties and external disturbances [154], Usually, this method uses the back-EMF generated by the motor to estimate rotor position and speed, such as back-EMF-based SMO.

IV.4.1.2.6. Robust Sliding Mode Observer

Despite uncertainties and disturbances, a robust sliding mode observer (SMO) can correctly estimate the states of a system. Specifically, the design of this type of observer enhances robustness against a wide range of uncertainties and disturbances, including non-linear and uncertain system dynamics[155].Systems also use robust SMOs for diagnosing actuator faults. It typically involves additional design criteria to maximize robustness.

IV.4.1.2. Implementation the SMO for sensorless control of 5P-PMSM

In this section, a slide model observer (SMO) is suggested to estimate the back-EMF and the 5Φ-PMSM speed as well as rotor position, where the stator voltages are considered measurable and taken as the observer inputs. The dynamic nonlinear model of the SMO can be constructed in the stationary reference frame ($\alpha 1-\beta 1-\alpha 2-\beta 2$) as follows:

$$\begin{cases} L_s \dfrac{d\hat{i}_{\alpha 1}}{dt} = -R_s \hat{i}_{\alpha 1} + V_{\alpha 1} - K_1 sat\left(s_{\alpha 1}\right) \\ L_s \dfrac{d\hat{i}_{\beta 1}}{dt} = -R_s \hat{i}_{\beta 1} + V_{\beta 1} - K_1 sat\left(s_{\beta 1}\right) \\ L_{ls} \dfrac{d\hat{i}_{\alpha 2}}{dt} = -R_s \hat{i}_{\alpha 2} + V_{\alpha 2} - K_2 sat\left(s_{\alpha 2}\right) \\ L_{ls} \dfrac{d\hat{i}_{\beta 2}}{dt} = -R_s \hat{i}_{\beta 2} + V_{\beta 2} - K_2 sat\left(s_{\beta 2}\right) \end{cases} \tag{IV.07}$$

Where, K_1 and K_2 are the observer gains. Also, $sat(s)$ is saturation function, which is expressed as [4.5]:

$$sat(s) = \begin{cases} 1 & if \quad s \succ \chi \\ \dfrac{s}{\chi} & if \quad |s| \le \chi \\ -1 & if \quad s \prec \chi \end{cases} \qquad \text{(IV.08)}$$

Where, χ is positive constant $S(X) = \begin{bmatrix} s_{\alpha 1} & s_{\beta 1} & s_{\alpha 2} & s_{\beta 2} \end{bmatrix}^T = \begin{bmatrix} \hat{i}_{\alpha\beta} - i_{\alpha\beta} \end{bmatrix}^T$ is sliding surface.

The stability of the SMO system based on the Lyapunov function is studied under two conditions, the first one is the Lyapunov function should be positive. While the second condition is the derivative of the sliding function is negative, which is selected as:

$$H = \frac{1}{2} S(X)^T S(X) \qquad \text{(IV.09)}$$

Its derivative is written as:

$$\dot{H} = \frac{1}{2} S(X)^T \dot{S}(X) = s_{\alpha 1}\dot{s}_{\alpha 1} + s_{\beta 1}\dot{s}_{\beta 1} + s_{\alpha 2}\dot{s}_{\alpha 2} + s_{\beta 2}\dot{s}_{\beta 2} < 0 \qquad \text{(IV.10)}$$

Thus, the derivative of estimation error can be computed as:

$$\begin{cases} L_s \dfrac{ds_{\alpha 1}}{dt} = -R_s s_{\alpha 1} + e_{\alpha 1} - K_1 sat(s_{\alpha 1}) \\ L_s \dfrac{ds_{\beta 1}}{dt} = -R_s s_{\beta 1} + e_{\beta 1} - K_1 sat(s_{\beta 1}) \\ L_{ls} \dfrac{ds_{\alpha 2}}{dt} = -R_s s_{\alpha 2} + e_{\alpha 2} - K_2 sat(s_{\alpha 2}) \\ L_{ls} \dfrac{ds_{\beta 2}}{dt} = -R_s s_{\beta 2} + e_{\beta 2} - K_2 sat(s_{\beta 2}) \end{cases} \qquad \text{(IV.11)}$$

By carefully selecting the observer gains, the presented SMO can achieve the separation between observer design and state feedback. When the system arrives to the sliding surface.

$$\dot{S}(X) = S(X) = 0 \qquad \text{(IV.12)}$$

Substituting (IV.12) into (IV.11) yields:

$$\begin{cases} e_{\alpha 1} = K_1 sat(\hat{i}_{\alpha 1} - i_{\alpha 1}) \\ e_{\beta 1} = K_1 sat(\hat{i}_{\beta 1} - i_{\beta 1}) \\ e_{\alpha 2} = K_2 sat(\hat{i}_{\alpha 2} - i_{\alpha 2}) \\ e_{\beta 2} = K_2 sat(\hat{i}_{\beta 2} - i_{\beta 2}) \end{cases} \qquad \text{(IV.13)}$$

On the other hand, a simple algorithm of speed sensorless control is built to extract the back EMF value for good filtering so to estimate the 5Φ-PMSM speed, which can be written as follows:

$$\begin{cases} \dfrac{d\tilde{e}_{\alpha1}}{dt} = -\tilde{\omega}_r\hat{e}_{\beta1} - \omega_r\tilde{e}_{\beta1} - m\tilde{e}_{\alpha1} \\ \dfrac{d\tilde{e}_{\beta1}}{dt} = \tilde{\omega}_r\hat{e}_{\alpha1} + \omega_r\tilde{e}_{\alpha1} - m\tilde{e}_{\beta1} \\ \dfrac{d\tilde{e}_{\alpha2}}{dt} = -m_1\tilde{e}_{\alpha2} \\ \dfrac{d\tilde{e}_{\beta2}}{dt} = -m_1\tilde{e}_{\beta2} \end{cases} \tag{IV.14}$$

Where, $\tilde{e}_{\alpha1} = \hat{e}_{\alpha1} - e_{\alpha1}$, $\tilde{e}_{\beta1} = \hat{e}_{\beta1} - e_{\beta1}$, $\tilde{e}_{\alpha2} = \hat{e}_{\alpha2} - e_{\alpha2}$, $\tilde{e}_{\beta2} = \hat{e}_{\beta2} - e_{\beta2}$ and $\tilde{\omega}_r = \hat{\omega}_r - \omega_r$.

Also, m, m_1 are constants that are obtained by applying the given stability conditions.

Therefore, to demonstrate the stability of system (IV.14), a new Lyapunov function is given as follows [11]:

$$H_1 = \frac{\tilde{e}_{\alpha1}^2 + \tilde{e}_{\beta1}^2 + \tilde{e}_{\alpha2}^2 + \tilde{e}_{\beta2}^2}{2} + \frac{\tilde{\omega}_r^2}{2\lambda} \tag{IV.15}$$

Its derivative is written as:

$$\dot{H}_1 = \dot{\tilde{e}}_{\alpha1}\tilde{e}_{\alpha1} + \dot{\tilde{e}}_{\beta1}\tilde{e}_{\beta1} + \dot{\tilde{e}}_{\alpha2}\tilde{e}_{\alpha2} + \dot{\tilde{e}}_{\beta2}\tilde{e}_{\beta2} + \frac{1}{\lambda}\tilde{\omega}_r\dot{\hat{\omega}}_r \tag{IV.16}$$

Were, $\lambda > 0$

Substituting (IV.14) into (IV.16) yields:

$$\dot{H}_1 = -m\left(\tilde{e}_{\alpha1}^2 + \tilde{e}_{\beta1}^2\right) - m_1\left(\tilde{e}_{\alpha2}^2 + \tilde{e}_{\beta2}^2\right) + \tilde{\omega}_r\left(\hat{e}_{\alpha1}\tilde{e}_{\beta1} - \hat{e}_{\beta1}\tilde{e}_{\alpha1} + \frac{1}{\lambda}\dot{\hat{\omega}}_r\right) \tag{IV.17}$$

The function H_1 is positive. Thus, the first stability requirement is satisfied. The second requirement is that the derivative of the H_1 be smaller than zero. It is important for them $\dot{H}_1$ to be negative as:

$$\begin{cases} -m\left(\tilde{e}_{\alpha1}^2 + \tilde{e}_{\beta1}^2\right) - m_1\left(\tilde{e}_{\alpha2}^2 + \tilde{e}_{\beta2}^2\right) < 0 \\ \tilde{\omega}_r\left(\hat{e}_{\alpha1}\tilde{e}_{\beta1} - \hat{e}_{\beta1}\tilde{e}_{\alpha1} + \dfrac{1}{\lambda}\dot{\hat{\omega}}_r\right) = 0 \end{cases} \tag{IV.18}$$

Based on the estimated back EMF value, the estimated 5Φ-PMSM speed as follows:

$$\hat{\omega}_r = \lambda\int\left(\tilde{e}_{\alpha1}\hat{e}_{\beta1} - \tilde{e}_{\beta1}\hat{e}_{\alpha1}\right)\, dt \tag{IV.19}$$

Finally, the adaptation law based on PI controller is computed as:

$$\hat{\omega}_r = K_{P\omega}\left(\tilde{e}_{\alpha 1}\hat{e}_{\beta 1} - \tilde{e}_{\beta 1}\hat{e}_{\alpha 1}\right) + K_{I\omega}\int\left(\tilde{e}_{\alpha 1}\hat{e}_{\beta 1} - \tilde{e}_{\beta 1}\hat{e}_{\alpha 1}\right) dt \qquad \text{(IV.20)}$$

$$\hat{\theta}_r = -\arctan\left(\frac{\hat{e}_{\alpha 1}}{\hat{e}_{\beta 1}}\right) \qquad \text{(IV.21)}$$

Where, $K_{P\omega}$ and $K_{I\omega}$ are the PI speed gains. The constant gains used in SMO are chosen in Table IV.2, which is used in the real time simulation tests.

Table IV.2. Constant gains of SMO algorithm

K_1	K_2	$K_{P\omega}$	$K_{I\omega}$
700	300	25	0.15

The general structure of the suggested observer for 5P-PMSM drive is presented in Figure (IV.11). As can be seen, the feedback currents $i_{\alpha 1}$, $i_{\beta 1}$, $i_{\alpha 2}$, $i_{\beta 2}$ and the stator voltage $V_{\alpha 1}$, $V_{\beta 1}$, $V_{\alpha 2}$, $V_{\beta 2}$ are the SMO inputs. While the estimated 5P-PMSM speed and rotor position are the outputs of the suggested observer.

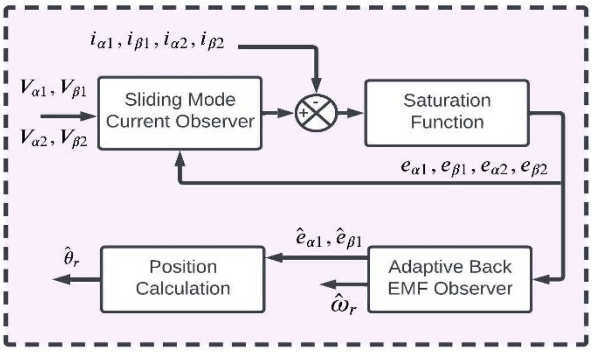

Figure. (IV.11). General structure of the suggested observer for 5P-PMSM drive.

IV.4.2. Real time implementation

Using the real-time implementation aims to test the control system to make simulation and implementation happen quickly in real-time. This method makes it easier to create and test control strategies in real-world situations, which ensures that the performance of the control system is accurately evaluated and improved. A key feature of the created control algorithm is its ability to operate in real-time. This is because computer technology and control theory are always being used and improved in the area of automation. As the name suggests, real-time systems can run programs that need to be run within a certain amount of time[156].Real-time simulation tools like OPL 4500 make it possible to integrate advanced control algorithms and test them in a changing environment, which is essential for the successful use of control systems in many situations.

OPAL-RT is the world leader in making PC/FPGA-based real-time simulators, Hardware-in-the-Loop (HIL) testing equipment, and Rapid Control Prototyping (RCP) systems. To make real-time apps that can run on PC, ARM, DSP, and other platforms, it turns Simulink models into source code spatially in language C [157],These are used to design, test, and improve control and protection systems, making it suitable for applications in power systems, aerospace, automotive, and other engineering fields.

The OPAL 4500 real-time estimator, integrated with RT-LAB for real-time execution are designed for optimization using both Genetic Algorithms (GA) and Sliding Mode Observer (SMO), The control logic is compiled into code via RT-LAB, a platform that allows for real-time testing and execution. The compiled code is then fed into the OPAL 4500 real-time estimator, which performs high-fidelity real-time simulations to evaluate and optimize the control parameters. This configuration facilitates the precise tuning and performance evaluation of the backstepping controller in real-world scenario.

The benefits of the suggested backstepping method based on the genetic algorithm of the 5Φ-PMSM drive and the accuracy of the robust slide model observer shown in this work are checked using the OPAL-RT 4500 computer in real time. Several real-time models are run to see how the suggested control works in different situations, such as when the load is applied, when the motor parameters change, and when the industrial test paths are taken. The schematic plan of the OPAL-RT 4500 simulator setup for real time is shown in Figure (IV.12).

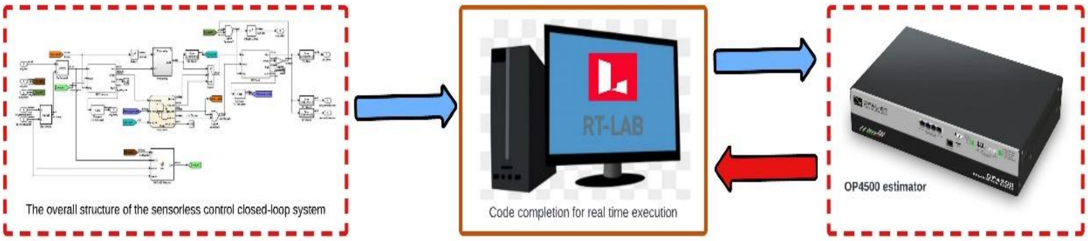

Figure (IV.12).The overall structure of the sensorless control closed-loop system.

IV.4.3. Results and Discussions of Real-time Simulation on Sensorless Control

IV.4.3.1. First test: Load torque change

The first test is done to show that the way without sensors that was suggested works and is useful. Where, the estimated speed is used instead of the actual speed. The Figure (IV.13), which shows the real-time result of the recommended sensorless control-based AG with SMO system when the load torque changes,where Figure (IV.13a) illustrate the real speed and estimated speed and the speed tracking error in Figure (IV.13b),the developed torque and imposed load torque in

Figure(IV.13c), the five-phase currents in Figure (IV.13d), the real rotor position and estimated position signal in Figure (IV.13e), and the rotor position error in Figure (IV.13f). The imposed reference speed is fixed at 100 rad/s and the applied load torque is 5 N.m at 0.5 s.

Figure IV.13(a) shows the actual speed of the 5P-PMSM drive and the estimated speed. It's clear that the estimated speed closely matches the actual speed based on the set reference speed, with no overshoot. This shows that the sensorless control solution that was offered works. In Figure (IV.13 b), you can also see the tracking error in speed between the real speed and the expected speed. This tracking error is about the same as 0.02 rad/s when the motor is in a steady state, and it's very small when the load force changes. As it turns out, the error in speed tracking is a lot smaller than the error seen in[3],[158],[4], [9],[13],and[18]. Thus, the suggested SMO system gives accurate estimates and good tracking dynamics. While Figure (IV.13c)shows the developed torque and the forced load torque that was put on the 5Φ-PMSM. It can be observed the motor torque represents high and accurate dynamics after load torque change and it is equal to the imposed load torque in steady state operation with acceptable ripples compared to the results presented in [159],[14], [12],[18], [20].Figure(IV.13d)plots that the five-phase currents of the 5Φ-PMSM drive have a balanced sinusoidal waveform with reduced chattering compared to the chattering noticed in previous works [4], [9], [11]. On the other hand, the estimated rotor position, obtained from the SMO system is compared with the real rotor position as given in Figure (IV.13e). It can be said that the rotor position presents periodic function and it varies between zero and 2π rad. Furthermore, the estimated position follows perfectly to the real rotor position with the rotor position error is very small, as given in Figure (IV.13f).

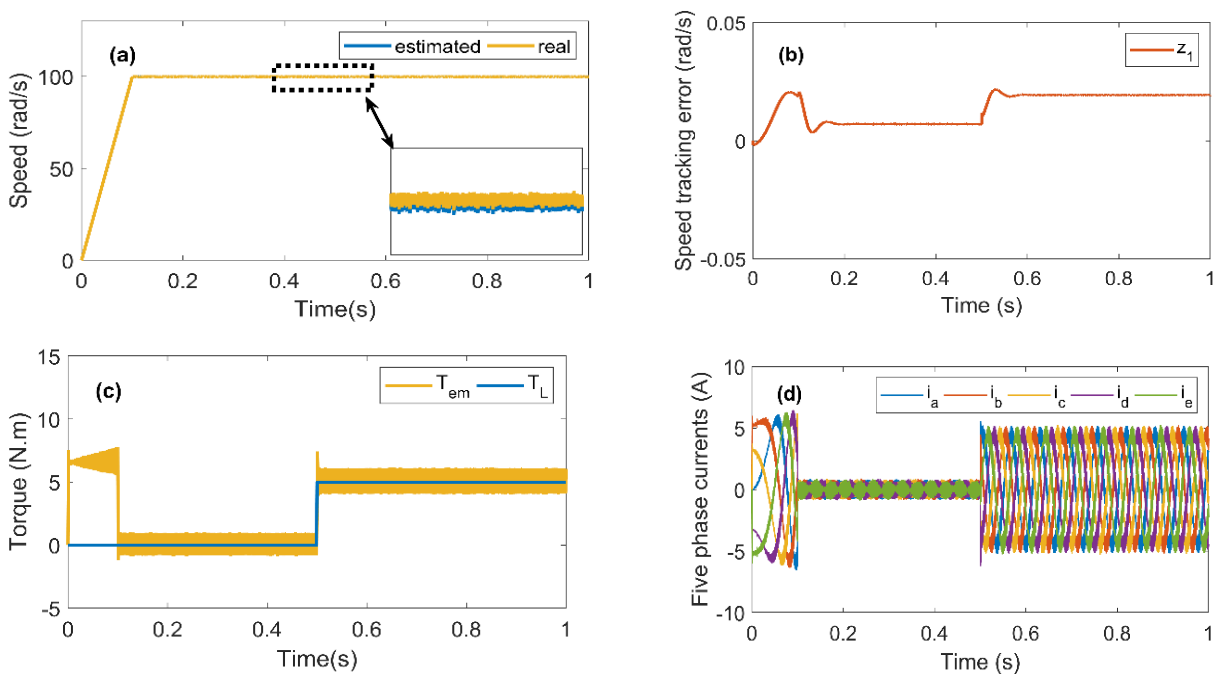

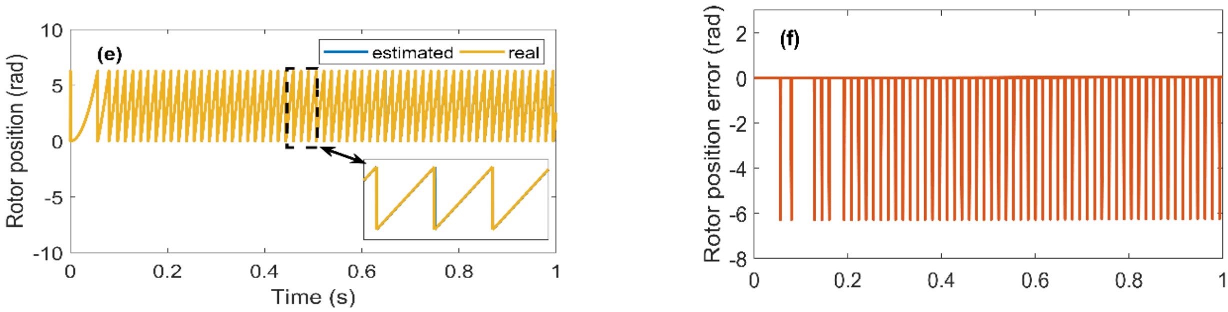

Figure (IV.13). Results of real time simulation of suggested sensorless algorithm under load torque change.

IV.4.3.2. Second test: Robustness test

So that we can see how well the suggested sensorless control works at a low speed, we set the step to 5 rad/s and applied 5 Nm of torque over 0.5 s. We need to look into what the 5P-PMSM drive does when the parameters aren't known. Because of this, the changes in the motor parameters are shown in Figure (IV.14a) and are written as

$$R_s = \begin{cases} 0.18\Omega & 0 < t < 0.2 \\ 0.27\Omega & 0.2 < t < 1 \end{cases}, \quad L_s = \begin{cases} 2.1mH & 0 < t < 0.4 \\ 3.15mH & 0.4 < t < 1 \end{cases} \quad \text{and} \quad J = \begin{cases} 0.0011Kg.m^2 & 0 < t < 0.7 \\ 0.00165Kg.m^2 & 0.7 < t < 1 \end{cases}$$

Such a test would show what happens when motor parameters change in relation to the suggested control method. Figure(IV.14) shows the real-time result of the suggested sensorless control-based AG with SMO system when the parameters are uncertainties, where the Figure (IV.14(a-d)) plot the motor parameter variation of 5Φ-PMSM drive in Figure (IV.14a), the estimated speed and measured one in Fig. (4.14b), the speed tracking error in Figure (IV.14c), the five-phase currents in Figure (IV.14d).

At a low speed of 5 rad/s, Figure (IV.14b) shows the recorded real speed and the estimated one. The predicted speed and the actual speed are very close to each other, even when the speed is low. There is no overshoot. Also, it's clear that changing the motor settings doesn't have any effect on how well the sensorless algorithm tracks compared to the results shown in[2], [4], [10]. While the speed tracking error is reduced from 6% to 0.8% compared to the results presented in [2], [158], [4], [9], [18], as given in Figure(IV.14c). This result demonstrates the good performance of the used sensorless control in ensuring advantageous stable operation mode of the 5Φ-PMSM drive even during low-speed operation (within 5 rad/s) in comparison to the earlier presented controllers. On the other side, as can be noticed from Figure (IV.14d) the five phase currents of 5Φ-PMSM drive present sinusoidal waveforms during motor parameter changes and low-speed operation.

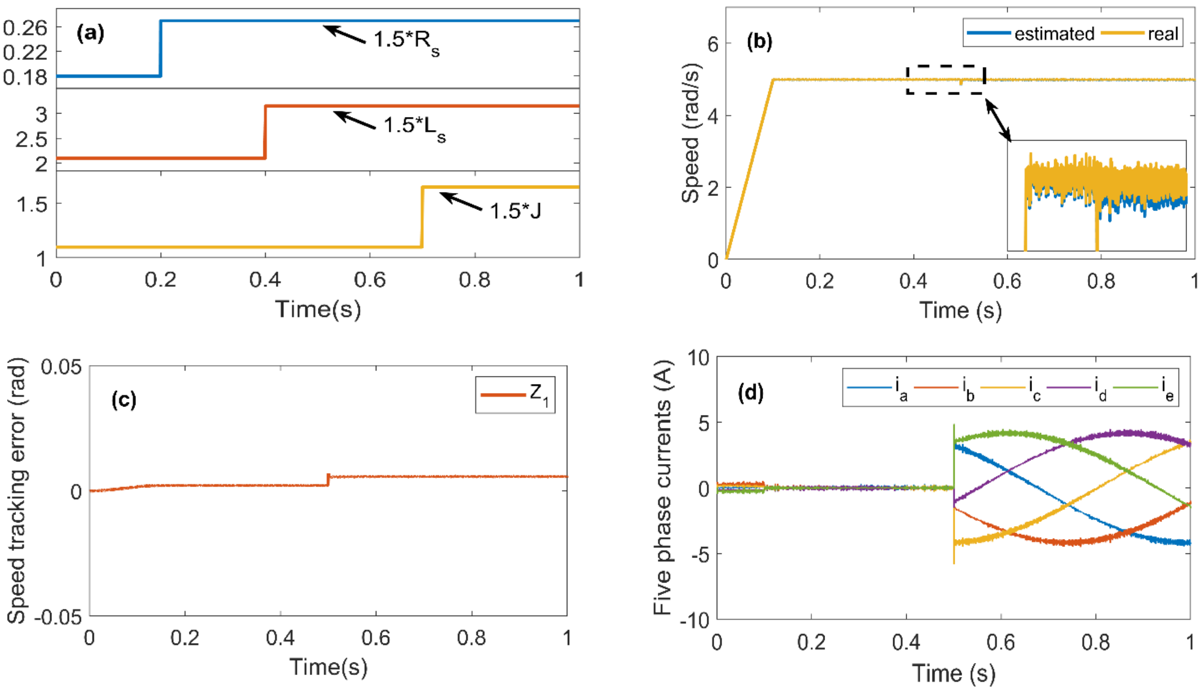

Figure (IV.14). Results of real time simulation of suggested sensorless algorithm under parameter uncertainties at 5 rad/s.

IV.4.3.3. Third test: industrial test trajectories

The suggested sensorless algorithm is tested with a 5Φ-PMSM drive operating profile that is the same as the one given in [14]. As illustrated in Figures. (IV.15a) and (IV.15b), this profile was chosen because it comprises consecutive situations throughout a large range of reference speed changes and load torque variations. Figure (IV.15c) indicates the measured real speed and the estimated value. It is clearly concluded from this figure, the estimated and real one converges to the reference profile very closely at various speed changes without any overshoot. While the speed tracking error is very small even under different values of imposed reference speed and applied load torque, which can be observed in Figure (IV.15d). Hence, the suggested sensorless algorithm based on SMO exhibits excellent tracking dynamics and satisfactory accuracy. The amplitude of five phase currents behave according to the dynamic behaviour of the 5Φ-PMSM operation under several situations as illustrated in Figure (IV.15e). Furthermore, the five phase currents behave as DC currents during the time interval when the motor speed is equal to zero. On the other side, the estimated rotor position follows the real signal very well with high accuracy, as shown in Figure (IV.15f).

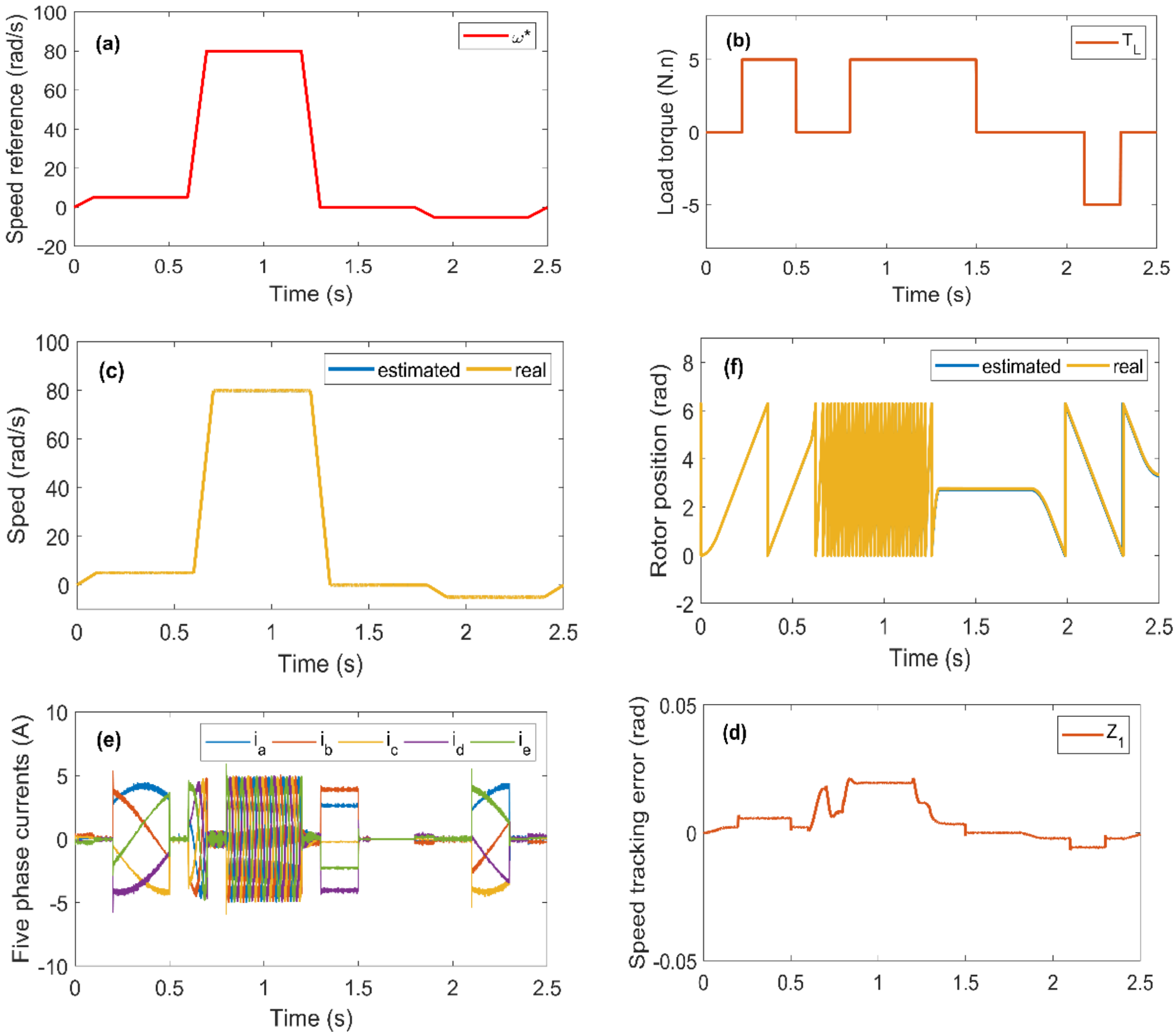

Figure (IV.15). Results of real time simulation of suggested sensorless algorithm under industrial operation profile.

Finally, based on the three tests that were already done. A new backstepping method based on the genetic algorithm and the SMO system can quickly and correctly adapt to changes in load torque over a wide range of changes in reference speed. However, the outcomes reveal that the SMO algorithm utilised in the suggested sensorless control continues to work well even when the motor settings transition. You can use this motor in a lot of different industrial settings by using the suggested backstepping method on the 5Φ-PMSM drive.

IV.5. Conclusion

This chapter has detailed the optimization of backstepping control using genetic algorithms (GA) and the implementation of sensorless control via a sliding mode observer (SMO) to make control possible without sensors. Moreover, this chapter covered more detail in its theory section on genetic algorithm theory with the optimization method of backstepping control and the sliding mode observer (SMO) It was detailed for use as a sensorless control observer. Furthermore, the OPAL 4500 estimator has been used to do thorough real-time testing to prove that these methods work., several tests, such as load torque change, robustness assessments, and industry trajectory tests, these real-time data show that the suggested sensorless control of 5Φ-PMSM drive works well even when there are unknowns in the parameters, like the stator resistance, friction coefficient, and stator inductance. These are the most important changes that can happen in a 5Φ-PMSM drive system., have shown that the proposed control strategies work very well even when the motor settings are changed. It provides an effective sensorless method for real-world uses.

The integration of GA for optimizing the backstepping controller has shown significant improvements in control precision and adaptability. Similarly, the sensorless control approach using SMO has effectively eliminated the need for direct measurement sensors, thereby reducing system complexity and cost. these control strategies are highly effective in various industrial and automotive applications. This proposed control on five-phase machines opens us up several prospects in the field and we will endeavour to perform several enhancements.

General Conclusion

General Conclusion

The goal of this thesis was to look into a new advanced control method that uses backstepping control along with the genetic algorithm to control a five-phase permanent magnet synchronous motor (5Φ-PMSM). These machines are usually more efficient because they lose less power and make better use of magnetic materials. They also provide a larger power factor, which can lower the need for reactive power and increase system efficiency as a whole. Better controllability, which enables more accurate torque and speed control, is another benefit of MSAP machines, which broadens their applicability. Furthermore, the comprehensive modeling of five-phase permanent magnet synchronous motors (5Φ-PMSM) within three distinct reference frames was conducted to facilitate the control of 5Φ-PMSM motors, where the performance was verified using Matlab Simulink software

On other hand, due their effectiveness for managing nonlinear systems by breaking them down into simpler sequential problems, backstepping control was proposed to control these machines where the effectiveness of this control strategy was rigorously tested under various conditions. The simulation results demonstrated the robust performance of the backstepping control in managing load torque variations, reversing motor speed, and handling fault conditions such as an open-phase fault. even though they have trouble getting optimal efficiency due to adjusting of the control gains.

To achieve optimal efficiency of backstepping control, one method was realised by the integration of Genetic Algorithm for optimizing the backstepping control is especially important to identify the gain values to produce the optimum performance. On the other side, the sensorless control using a Sliding Mode Observer (SMO), which is designed to estimate the back-EMF and the 5Φ-PMSM speed, as well as the rotor position, that lead more accurate and reliable motor operation without the need for physical sensors., which reduces costs and maintenance requirements, significantly enhances performance and efficiency of control systems. Furthermore, through extensive modelling, simulation, and experimental validation, the estimation of speed under changed parameters such the stator resistance and the magnetizing inductance, was a secondary topic of the study that was presented. In fact, all of the previously stated processes have been examined using the real-time OL-4500 estimators through simulation testing under various operating conditions of the motor under study, particularly when there is a change in load, speed, rotation, low speed, motor parameter changes, and open phase failures. the research demonstrates that GA-optimized sensorless control achieves superior speed and torque control, improving the dynamic response and robustness of the motor system, which plays a crucial role in automating complex industrial systems like robotics, manufacturing lines, and energy systems, improving throughput and consistency.

Futures woks

The results indicate that more investigation into the integration of hybrid approaches and additional optimization techniques may be necessary to further improve sensorless control strategies and guarantee even higher performance and economy in sophisticated motor control systems. These include the following proposals:

- It is possible to improve performance and resilience by combining different control systems, such as sliding mode control and backstepping control.
- Investigation into fault tolerant properties of sensorless control strategies.
- Integration of two or more artificial techniques .It can help get newer results, especially to handle the backstepping control performance.
- Using motor parameter estimates, experimental validation of suggested backstepping control schemes
- The proposed control strategies can be applied to other types of machines such us asynchronous motor.

ANNEXE

A-The equivalent circuit of 5P-PMSM drive

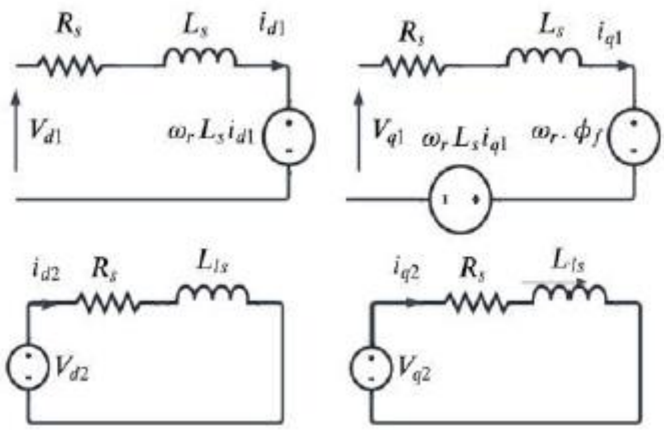

B- The five-phase permanent magnet synchronous motor parametres :

Nominal data	Values
n_p	2
L_{ls}	0.13 mH
R_s	0.18 Ω
φ_f	0.163 Vs
J	0.11 Kg.m^2

C- Genetic algorithm parameters

GA parameters	Value
Population size	20
Number of genes	4
Selection Type	Threshold & Probabilistic Tournament
Mumber of generation	1000
Selection Probability	0.8
Crossover Type	Linear crossing (Wright)
Mutation rate	[0% , 30%]
Sampling frequency	0.0001s

Bibliographies

Bibliographies

[1] W. Wang, X. Chen, and J. Wang, "Motor / Generator Applications in Electrified Vehicle Chassis-A survey," no. 1, p. 1.

[2] L. Dhamo and A. Spahiu, "An Improved Performance of Sensorless PMSM Drive Control with Sliding Mode Observer in Low Speed Operation," *Appl. Power Electron. Conf. Expo. 2004. APEC '04. Ninet. Annu. IEEE*, vol. 4, no. May, pp. 2205–2211, 2013.

[3] L. Guo and L. Parsa, "Model reference adaptive control of five-phase IPM motors based on neural network," *IEEE Trans. Ind. Electron.*, vol. 59, no. 3, pp. 1500–1508, 2012, doi: 10.1109/TIE.2011.2163371.

[4] X. Zhang and Z. Li, "Sliding-mode observer-based mechanical parameter estimation for permanent magnet synchronous motor," *IEEE Trans. Power Electron.*, vol. 31, no. 8, pp. 5732–5745, 2016, doi: 10.1109/TPEL.2015.2495183.

[5] F. Mekri, J. F. Charpentier, and E. Semail, "An efficient control of a series connected two-synchronous motor 5-phase with non sinusoidal EMF supplied by a single 5-leg VSI: Experimental and theoretical investigations," *Electr. Power Syst. Res.*, vol. 92, pp. 11–19, 2012, doi: 10.1016/j.epsr.2012.05.012.

[6] P. Tang, Y. Dai, and Z. Li, "Unified predictive current control of PMSMs with parameter uncertainty," *Electron.*, vol. 8, no. 12, pp. 1–18, 2019, doi: 10.3390/electronics8121534.

[7] A. K. Singh and O. P. Roy, "Performance analysis of a PMSM drive using PID controllers," *Electron. Inf. Plan.*, vol. 37, no. 3, pp. 80–87, 2010.

[8] W. Lina, X. Kun, L. De Lillo, L. Empringham, and P. Wheeler, "PI controller relay auto-tuning using delay and phase margin in PMSM drives," *Chinese J. Aeronaut.*, vol. 27, no. 6, pp. 1527–1537, 2014, doi: 10.1016/j.cja.2014.10.019.

[9] A. Hosseyni, R. Trabelsi, M. F. Mimouni, A. Iqbal, and R. Alammari, "Sensorless sliding mode observer for a five-phase permanent magnet synchronous motor drive," *ISA Trans.*, vol. 58, pp. 462–473, 2015, doi: 10.1016/j.isatra.2015.05.007.

[10] S. Rebouhl, A. Kaddouri, R. Abdessemed, and A. Haddoun, "Nonlinear control by input-output linearization scheme for EV permanent magnet synchronous motor," *VPPC 2007 - Proc. 2007 IEEE Veh. Power Propuls. Conf.*, no. 213, pp. 185–190, 2007, doi: 10.1109/VPPC.2007.4544122.

[11] M. L. Corradini, G. Ippoliti, S. Longhi, and G. Orlando, “A quasi-sliding mode approach for robust control and speed estimation of PM synchronous motors,” *IEEE Trans. Ind. Electron.*, vol. 59, no. 2, pp. 1096–1104, 2012, doi: 10.1109/TIE.2011.2158035.

[12] C. Xia, J. Zhao, Y. Yan, and T. Shi, “A novel direct torque control of matrix converter-fed PMSM drives using duty cycle control for torque ripple reduction,” *IEEE Trans. Ind. Electron.*, vol. 61, no. 6, pp. 2700–2713, 2014, doi: 10.1109/TIE.2013.2276039.

[13] X. Liu, G. Zhang, L. Mei, and D. Wang, “Backstepping control with speed estimation of PMSM based on MRAS,” *Autom. Control Comput. Sci.*, vol. 50, no. 2, pp. 116–123, 2016, doi: 10.3103/S0146411616020036.

[14] M. A. Hamida, J. de Leon, and A. Glumineau, “Experimental sensorless control for IPMSM by using integral backstepping strategy and adaptive high gain observer,” *Control Eng. Pract.*, vol. 59, no. November 2016, pp. 64–76, 2017, doi: 10.1016/j.conengprac.2016.11.012.

[15] S. Chaouch, L. Abdou, S. Drid, and L. Chrifi-Alaoui, “Optimized Torque Control via Backstepping Using Genetic Algorithm of Induction Motor,” *Autom. – J. Control. Meas. Electron. Comput. Commun.*, vol. 57, no. 2, 2016, doi: 10.7305/automatika.2016.10.1345.

[16] A. Marvi Moghadam and S. Balochian, “Design of combined sliding mode controller back stepping using genetic algorithm,” *J. Eng. (United Kingdom)*, vol. 2013, 2013, doi: 10.1155/2013/614803.

[17] H. M. Kojabadi and M. Ghribi, “MRAS-based adaptive speed estimator in PMSM drives,” *Int. Work. Adv. Motion Control. AMC*, vol. 2006, no. 1, pp. 569–572, 2006, doi: 10.1109/AMC.2006.1631722.

[18] A. Kirad, S. Groini, and Y. Soufi, “Improved sensorless backstepping controller using extended Kalman filter of a permanent magnet synchronous machine,” *Bull. Electr. Eng. Informatics*, vol. 11, no. 2, pp. 658–671, 2022.

[19] G. Zhang, G. Wang, D. Xu, and N. Zhao, “ADALINE-network-based PLL for position sensorless interior permanent magnet synchronous motor drives,” *IEEE Trans. Power Electron.*, vol. 31, no. 2, pp. 1450–1460, 2016, doi: 10.1109/TPEL.2015.2424256.

[20] T. Kamel, D. Abdelkader, B. Said, S. Padmanaban, and A. Iqbal, “Extended Kalman filter based sliding mode control of parallel-connected two five-phase PMSM drive system,” *Electron.*, vol. 7, no. 2, 2018, doi: 10.3390/electronics7020014.

[21] M. A. Mossa, H. Echeikh, A. Iqbal, T. D. Do, and A. S. Al-Sumaiti, “A novel sensorless

control for multiphase induction motor drives based on singularly perturbed sliding mode observer-experimental validation," *Appl. Sci.*, vol. 10, no. 8, 2020, doi: 10.3390/APP10082776.

[22] L. Parsa, "On advantages of multi-phase machines," *IECON Proc. (Industrial Electron. Conf.*, vol. 2005, pp. 1574–1579, 2005, doi: 10.1109/IECON.2005.1569139.

[23] K. Saad, K. Abdellah, H. Ahmed, and A. Iqbal, "Investigation on SVM-Backstepping sensorless control of five-phase open-end winding induction motor based on model reference adaptive system and parameter estimation," *Eng. Sci. Technol. an Int. J.*, vol. 22, no. 4, pp. 1013–1026, 2019, doi: 10.1016/j.jestch.2019.02.008.

[24] S. K. Sul and S. Kim, "Sensorless control of IPMSM: Past, present, and future," *IEEJ J. Ind. Appl.*, vol. 1, no. 1, pp. 15–23, 2012, doi: 10.1541/ieejjia.1.15.

[25] Y. Lee and S. K. Sul, "Model-based sensorless control of IPMSM enhancing robustness based on the estimation of speed error," *2016 IEEE 7th Int. Symp. Sensorless Control Electr. Drives, SLED 2016*, 2016, doi: 10.1109/SLED.2016.7518796.

[26] S. Li *et al.*, "Sensorless control strategy for multiphase induction motor with stator and rotor resistance identification based on injecting third harmonic current," *2020 IEEE 1st China Int. Youth Conf. Electr. Eng. CIYCEE 2020*, pp. 1–7, 2020, doi: 10.1109/CIYCEE49808.2020.9332680.

[27] K. H. Ang, G. Chong, and Y. Li, "PID control system analysis, design, and technology," *IEEE Trans. Control Syst. Technol.*, vol. 13, no. 4, pp. 559–576, 2005, doi: 10.1109/TCST.2005.847331.

[28] R. Kumar, S. Das, P. Syam, and A. K. Chattopadhyay, "Review on model reference adaptive system for sensorless vector control of induction motor drives," *IET Electr. Power Appl.*, vol. 9, no. 7, pp. 496–511, 2015, doi: 10.1049/iet-epa.2014.0220.

[29] M. Synchrones, "Amor KHLAIEF," 2012.

[30] W. Zine, "HF signal injection and Machine Learning for the sensorless control of IPMSM-based EV drives," *Ph. D. thesis*, 2017.

[31] Y. Mini, N. K. Nguyen, E. Semail, and D. T. Vu, "Enhancement of Sensorless Control for Non-Sinusoidal Multiphase Drives-Part I: Operation in Medium and High-Speed Range," *Energies,* vol. 15, no. 2, pp. 1–27, 2022, doi: 10.3390/en15020607.

[32] R. Bojoi, S. Rubino, A. Tenconi, and S. Vaschetto, "Multiphase electrical machines and drives: A viable solution for energy generation and transportation electrification," *Proc. 2016*

Int. Conf. Expo. Electr. Power Eng. EPE 2016, no. Epe, pp. 632–639, 2016, doi: 10.1109/ICEPE.2016.7781416.

[33] S. Khadar, K. Abdellah, and M. M. Rezaoui, “Contribution to control of five phase induction motor with open end windings in normal and degraded modes,” no. July, 2021.

[34] C. A. Reusser, “Power Converter Topologies for Multiphase Drive Applications,” *Electr. Power Convers.*, pp. 1–22, 2019, doi: 10.5772/intechopen.81977.

[35] A. S. Abdel-Khalik, M. I. Masoud, and B. W. Williams, “Vector controlled multiphase induction machine: Harmonic injection using optimized constant gains,” *Electr. Power Syst. Res.*, vol. 89, pp. 116–128, Aug. 2012, doi: 10.1016/j.epsr.2012.03.001.

[36] M. Jones, S. N. Vukosavic, D. Dujic, and E. Levi, “A synchronous current control scheme for multiphase induction motor drives,” *IEEE Trans. Energy Convers.*, vol. 24, no. 4, pp. 860–868, 2009, doi: 10.1109/TEC.2009.2025419.

[37] I. Bakhti, S. Chaouch, A. Makouf, and T. Douadi, “Speed control of permanent magnet synchronous motor using different strategy of sliding mode approach,” *J. Eng. Sci. Technol.*, vol. 12, no. 10, pp. 2778–2791, 2017.

[38] H. Li, X. Zhang, S. Yang, and S. Liu, “Unified Graphical Model of High-Frequency Signal Injection Methods for PMSM Sensorless Control,” *IEEE Trans. Ind. Electron.*, vol. 67, no. 6, pp. 4411–4421, 2020, doi: 10.1109/TIE.2019.2924863.

[39] S. C. Yang, S. M. Yang, and J. H. Hu, “Robust initial position estimation of permanent magnet machine with low saliency ratio,” *IEEE Access*, vol. 5, no. c, pp. 2685–2695, 2017, doi: 10.1109/ACCESS.2017.2666156.

[40] P. Xu and Z. Zhu, “Carrier signal injection-based sensorless control for permanent magnet synchronous machine drives with tolerance of signal processing delays,” *IET Electr. Power Appl.*, vol. 11, no. 6, pp. 1140–1149, 2017, doi: 10.1049/iet-epa.2017.0025.

[41] J. Riveros, B. Bogado, J. Prieto, F. Barrero, S. Toral, and M. Jones, “Multiphase machines in propulsion drives of electric vehicles,” *Proc. EPE-PEMC 2010 - 14th Int. Power Electron. Motion Control Conf.*, no. November 2014, 2010, doi: 10.1109/EPEPEMC.2010.5606658.

[42] K. Iffouzar, “Etude et contrôle des machines asynchrones polyphasées en mode normal et dégradé. Application dans un système embarque.” Université de Béjaia-Abderrahmane Mira, 2016.

[43] E. Technology, “Types of Inverters and their Applications,” *2012-2024*, 2012.

[44] R. K. Singh, “Multiphase Inverter Topology and its Modulation V3ua,” vol. 00, 2006.

[45] V. Sharna, "DIiode clambed multilevel Iinverter switching topologies," pp. 185–189, 2017.

[46] T. Advantages and C. Inverter, "Flying Capacitor Inverter The Advantages and Operation of Flying Capacitor Inverter," pp. 1–17.

[47] Y. Park, H. Ryu, H. Lee, M. Jung, and S. Lee, "Design of a Cascaded H-Bridge Multilevel Inverter Based on Power Electronics Building Blocks and Control for High Performance," vol. 10, no. 3, pp. 262–269, 2010.

[48] E. Levi, "Multiphase electric machines for variable-speed applications," *IEEE Trans. Ind. Electron.*, vol. 55, no. 5, pp. 1893–1909, 2008, doi: 10.1109/TIE.2008.918488.

[49] T. Kamel, D. Abdelkader, and B. Said, "Vector control of five-phase permanent magnet synchronous motor drive," *2015 4th Int. Conf. Electr. Eng. ICEE 2015*, vol. 2, no. 2, pp. 1–4, 2016, doi: 10.1109/INTEE.2015.7416853.

[50] "Speed Control of Permanent Magnet Synchronous Motor for Elevator," *J. Korean Inst. Illum. Electr. Install. Eng.*, vol. 18, no. 5, pp. 74–82, 2004, doi: 10.5207/jieie.2004.18.5.074.

[51] A. T. Woldegiorgis, X. Ge, S. Li, and M. Hassan, "Extended Sliding Mode Disturbance Observer-Based Sensorless Control of IPMSM for Medium and High-Speed Range Considering Railway Application," *IEEE Access*, vol. 7, pp. 175302–175312, 2019, doi: 10.1109/ACCESS.2019.2957274.

[52] P. Kachroo and M. Tomizuka, "Chattering reduction and error convergence in the sliding-mode control of a class of nonlinear systems," *IEEE Trans. Automat. Contr.*, vol. 41, no. 7, pp. 1063–1068, 1996, doi: 10.1109/9.508917.

[53] A. Kouzou, S. Khadar, and A. Teta, "Speed Tracking nonlinear Control using Second order Luenberger observer of Five Phase Permanent-Magnet Synchronous Motor Supplied by a Flying Capacitor Multi-cellular Inverter," *Proc. - 2022 5th Int. Conf. Power Electron. their Appl. ICPEA 2022*, vol. 1, no. March, pp. 1–6, 2022, doi: 10.1109/ICPEA51060.2022.9791191.

[54] I. Vesely, L. Vesely, and Z. Bradac, "MRAS identification of permanent magnet synchronous motor parameters," *IFAC-PapersOnLine*, vol. 51, no. 6, pp. 250–255, 2018, doi: 10.1016/j.ifacol.2018.07.162.

[55] S. U. Rahman and C. Xia, "Rotor Speed and Position Estimation Analysis of Interior PMSM Machines in Low and Medium-High Speed Regions Adopting an Improved Flux Observer for Electric Vehicle Applications," *Machines*, vol. 11, no. 5, 2023, doi: 10.3390/machines11050574.

[56] M. Brodatzki, J. Richter, J. Kolb, and M. Braun, “Position and Speed Estimation Algorithm for Permanent Magnet Synchronous Machines Considering Nonlinear Magnetic Effects,” *ICPE 2019 - ECCE Asia - 10th Int. Conf. Power Electron. - ECCE Asia*, pp. 724–731, 2019, doi: 10.23919/icpe2019-ecceasia42246.2019.8796980.

[57] S. Vaez-Zadeh, “242Rotor Position and Speed Estimation,” *Control of Permanent Magnet Synchronous Motors*. Oxford University Press, p. 0, Mar. 01, 2018. doi: 10.1093/oso/9780198742968.003.0006.

[58] R. Ortega, L. Praly, A. Astolfi, J. Lee, and K. Nam, “Estimation of Rotor Position and Speed of Permanent Magnet Synchronous Motors With Guaranteed Stability,” *Control Syst. Technol. IEEE Trans.*, vol. 19, pp. 601–614, Jun. 2011, doi: 10.1109/TCST.2010.2047396.

[59] J. J. Guedes, M. F. Castoldi, A. Goedtel, C. M. Agulhari, and D. S. Sanches, “Parameters estimation of three-phase induction motors using differential evolution,” *Electr. Power Syst. Res.*, vol. 154, pp. 204–212, 2018, doi: 10.1016/j.epsr.2017.08.033.

[60] J. Treetrong, J. Sinha, F. Gu, and A. Ball, “Parameter Estimation for Electric Motor Condition Monitoring,” *Adv. Vib. Eng.*, vol. 11, pp. 75–83, Jan. 2012.

[61] M. Riera-Guasp, J. A. Antonino-Daviu, and G. A. Capolino, “Advances in electrical machine, power electronic, and drive condition monitoring and fault detection: State of the art,” *IEEE Trans. Ind. Electron.*, vol. 62, no. 3, pp. 1746–1759, 2015, doi: 10.1109/TIE.2014.2375853.

[62] J. C. Gamazo-Real, E. Vázquez-Sánchez, and J. Gómez-Gil, “Position and speed control of brushless dc motors using sensorless techniques and application trends,” *Sensors*, vol. 10, no. 7, pp. 6901–6947, 2010, doi: 10.3390/s100706901.

[63] H. Abu-Rub, M. Rizwan Khan, A. Iqbal, and S. K. Moin Ahmed, “MRAS-based sensorless control of a five-phase induction motor drive with a predictive adaptive model,” *IEEE Int. Symp. Ind. Electron.*, pp. 3089–3094, 2010, doi: 10.1109/ISIE.2010.5637858.

[64] Y. Zhang, Z. Zhao, T. Lu, L. Yuan, W. Xu, and J. Zhu, “A comparative study of luenberger observer, sliding mode observer and extended Kalman filter for sensorless vector control of induction motor drives,” *2009 IEEE Energy Convers. Congr. Expo. ECCE 2009*, pp. 2466–2473, 2009, doi: 10.1109/ECCE.2009.5316508.

[65] W. Zine, Z. Makni, E. Monmasson, K. Chen, L. Idkhajine, and B. Condamin, “Hybrid sensorless control strategy for EV applications based on high frequency signal injection and machine learning,” *2017 IEEE Veh. Power Propuls. Conf. VPPC 2017 - Proc.*, vol. 2018-

Janua, pp. 1–5, 2018, doi: 10.1109/VPPC.2017.8330887.

[66] U. P. De Catalunya, J. Manuel, U. P. De Catalunya, U. P. De Catalunya, R. Martinez, and J. Luis, "Observer Based Open Transistor Fault Diagnosis and Fault- Tolerant Control of Five-Phase PM Motor Drive for Application in Electric Vehicles," 2014.

[67] M. H. Iftikhar, B. G. Park, and J. W. Kim, "Design and analysis of a five-phase permanent-magnet synchronous motor for fault-tolerant drive," *Energies*, vol. 14, no. 2, 2021, doi: 10.3390/en14020514.

[68] M. J. Duran, E. Levi, and F. Barrero, "Multiphase Electric Drives: Introduction," *Wiley Encycl. Electr. Electron. Eng.*, no. i, pp. 1–26, 2017, doi: 10.1002/047134608x.w8364.

[69] B. Tian, G. Mirzaeva, Q. T. An, L. Sun, and D. Semenov, "Fault-Tolerant Control of a Five-Phase Permanent Magnet Synchronous Motor for Industry Applications," *IEEE Trans. Ind. Appl.*, vol. 54, no. 4, pp. 3943–3952, 2018, doi: 10.1109/TIA.2018.2820060.

[70] H. De Jong, "Modeling and Simulation of Five Phase Permanent Magnet Synchronous Motor," vol. I, no. 2, pp. 111–118, 2003.

[71] G. Umoh, C. Ogbuka, and E. Obe, "Modelling and analysis of five-phase permanent magnet synchronous motor in machine variables," *Prz. Elektrotechniczny*, vol. 96, no. 1, pp. 87–92, 2020, doi: 10.15199/48.2020.01.21.

[72] D. Post-graduation and R. Scientifique, "Mémoire de Magister," pp. 21–28, 2014.

[73] M. A. Mossa, H. Echeikh, and A. Ma'arif, "Dynamic Performance Analysis of a Five-Phase PMSM Drive Using Model Reference Adaptive System and Enhanced Sliding Mode Observer," *J. Robot. Control*, vol. 3, no. 3, pp. 289–308, 2022, doi: 10.18196/jrc.v3i3.14632.

[74] Y. Bensalem, A. Kouzou, R. Abbassi, H. Jerbi, R. Kennel, and M. Abdelrahem, "Sliding-mode-based current and speed sensors fault diagnosis for five-phase pmsm," *Energies*, vol. 15, no. 1, 2022, doi: 10.3390/en15010071.

[75] M. Academique, "Conception et commande d ' une MSAP pentaphasé".

[76] G. Kenne, J. D. D. Nguimfack Ndongmo, R. Fochie Kuate, and H. B. Fotsin, "An Online Simplified Nonlinear Controller for Transient Stabilization Enhancement of DFIG in Multi-Machine Power Systems," *IEEE Trans. Automat. Contr.*, vol. 60, no. 9, pp. 2464–2469, 2015, doi: 10.1109/TAC.2015.2427591.

[77] M. JANASZEK, "EXTENDED CLARKE TRANSFORMATION FOR n-PHASE SYSTEMS," *Proc. Electrotech. Inst.*, vol. 63, no. 0, pp. 5–26, 2016, doi: 10.5604/01.3001.0009.4333.

[78] N. Bounasla, S. Barkat, E. Benyoussef, and K. Tounsi, “Sensorless sliding mode control of a five-phase PMSM using extended Kalman filter,” *Proc. 2016 8th Int. Conf. Model. Identif. Control. ICMIC 2016*, no. 1, pp. 97–102, 2017, doi: 10.1109/ICMIC.2016.7804280.

[79] A. Hezzi, Y. Bensalem, S. Ben Elghali, and M. N. Abdelkrim, “Sliding Mode Observer based sensorless control of five phase PMSM in electric vehicle,” *19th Int. Conf. Sci. Tech. Autom. Control Comput. Eng. STA 2019*, no. 1, pp. 530–535, 2019, doi: 10.1109/STA.2019.8717290.

[80] A. Iqbal, S. Moinuddin, and M. R. Khan, “Space Vector Model of A Five-Phase Voltage Source Inverter,” pp. 488–493, 2006.

[81] K. Tounsi, D. Abdelkader, and S. Barkat, “Vector Control of Five-Phase Permanent Magnet Synchronous Motor Drive,” no. October 2016, 2015, doi: 10.1109/INTEE.2015.7416853.

[82] F. Acosta-Cambranis, J. Zaragoza, L. Romeral, and N. Berbel, “Comparative analysis of svm techniques for a five-phase vsi based on sic devices,” *Energies*, vol. 13, no. 24, 2020, doi: 10.3390/en13246581.

[83] L. Gao and J. E. Fletcher, “A Space Vector Switching Strategy for Three-Level Five-Phase Inverter Drives,” vol. 57, no. 7, pp. 2332–2343, 2010.

[84] M. A. Patel, A. R. Patel, and D. R. Vyas, “Use of PWM Techniques for Power Quality Improvement,” no. May, pp. 2–6, 2009.

[85] A. Mushtaq, “What are the types of Pulse Width Modulation Techniques,” *May 25, 2022*, 2022.

[86] Geeksforgeeks, “Pulse Width Modulation (PWM),” *https://www.geeksforgeeks.org/pulse-width-modulation-pwm/*.

[87] F. F. Jaber and A. F. Abdulhasan, “Mathematical Model of Permanent Magnet Synchronous Motor,” *Univ. Thi -Qar J. Eng. Sci.*, vol. 12, no. 2, pp. 10–14, 2022, [Online]. Available: http://www.doi.org/10.31663/tqujes.12.2.444

[88] N. Bianchi and M. Dai Pre, “Active power filter control using neural network technologies,” *IEE Proceedings-Electric Power Appl.*, vol. 150, no. 2, pp. 139–145, 2003, doi: 10.1049/ip-epa.

[89] H. Echeikh, R. Trabelsi, A. Iqbal, M. F. Mimouni, and R. Alammari, “Online adaptation of rotor resistance based on sliding mode observer kwith backstepping control of a five-phase induction motor drives,” *Int. J. Power Electron. Drive Syst.*, vol. 7, no. 3, pp. 648–655, 2016, doi: 10.11591/ijpeds.v7.i3.pp648-655.

[90] P. V. Kokotović, “The Joy of Feedback: Nonlinear and Adaptive,” *IEEE Control Systems*, vol. 12, no. 3. pp. 7–17, 1992. doi: 10.1109/37.165507.

[91] A. Humaidi and M. Hameed, “Development of a new adaptive backstepping control design for a non-strict and under-actuated system based on a PSO tuner,” *Inf.*, vol. 10, no. 2, 2019, doi: 10.3390/info10020038.

[92] C. W. Chung and Y. Chang, “Backstepping control of multi-input non-linear systems,” *IET Control Theory Appl.*, vol. 7, no. 14, pp. 1773–1779, 2013, doi: 10.1049/iet-cta.2012.0529.

[93] M. Kamarudin, A. Husain, and M. Ahmad, “Stabilization of Uncertain Systems using Backstepping and Lyapunov Redesign,” *Eprints2.Utem.Edu.My*, no. January, pp. 160–163, 2013, doi: 10.13140/RG.2.1.4714.1929.

[94] D. Ricci, M. Romero, and M. Seron, “Lyapunov-Function-Free Backstepping Design with Application to the Lorenz System,” *IFAC-PapersOnLine*, vol. 51, no. 33, pp. 223–228, 2018, doi: 10.1016/j.ifacol.2018.12.086.

[95] A. Hosseyni, R. Trabelsi, A. Iqbal, and M. F. Mimouni, “Backstepping control for a five-phase permanent magnet synchronous motor drive,” *Int. J. Power Electron. Drive Syst.*, vol. 6, no. 4, pp. 842–852, 2015, doi: 10.11591/ijpeds.v6.i4.pp842-852.

[96] A. Hosseyni, R. Trabelsi, P. Sanjeevikumar, A. Iqbal, and M. F. Mimouni, “Sensorless back stepping control for a five-phase permanent magnet synchronous motor drive based on sliding mode observer,” *Lect. Notes Electr. Eng.*, vol. 436, pp. 251–261, 2017, doi: 10.1007/978-981-10-4394-9_26.

[97] A. M. B.BELABBES, M.K.FELLAH, A.LOUSDAD, A.MEROUFEL, “Speed Control By Backstepping With Nonlinear Observer of a Permanent Magnet Synchronous Motor,” vol. 6, no. 4, pp. 1–7, 2006.

[98] N. Ali, W. Alam, M. Pervaiz, and J. Iqbal, “Nonlinear adaptive backstepping control of permanent magnet synchronous motor,” *Rev. Roum. des Sci. Tech. Ser. Electrotech. Energ.*, vol. 66, no. 1, pp. 9–14, 2021.

[99] B. M. Safinaz, B. Mohammed, and B. Ahmed, “Observer Backstepping Design for Flight Control †,” *Eng. Proc.*, vol. 29, no. 1, 2023, doi: 10.3390/engproc2023029003.

[100] C. To, A. Control, T. Nonlinear, and S. With, “Contribution To Adaptive Control of,” 2020.

[101] J. M. Hughes *et al.*, “Backstepping Backstepping adaptatif pour le contrôle la poursuite et la synchronisation des Remerciements,” *Thesis*, p. 171, 2013, [Online]. Available: PhD Thesis

[102] H. A. Mintsa, G. E. Eny, N. Senouveau, and R. M. A. Nzue, “Analysis of the Gains Tuning

Problem in a Backstepping Controller Applied to an Electrohydraulic Drive," *WSEAS Trans. Syst. Control*, vol. 18, no. June, pp. 166–173, 2023, doi: 10.37394/23203.2023.18.17.

[103] H. D. Long, "Tuning Parameters of Backstepping Control Using TLBO Algorithm for Inverted Pendulum," *Proc. 2024 Conf. Young Res. Electr. Electron. Eng. ElCon 2024*, no. January, pp. 363–366, 2024, doi: 10.1109/ElCon61730.2024.10468274.

[104] A. Boulmane, Y. Zidani, D. Belkhayat, and M. Bouchouirbat, "A GA-based adaptive mechanism for sensorless vector control of induction motor drives for urban electric vehicles," *Turkish J. Electr. Eng. Comput. Sci.*, vol. 28, no. 3, pp. 1731–1746, 2020, doi: 10.3906/elk-1910-39.

[105] N. Weiner, "The appeal 08: ewolufiqm," 1995.

[106] M. Mitchell, S. Fe, and S. Forrest, "Artificial Life 1 Introduction 2 Overview of Genetic Algorithms," *Optimization*, pp. 1–28, 1993.

[107] S. Forrest and M. Mitchell, "Adaptive computation: The multidisciplinary legacy of John H. Holland," *Commun. ACM*, vol. 59, no. 8, pp. 58–63, 2016, doi: 10.1145/2964342.

[108] "Holland's Theory - an overview | ScienceDirect Topics." https://www.sciencedirect.com/topics/psychology/hollands-theory (accessed Apr. 18, 2024).

[109] A. Lambora, K. Gupta, and K. Chopra, "Genetic Algorithm- A Literature Review," *Proc. Int. Conf. Mach. Learn. Big Data, Cloud Parallel Comput. Trends, Prespectives Prospect. Com. 2019*, no. 1998, pp. 380–384, 2019, doi: 10.1109/COMITCon.2019.8862255.

[110] "Genetic Reproduction Reproduction," no. 4, pp. 5–6.

[111] J. McCall, "Genetic algorithms for modelling and optimisation," *J. Comput. Appl. Math.*, vol. 184, no. 1, pp. 205–222, 2005, doi: 10.1016/j.cam.2004.07.034.

[112] M. A. Albadr, S. Tiun, M. Ayob, and F. Al-Dhief, "Genetic algorithm based on natural selection theory for optimization problems," *Symmetry (Basel).*, vol. 12, no. 11, pp. 1–31, 2020, doi: 10.3390/sym12111758.

[113] J. Holland, "Genetic algorithm : Discover the 6 steps Understanding the steps of the genetic algorithm," 2024.

[114] H. Kour, P. Sharma, and P. Abrol, "Analysis of fitness function in genetic algorithms," *J. Sci. Tech. Adv.*, vol. 1, no. 3, pp. 87–89, 2015, [Online]. Available: http://in.mathworks.com/help/gads/examples/coding-and-minimizing-a-

[115] S. Editors *et al.*, "Natural Computing Series".

[116] "Goldberg_Genetic_Algorithms_in_Search.pdf."

[117] A. E. Eiben, “Genetic algorithms + data structures = evolution programs,” *Artificial Intelligence in Medicine*, vol. 9, no. 3. pp. 283–286, 1997. doi: 10.1016/s0933-3657(96)00378-8.

[118] R. retno Jati, “No Title*עלון הנוטע*,” תמונת מצב: ענף הקיווי, vol. 66, pp. 37–39, 2016.

[119] A. Shukla, H. M. Pandey, and D. Mehrotra, “Comparative review of selection techniques in genetic algorithm,” *2015 1st Int. Conf. Futur. Trends Comput. Anal. Knowl. Manag. ABLAZE 2015*, pp. 515–519, 2015, doi: 10.1109/ABLAZE.2015.7154916.

[120] S. A. Smith, “ScholarWorks at University of Montana Let us know how access to this document benefits you .,” vol. 1972, no. Spring, pp. 1–16, 1959.

[121] C. A. C. Coello, G. B. Lamont, D. A. Van Veldhuizen, D. E. Goldberg, and J. R. Koza, *Evolutionary Algorithms for Solving Multi-Objective Problems Second Edition Genetic and Evolutionary Computation Series Series Editors Selected titles from this series :* 2007.

[122] V. Filipović, “Fine-grained tournament selection operator in genetic algorithms,” *Comput. Informatics*, vol. 22, no. 2, pp. 143–161, 2003.

[123] S. Yang, “Genetic algorithms with elitism-based immigrants for changing optimization problems,” *Lect. Notes Comput. Sci. (including Subser. Lect. Notes Artif. Intell. Lect. Notes Bioinformatics)*, vol. 4448 LNCS, pp. 627–636, 2007, doi: 10.1007/978-3-540-71805-5_69.

[124] “Cross-over Mutation - an overview | ScienceDirect Topics.” https://www.sciencedirect.com/topics/computer-science/cross-over-mutation (accessed Apr. 26, 2024).

[125] “Point Crossover - an overview | ScienceDirect Topics.” https://www.sciencedirect.com/topics/computer-science/point-crossover (accessed Apr. 27, 2024).

[126] U. A.J. and S. P.D., “Crossover Operators in Genetic Algorithms: a Review,” *ICTACT J. Soft Comput.*, vol. 06, no. 01, pp. 1083–1092, 2015, doi: 10.21917/ijsc.2015.0150.

[127] R. Hinterding, H. Gielewski, and T. Peachey, “The Nature of Mutation in Genetic Algorithms.,” *Proc. Sixth Int. Conf. Genet. Algorithms*, pp. 65–72, 1995, [Online]. Available: http://pdf.aminer.org/000/310/686/the_nature_of_mutation_in_genetic_algorithms.pdf

[128] M. Harman, “An Evaluation of Mutation Operators for Equivalent Mutants,” no. September, pp. 1–99, 2006.

[129] L. Núñez-Letamendia, “Fitting the control parameters of a genetic algorithm: An application to technical trading systems design,” *Eur. J. Oper. Res.*, vol. 179, no. 3, pp. 847–868, Jun.

2007, doi: 10.1016/J.EJOR.2005.03.067.

[130] A. Chitra and A. Rajkumar, “Genetic algorithm based feature selection for paraphrase recognition,” *Int. J. Artif. Intell. Tools*, vol. 22, no. 2, pp. 1–17, 2013, doi: 10.1142/S0218213013500073.

[131] E. S. Jabber, “Optimal Population Size for Genetic Algorithm Using Fuzzy System,” *Basrah J. Sci.*, vol. 25, no. 2A english, pp. 66–77, 2007.

[132] “Population-sizing-in-genetic-algorithms-Too-small-and-the-user-pays-a-quality-penalty.”

[133] G. D’Angelo and F. Palmieri, “GGA: A modified genetic algorithm with gradient-based local search for solving constrained optimization problems,” *Inf. Sci. (Ny).*, vol. 547, pp. 136–162, 2021, doi: 10.1016/j.ins.2020.08.040.

[134] A. Hassanat, K. Almohammadi, E. Alkafaween, E. Abunawas, A. Hammouri, and V. B. S. Prasath, “Choosing mutation and crossover ratios for genetic algorithms-a review with a new dynamic approach,” *Inf.*, vol. 10, no. 12, 2019, doi: 10.3390/info10120390.

[135] “Termination Criterion - an overview | ScienceDirect Topics.” https://www.sciencedirect.com/topics/computer-science/termination-criterion (accessed Apr. 28, 2024).

[136] P. L. Morrell, D. M. Toleno, K. E. Lundy, and M. T. Clegg, “Estimating the contribution of mutation, recombination and gene conversion in the generation of haplotypic diversity,” *Genetics*, vol. 173, no. 3, pp. 1705–1723, 2006, doi: 10.1534/genetics.105.054502.

[137] “Cross-over Mutation - an overview | ScienceDirect Topics.” https://www.sciencedirect.com/topics/computer-science/cross-over-mutation (accessed Apr. 28, 2024).

[138] P. Bajpai, “Genetic Algorithm – an Approach to Solve Global Optimization Problems,” vol. 1, no. 3, pp. 199–206.

[139] J. Fang, Y. Wang, C. Lei, and R. C. Feng, “The way of solving traveling salesman problem the research on scheduling in AS/RS,” *Procedia Eng.*, vol. 16, pp. 601–607, 2011, doi: 10.1016/j.proeng.2011.08.1130.

[140] M. L. Shahab, F. Azizi, B. A. Sanjoyo, M. I. Irawan, N. Hidayat, and A. M. Rukmi, “A genetic algorithm for solving large scale global optimization problems,” *J. Phys. Conf. Ser.*, vol. 1821, no. 1, 2021, doi: 10.1088/1742-6596/1821/1/012055.

[141] J. Lässig, K. H. Hoffmann, and M. Enachescu, “Threshold selecting,” no. July 2008, pp. 2181–2186, 2008, doi: 10.1145/1388969.1389044.

[142] R. Matoušek, “Genetic algorithm and advanced tournament selection concept,” *Stud. Comput. Intell.*, vol. 236, pp. 189–196, 2009, doi: 10.1007/978-3-642-03211-0_16.

[143] C. Heitzinger, “8.3.3 Mutation,” 2003.

[144] D. Ginoya, P. D. Shendge, and S. B. Phadke, “Sliding mode control for mismatched uncertain systems using an extended disturbance observer,” *IEEE Trans. Ind. Electron.*, vol. 61, no. 4, pp. 1983–1992, 2014, doi: 10.1109/TIE.2013.2271597.

[145] C. S. T. Dong, H. H. Vo, T. C. Tran, P. Brandstetter, and P. Simonik, “Application of sensorless sliding mode observer in control of induction motor drive,” *Adv. Electr. Electron. Eng.*, vol. 15, no. 5, pp. 747–753, 2017, doi: 10.15598/aeee.v15i5.2626.

[146] L. Long, T. Sun, and J. Liang, “Five phase permanent magnet synchronous motor decoupled model with dual frame frequency adaptive flux observer,” *Energy Reports*, vol. 6, pp. 1403–1408, 2020, doi: 10.1016/j.egyr.2020.11.010.

[147] C. Li and M. Elbuluk, “A sliding mode observer for sensorless control of permanent magnet synchronous motors,” *Conf. Rec. - IAS Annu. Meet. (IEEE Ind. Appl. Soc.*, vol. 2, no. C, pp. 1273–1278, 2001, doi: 10.1201/b18777-5.

[148] J. Davila, L. Fridman, and A. Levant, “Second-order sliding-mode observer for mechanical systems,” *IEEE Trans. Automat. Contr.*, vol. 50, no. 11, pp. 1785–1789, 2005, doi: 10.1109/TAC.2005.858636.

[149] A. S. and M. G. Slim DHAHRI, Fayçal BEN HMIDA, “LMI-based sliding-mode observer design method for reconstruction of actuator and sensor faults. ,” *Int. J. Sci. Tech. Autom. Control.*, vol. 1, no. 1, pp. 91–107, 2007.

[150] S. Y. Yang, D. W. Ding, X. Li, and X. Zhang, “Back-EMF based sliding mode observer for vector control of induction machine,” *Dianji yu Kongzhi Xuebao/Electric Mach. Control*, vol. 20, no. 10, pp. 23–30, 2016, doi: 10.15938/j.emc.2016.10.004.

[151] Y. S. Kung, R. Risfendra, Y. De Lin, and L. C. Huang, “FPGA-realization of a sensorless speed controller for PMSM drives using novel sliding mode observer,” *Microsyst. Technol.*, vol. 24, no. 1, pp. 79–93, 2018, doi: 10.1007/s00542-016-3179-6.

[152] H. Zhang and G. Liu, “High-performance control method for the MSTMP motor,” *IET Power Electron.*, vol. 13, no. 2, pp. 266–274, 2020, doi: 10.1049/iet-pel.2019.0488.

[153] H. Niederwieser, M. Tranninger, R. Seeber, and M. Reichhartinger, “Unknown input observer design for linear time-invariant multivariable systems based on a new observer normal form,” *Int. J. Syst. Sci.*, vol. 53, no. 10, pp. 2180–2206, 2022, doi:

10.1080/00207721.2022.2046201.

[154] Y. Zhu and S. Zhu, “Adaptive Sliding Mode Control Based on Uncertainty and Disturbance Estimator,” *Math. Probl. Eng.*, vol. 2014, 2014, doi: 10.1155/2014/982101.

[155] X. G. Yan and C. Edwards, “Robust sliding mode observer-based actuator fault detection and isolation for a class of nonlinear systems,” *Int. J. Syst. Sci.*, vol. 39, no. 4, pp. 349–359, 2008, doi: 10.1080/00207720701778395.

[156] B. An, G. Liu, and C. Senchun, “Design and implementation of real-time control system using RTAI and Matlab/RTW,” *Proc. 2012 UKACC Int. Conf. Control. Control 2012*, no. September 2012, pp. 834–839, 2012, doi: 10.1109/CONTROL.2012.6334740.

[157] C. Gherasim, J. Van den Keybus, J. Driesen, and R. Belmans, “DSP implementation of power measurements according to the IEEE trial-use Standard 1459,” *IEEE Trans. Instrum. Meas.*, vol. 53, no. 4, pp. 1086–1092, 2004, doi: 10.1109/TIM.2004.831509.

[158] R. Ramírez-Villalobos, L. T. Aguilar, and L. N. Coria, “Sensorless H∞ speed-tracking synthesis for surface-mount permanent magnet synchronous motor,” *ISA Trans.*, vol. 67, pp. 140–150, 2017, doi: 10.1016/j.isatra.2017.01.007.

[159] “Optimized Sensorless Control of a Five-Phase Permanent Magnet Synchronous Motor using Genetic Algorithm”.